Synthesis, spectroscopic characterization, and cyclic voltammetry studies for salicylaldehyde Schiff base ligands and their copper (II) salicylaldimine compounds.

By

Siyasanga Booysen

In fulfillment of the requirement for the degree of

Magister Scientiae in Chemical Science

Faculty of Natural Sciences, University of the Western Cape

Bellville, Cape Town, South Africa

Supervisors: Dr Asanda Busa and Prof. Martin O. Onani
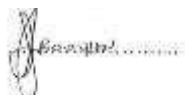
May 2022

Declaration

I hereby declare that Synthesis, spectroscopic characterization, and cyclic voltammetry studies for salicylaldehyde Schiff base ligands and their copper (II) salicylaldimine compounds submitted to the University of the Western Cape is my work, except where indicated by referencing which are completely and accurately reported.

Siyasanga Booysen   May 2022

Signature:

Supervisors: Dr A.V. Busa, Prof. M.O. Onani

i

Dedication

This work is dedicated to my late Grandma (Nominithi Dane Booysen) and my one and only

brother (Mandilakh Xolisa Booysen). You may be gone but you will always be in my heart, I

have lost you on flesh but surly I have gained very strong guardian angels. May your souls

continue to rest in power!!!!! I love you always.

Acknowledgments

Philippians 4 vs 13

"I can do all things through Christ who strengthens me" with those words I would like to thank the Lord, God for his everlasting love, His love and protection through this journey till today He has been faithful to me. Dear Lord, I am grateful for all your blessings without Him this work wouldn't have been possible.

To my Supervisor Prof Martin.O. Onani from the bottom of my heart, I want to thank you for being a father and an academic father, during the course of this work I faced so many challenges and you held my hand and made sure I never gave up. For your guidance and your teachings, I lack words of how to thank you, May God bless you for everything.

To my supervisor Dr Asanda Vincent Busa I know I haven't been the best student, but you never gave up on me. Thank you for your guidance and your teachings. May God bless you on my behalf.
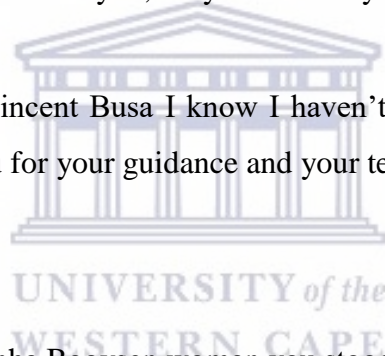
To my mother Nonkoliseko Sannha Booysen woman you stood by my side and supported me through this journey I want to say thank you for everything you know how much I love you To my sister Andiswa Camagwini Booysen Ngwenya , I want to thank you for your love and support. If I were given a chance to choose a sister again with no doubt, I would choose you any time. No amount of words can ever express how thankful I am to you.

To my big brother Mr Ayanda Ngwenya, bhuti you always made sure I never lack anything, from days where I lost hope you would remind me that if I put my mind to something I will definitely achieve it, thank you for taking the responsibility of being a big brother to me. I love you infinity * infinity.

iii

To Onalo Siyamthanda Booysen it has been difficult to be separated to you since you were 3 you never got a chance to spend time with me but I want you to know all these efforts are to make a brighter future for you my sweetheart. I love you my baby.

To my colleagues and friends (Andisiwe Ngwekazi, Zimkhitha Nqakala,Walter Masingi, Masande Yalo, Kelechi Nwambaekwe, Malamba Tsedu, Dr. Nandipha Botha, Babalo Marantsele and Tin Hlanjwa) I lack word on how to thank you for your endless support when I was going through the most you guys opened your arms and allowed me to bother you with my problems, I am truly grateful for everything that you have done for me, during this pandemic of academics you have been a shoulder to cry on. I am truly grateful for each and every one of you May God bless you I love your infinity * infinity.

I also extend my appreciation to:

The department of chemistry at the University of the Western Cape for the opportunity to carry out this research project and the technical staff members who assisted in various ways. The Organometallics and Nanomaterials Research group and Organic research group for assistance and advice.

NRF for the bursary.

Stellenbosch University for assisting with their instruments (Elemental Analysis).

UWC residential services (Res-Life) for the job that covered my living expenses and month-month-month.

To my extended family thank you for your consistent love and support.

Abstract

Schiff base compounds are a significant class of ligands in coordination chemistry which have been applied widely as they are precise and versatile towards different metal salts. These compounds could be commonly chelating operators, particularly when a compound attached like hydroxide or alkyl thiols (– OH or – SH) is available near the azomethine group to form a five or six-membered ring with the metal center. The metal complexes of Schiff bases contracted from substituted salicylaldehydes, particularly the heterocyclic based metal complexes and different amines have been highly explored due to their broad applicability in mild oxidation catalysis.In this study, five Schiff base ligands namely { **HL^1** : (E)-4-(tert-butyl)-2-(((2-(thiophen-2-yl) ethyl) imino) methyl) phenol. **HL^2**: (E)-2, 4-di-tert-butyl-6-(((furan-2-ylmethyl) imino) methyl) phenol. **HL^3**: (E)-4-chloro-2-(((furan-2-ylmethyl) imino) methyl) phenol. **HL^4** : (E)-2bromo-4chloro-6-(((2-(thiophen-2-yl) ethyl) imino) methyl) phenol. **HL^5**: (E)-4-nitro-2-(((2(thiophen2-yl) ethyl) imino) methyl) phenol.} were synthesized and fully characterized for use in the synthesis of copper (II) salicylaldimine compounds. The ligands, HL^1–HL^5, reported herein were synthesized by reacting the commercially available,2-hydroxy-5-methylbenzaldehyde,3,5-di-*tert*-2-hydroxybenzaldehyde,5- chlorosalicylaldehyde, 3-bromo-5-chloro-salicyaldehyde and 2-hydroxy-5-nitrobenzaldehyde with either 2-thiopheneethylamine or 2-furfurylmethylamine, respectively. The reactions were stirred at room temperature for 12 hours in the presence of a drying agent, anhydrous magnesium sulfate, in dry ethanol. The ligands were isolated as stable yellow solids with yields ranging from 70% to 97%. The ligands were soluble in most common organic solvents such as dichloromethane, chloroform, and acetonitrile. The complexes were derived from the ligands (HL^1–HL^5) respectively, by reacting commercially available Cu (CH$_3$COO) $_2$, while the Et$_3$N was used to deprotonate the ligands to catalyze the reactions. Thereafter the solvent volume was then reduced under vacuum to ~3 mL and the complex precipitated with cold diethyl ether. The precipitate was filtered and washed with a copious amount of cold diethyl ether and isolated, the product was left to dry overnight in a fume cupboard. The characterizations of the synthesized ligands and their complexes was performed through NMR, FTIR spectroscopy, UV-Vis spectroscopy, Mass spectroscopy, Elemental Analysis, Cyclic voltammetry. The FTIR spectra demonstrated that the coordination sites are the azomethine nitrogen and carbonyl oxygen atoms of the Schiff base ligand. The compounds were further characterized by elemental analyses which showed that the compounds were relatively pure with the difference of at least

0.1. The mass spectrometer results of the ligands showed calculated molecular ion peak being in agreement with the experimental results observed. The Cu isotopes are known to be quadrupolar and usually yield broad signals in the NMR experiments. Therefore, the characterization using the NMR was not possible and thus a cyclic voltammetry study was carried out for the Cu (II) complexes instead. The CV of the complexes showed interesting results where the increase in the scan rate also increases the redox reaction.

UNIVERSITY of the
WESTERN CAPE

List of Abbreviations

%	percent
°C	degrees Celsius
^{13}C NMR	Carbon 13 nuclear magnetic resonance
^{1}H NMR	proton nuclear magnetic resonance
$CDCl_3$	deuterated chloroform
Cu	copper
CV	cyclic voltammetry
d	doublet
dd	doublets of doublet
E.A	elemental analysis
et al.	et alia
Fig.	figure
FTIR	fourier transform infrared spectroscopy
g	gram
GC-MS	gas chromatography mass spectrometry
H	hour
Hz	herz
J	coupling constant
L	liter
LMCT	ligand to metal charge transfer
m	multiplet
m/z	mass per charge
mg	milligram
mL	millilitre
Mol	moles
mM	millimolar
MS	mass spectrometry
NMR	nuclear magnetic resonance
OH	hydroxyl group
ppm	parts per million
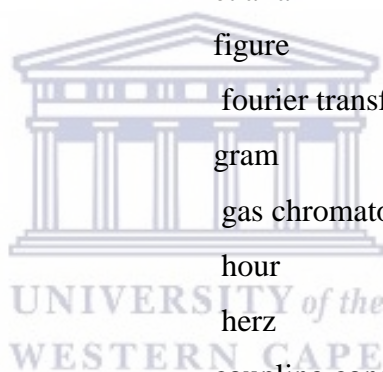
q	quartet
s	singlet
SB	Schiff base
t	triplet
UV-Vis	ultraviolet-visible spectroscopy
μg	microgram
μL	microliter

Table of Contents

List of schemes

Chapter 1

List of tables

List of figures

xiii

xiv

Chapter 1

1.1 Introduction

Coordination chemistry can be classified as the interaction between ligands and metal centre, where in the later, they can be complexing group that can accept or donate electron density from the metal atom, it is a substance in which a metal atom or ion accepts electrons from (and thus associates with) a group of neutral molecules or anions called ligands [1]. On the other side, ligands can be classified as either neutral molecules, or charged ions that carry lone electron pairs that interact with the metal centre in a variety of ways [2] [3]. Changes in the first coordination sphere of a metal ion can have a drastic impact on the entire complex and its chemical properties, according to the basic principles of coordination chemistry. To understand the chemical characteristics of metal complexes, it is critical to understand the bonding theories governing the ligands and metal atoms.

Copper is the third most abundant trace element in the body after zinc and iron. Copper, like silver and gold, is a noble metal. High thermal and electrical conductivity, low erosion, alloying capacity, and flexibility are all useful mechanical qualities. Electrical applications need a significant amount of metallic copper [4]. In general, simple Cu (I) mixtures do not stay stable in water and are quickly oxidized.

Cu (I) mixtures such as CuCl and CuCN, that are extremely insoluble. Cu (I) can also be used to frame structures using chelating ligands. Cu (I) complexes typically have four geometries: tetrahedral, trigonal– pyramidal (TBP), tetrahedral.There are also three and two facilitated Cu (I) structures, but five coordinated Cu(I) structures are aberrant and have at least one fundamentally protracted Cu–ligand link [5]. Cu (II) structures have recently received a lot of attention. They exhibit extremely interesting spectroscopic properties and changed reactant workouts because of their adaptability, aptitude to settle odd oxidation states, and successful execution in replicating specific geometries around metal focuses [6].

1.1.1   Schiff base ligands

A chemist from Germany who is also a Noble Prize winner called Hugo Schiff discovered Schiff base in the year 1864, and the ligands were then named after him [7] [8][9]. The Schiff bases are one of the most commonly used groups of chemical molecules. They are products of condensation reactions of a primary amine and a carbonyl compound. The Schiff bases all

1

possess azomethine (C=N-) as the main functional group [10][11]. The azomethine structure is made up of a carbon-nitrogen double bond, with the nitrogen attached to the alkyl or aryl group rather than the hydrogen, (see Scheme. 1.1) [12][13].
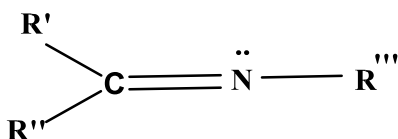
Scheme 1.1. Schiff base Schiff base reaction for the establishment of imines [12], where R', R", and R"' are alkyl, aryl, cycloalkyl, or heterocyclic groups that stabilize the Schiff base.

These compounds have the ability to coordinate with metal ions via imine nitrogen and any other group linked to a Schiff base. Because of the versatility of the active groups, Schiff base ligands are referred to as "privileged ligands" [14] [15]. The literature reports show a multidentate Schiff base ligands with different terminals containing the S, N, and O donor atoms with a wide range of applications [16].

1.1.2 Schiff base formation mechanism

The general mechanism of Schiff base is depicted in scheme 1.2 this occur during its formation, a nucleophilic added amine to the carbonyl group. The lone pair of electrons in the amine nitrogen attack the ketone or aldehyde during the first phase of the mechanism, producing an unstable carbinolamine [17] [18]. A 1.3-hydrogen shift takes place, which promotes the elimination of H_2O via acid/base catalysis. Because carbinolamine is an alcohol, it undergoes acid-catalysed dehydration [19][20].
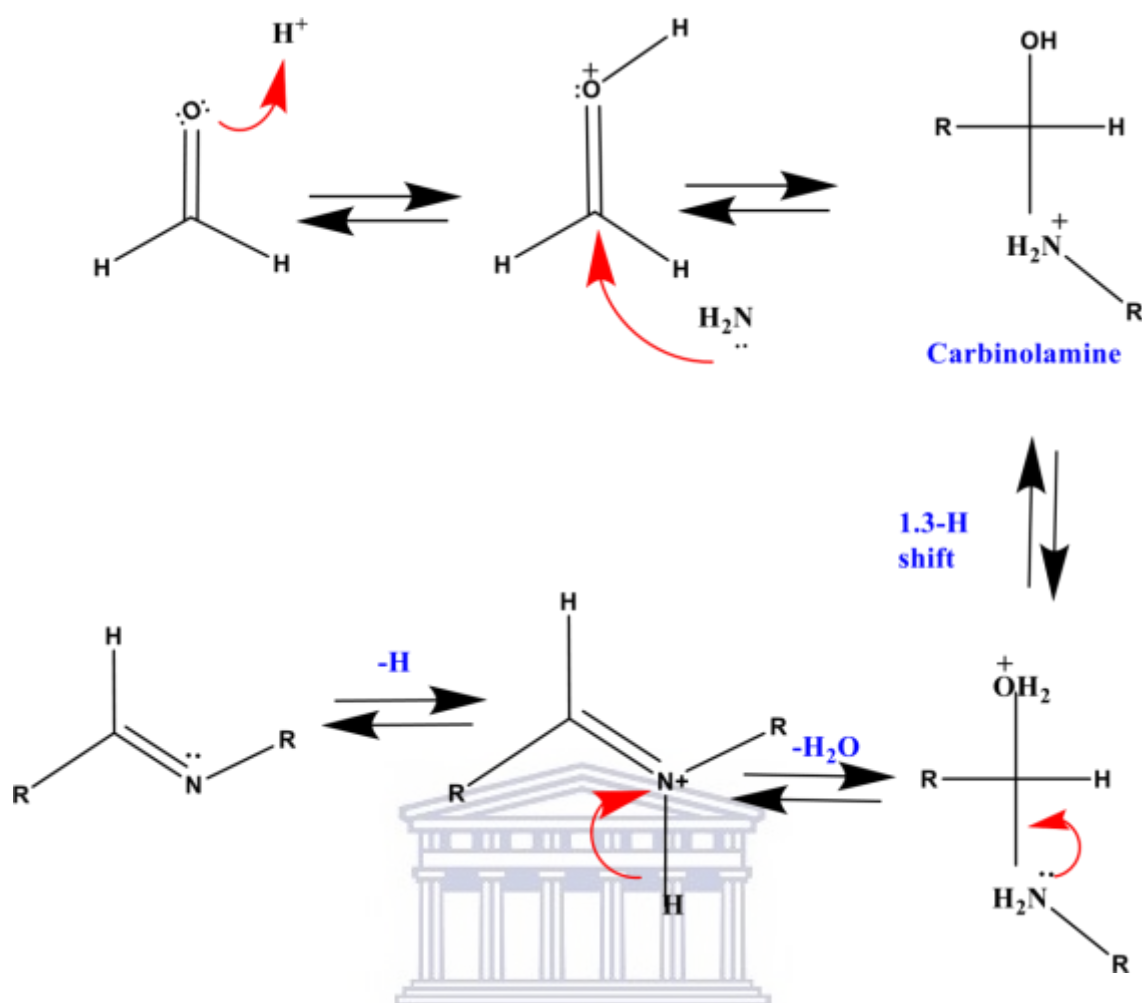
Scheme 1.2. The general mechanism of Schiff base, which is one of the possible pathways for the reaction of aldehydes with amines [20].

The dehydration of carbinolamine is the rate-determining step in the formation of the Schiff base [20] [21], consequently, acids or Lewis acids are used to catalyze this reaction. However, the concentration of acid present for catalysis cannot be greater than that of the amine. Deprotonation occurs, and the amine becomes non-nucleophilic [22], when equilibrium shifts to the left, the carbinolamine reverts to a ketone or aldehyde and a primary amine. Base catalysis is used in the dehydration of carbinolamines [23]. The elimination reaction is related to alkyl halide E2 elimination. Schiff base formation can be divided into two steps by adding an anionic intermediate (for example) followed by elimination. The geometry of the imine double bond is typically trans, which limits the steric interaction of the bulkier R group with R being an ether alkyl or aryl substituent [24][25] [26].

3

Under mild conditions, hydrolysis of the Schiff-base ligands reveals a remarkable problem with cleavage of the preceding imine bond. [27] [28]. Despite the use of anhydrous solvents throughout, the commercially obtained salts, in their hydrated forms, provided enough water into the system for imine bond hydrolysis to occur, which is aided by the presence of metal cations, which have Lewis acid properties and can speed up this bond cleavage scheme. 1.10 [29]. The mechanism for imine formation and its reversible response are depicted in Schemes 1.3 and 1.4 [39].
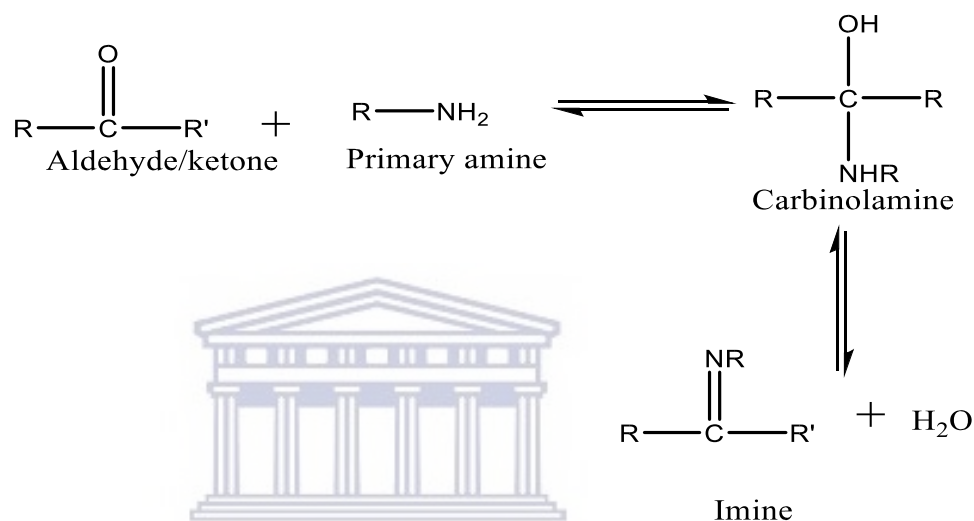
Scheme1.3. Mechanism of Schiff base formation **[**30]
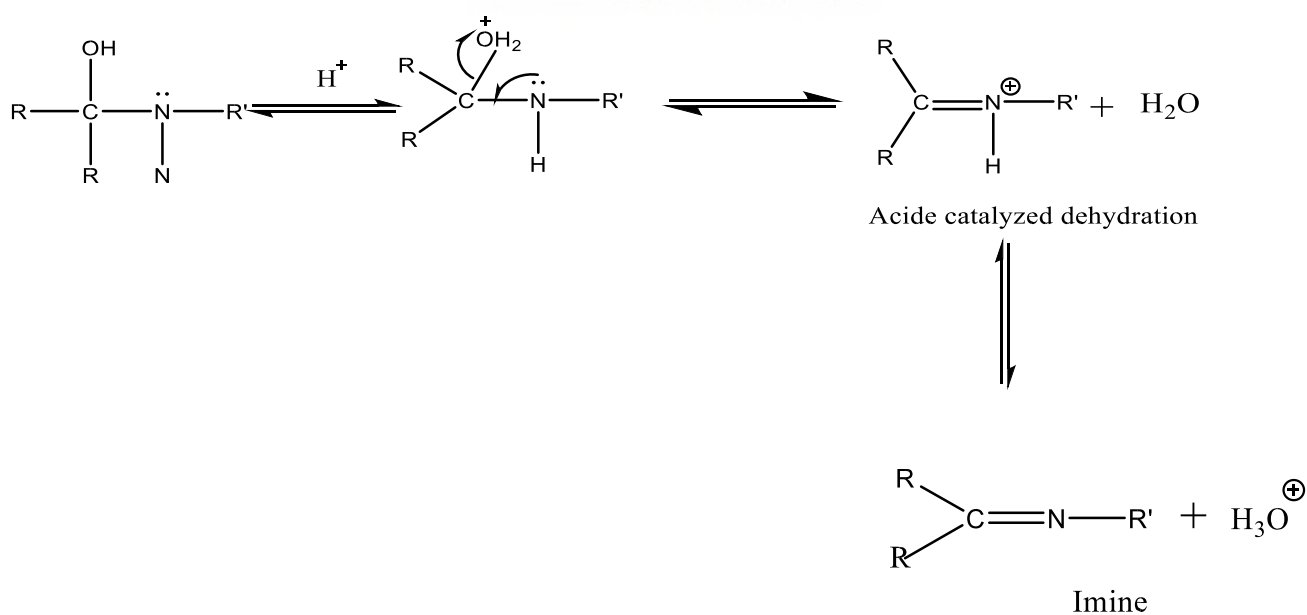
Scheme 1.4. Heating causes a reversible reaction of Schiff base from aldehyde/ketone under acid/base catalysis. [31].

In the development of imine-ligands, this hydrolysis could be reversible [29]. Nonetheless, imine-ligands are frequently very stable in acidic conditions. It is still unknown why some imine compounds withstand hydrolysis while others remain stable under similar conditions [32] [33]. Anhydrous $MgSO_4$ is always used to stop likely hydrolysis of the imine group in dichloromethane under gentle conditions to prevent the hydrolysis of the imine group thereby decomposing the product. [34].

1.1.3 Chelating properties of different types of Schiff base

Classes of Schiff base bidentate (1), tridentate (2), tetradentate (3) and others (Scheme 1.5-1.10) are known to be able to form stable complexes with transition metal ion and are easy to synthesize and can be obtained in good yield [35][36]. The resultant Schiff bases can act as mixed-donor ligands that can participate in bi-, tri-, tetra-, and higher coordination modes if they contain additional functional groups like –OH, –NH_2, or –SH. N,O- donor sites can be found in salicylaldimine Schiff base bidentate chelating ligands. The nitrogen atom is a soft donor atom that stabilizes lower oxidation state metal ions when they are coordinated, whereas oxygen is a strong donor atom that stabilizes high oxidation state metal ions [37].

Type 1: Bidentate
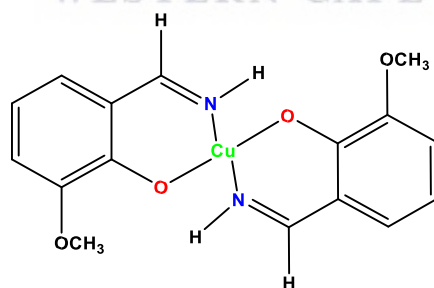
Scheme 1.5. O, N-bidentate Schiff base ligand donors [38].

5
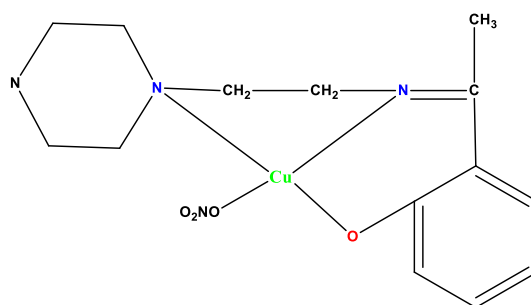
Type 2: Tridentate

Scheme 1.6. Schiff base ligand tridentate with O, N, donors [39].

Type 3: Tridentate
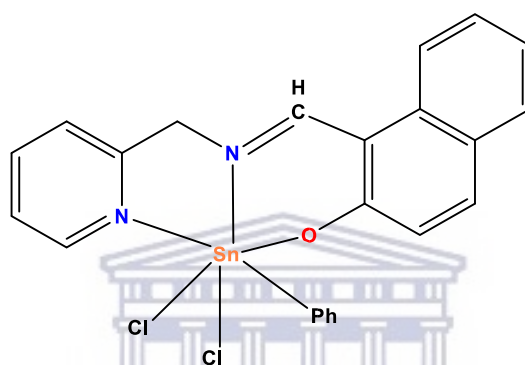
Scheme 1.7. Tridentate Schiff base ligand with donors of O, N, and N [40]

Type 4: Tridentate
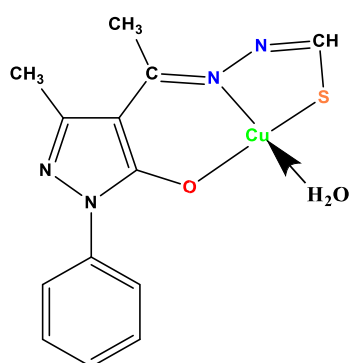
Scheme 1.8. Tridentate Schiff base ligand with donors of O, N, and S [41].

Type 5: Tetra dentate
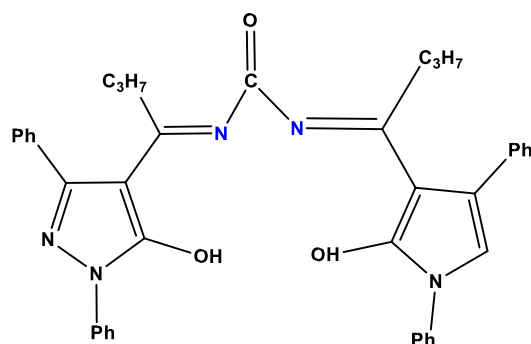
Scheme 1.9. Tetra dentate Schiff base ligands with donors of O, N, N, O Schiff base ligand structure proposed [42].
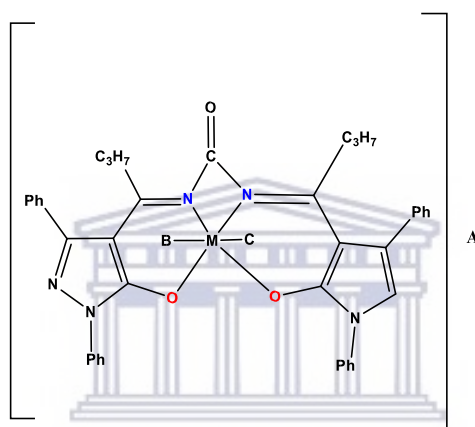
Scheme 1.10. Suggested metal complex structure with O, N, N, O donor Schiff base and A, B, C, and M being any of those listed in table 1.1 below. [42] [43].

Table 1.1 A,B,C and M symbols with what can be substituted in their space [42]

M	A	B	C
OV(IV)	-	H_2O	-
Cr(III) / Fe(III)	H_2O	H_2O	NO_3
Fe(II), Ni(II), Cu(II) or Zn(II)	H_2O	H_2O	-
UO2 (VI)	-	-	H_2O

7

The number of donor atoms contained in a ligand determines whether it is uni, di, tri, or quadridentate. When a ligand's donor sites occupy two or more coordination positions on the same central metal ion, a complex with a closed ring is formed, a phenomen which was coined in the year 1920 by Morgan and Drew [23][44][45]. The primarily nitrogen donor Schiff bases, can also function as bi-, tri-, tetra-, or polydentate mixed donors. The nature of donor of the ligand depends on the nature of 1° amine or diamine or the nature of aldehyde or ketone used in the synthesis [46].

1.1.4 Preparation of Schiff base ligands

Schiff base ligands are supporting ligands in the synthesis of metal complexes and organic products, as shown in Scheme 1.11 [47][48][49]. To form desirable metal complexes, Schiff base ligands coordinate to the metal centre [50]. Schiff base ligands offer a variety of biological and catalytic properties that seem to improve with metal center coordination [51]. Schiff base compounds containing functional groups such as thiosemicarbazones, imidazoles, indoles, pyrazoles, furylglyoxal, azomethine, ptoluidene, thiazole, benzothiazole, isatin, azo compounds, pyridoxal, hydrazones, and other fussed heterocyclic compounds have shown antibacterial, anticancer, antifungal, antimicrobial[52][53][54][55]. The features of Schiff base ligands make them attractive candidates for oxygenation, hydrolysis, electro-reduction, and decomposition in industry; plant management as insecticides in agriculture [56][57]; and therapeutic application as antiviral [55], antibacterial [58], and anticancer drugs [59]. Scheme

1.11shows the use of Schiff bases as intermediates in organic and inorganic synthesis.
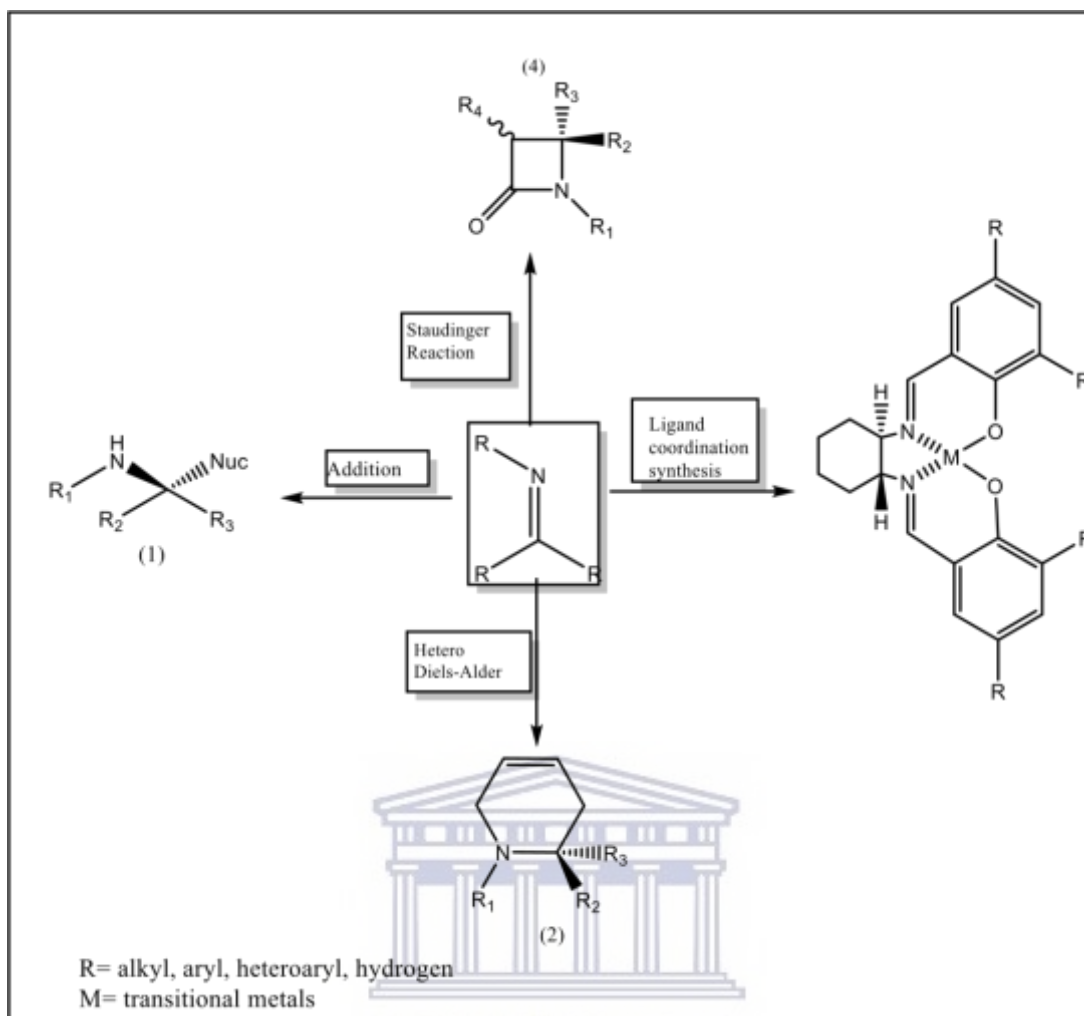
Scheme 1.11. Schiff bases as intermediate during synthesis [60].

1.1.5 Salicylaldimine Schiff Base Transition Metal Complexes

The salicylaldimine ligands are a sub-class of Schiff-base compounds that have been widely used as metal ligands because they have intriguing attractive, reactant, and redox properties and could be used as biomimetic models for various organic metal sites [61]. These compounds provide opportunities for inducing substrate chirality, fine-tuning the metal-focused electronic factors, and improving the solvency and security of homogeneous or heterogeneous catalysts. [62]. Such ligands are synthesized by means of by nucleophilic addition, some of these ligand that were studied were successfully synthesized from an amine and a carbonyl molecule, yielding a hemi-aminalfunctionality that was then dehydrated in situ to yield an imine functionality (vide supra). These ligands have a unique structure that is represented by the formula $RR_1C=NR_2$ (R = R_1 = R_2= alkyl, aryl, or hydrogen).

9

Schiff base ligands can either polymerize or decompose very fast, except there is at least one aryl group attached to carbon or nitrogen of the >C=N double bond [63]. As a result, Schiff base ligands with aryl substituents are significantly more stable and they are easy to synthesize, whereas on the other hand those with alkyl substituents are relatively unstable, Aliphatic aldehyde Schiff base are relatively unstable and polymerizable [64][65] , but those with aromatic aldehyde are efficient conjugation are more stable [66][67].
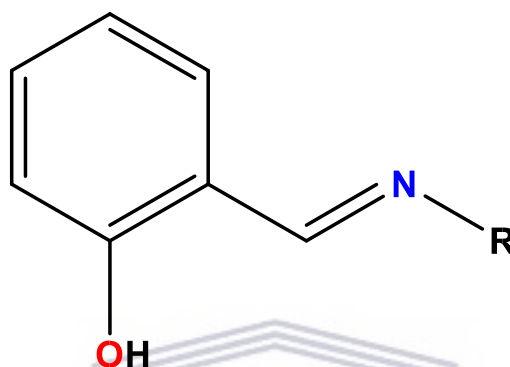
Scheme 1.12 Example of structure of Salicylaldime[68]

Condensation of aldehydes and amines occurs under various reaction conditions and in various solvents. Methanol or ethanol are the most common solvents used to make the SB ligands. The ligands can be prepared at room temperature or in a refluxing environment. $MgSO_4$ is a reagent that is mostly used to dehydrate water in the reaction [68] [69]. Literature shows that it is possible to develop new SB compounds as there is enough aldehydes and amines that can be reacted [70]. Schiff base ligands that are general mono-, di-, tri- and multi- dentate chelating are usually designed according to the binding environments of metal ions [71].

1.1.6 Methods that are used to prepare Schiff base ligands and their metal complexes

Direct ligand synthesis then complexation

The preparation, segregation and purification of Schiff base are carried out prior to complexation [72]. Thereafter the complexation is then carried out by treating the metal ion and Schiff bases with the desired metal salts. This method is advantageous because spectral characterization can

be easily performed to both ligands their metal complexes and it is easy to compare the data of both ligand and complexes [73].

Template Synthesis

According to Busch, the Template synthesis is an assembly of atoms, with respect to one or more geometry, in order to achieve particular linking of atoms. The technique prepares the complexes *in situ*, without the isolation of Schiff bases by amalgamating the metal compound, amine and aldehyde in one step reaction [74][75]. By using a reaction template, the metal ions do catalyze the process" [76]. This method has been previously used to carry out the assembles that have unusual topologies, such as rotaxanes, helicates, macro cycles and catenanes [77]. As a result, a templating agent is the organization of a set of building blocks so that they can be linked together in a specific manner.

Rearrangement of Heterocycles (oxazoles, thiazoles etc.)

The direct method of synthesizing a Schiff base by condensation of an o-hydroxy-, o-amino-, or o-mercaptoamine with a carbonyl molecule sometimes leads in an undesirable side reaction involving ring closure and the production of a heterocyclic compound [78] [79]. This technique was proposed by Schiff in 1869. It is where the Schiff base is prepared by a chelate of one of the starting materials (aldehyde or amine) with the other reacting with the metal complex [80]. Usually, the presence of metal ions, the benzothiazoline and benzoxazole rings are reported to open, and ring rearrangement results in the formation of corresponding metal chelates of the Schiff bases as shown in scheme 1.13 below[81].
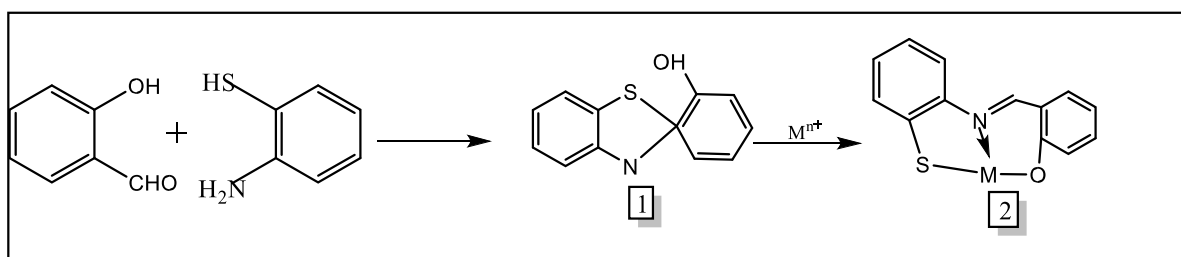
Scheme 1.13 2-(2-Hydroxyphenyl) benzothiazoline: (1)synthesis; (2) interaction with metal ion[81].

Literature reports indicate that Schiff base ligands are most convenient and highly attractive ligands for forming complexes [82]. The steric and electronic effects surrounding the metal complex can be finely tuned by incorporating bulky and/or electron withdrawing or donating

substituents into the Schiff bases [9] [73]. The chemistry changes when we have two donor atoms such as N and O, because they have opposing electronic effects. The phenolate oxygen is a hard donor that stabilizes the metal ion's with higher oxidation state, whereas the imine nitrogen is a border line donor that stabilizes the metal ion's with lower oxidation state [83].

The most popular method is actually the one step method of preparing the Schiff base ligand via the condensation reaction produces high quantitative yield [73]. Busa *et al* used this technique with compounds very close to our study. The direct ligand synthesis was followed by a metal salt complexation. The compounds were all subjected to the standard spectroscopic techniques such as FT-IR, UV-Vis, NMR, MS and elemental analysis to characterize them [68]. It can be concluded that the major advantage for this preparation method is simplicity of synthesis and high stability of the complexes with nitro- groups on ligands and thus produces good yield.

Schiff base compounds with nitrogen, oxygen, and Sulfur chelating groups in their structures have gotten a lot of attention in the field of research recently [62]. Other reports also demonstrated that copper (II) ions with salicylaldimine ligands have shown a high recoverability and stability [84].

Mononuclear Schiff-base structures are significant in demonstrating metalloenzymes, just as they are from a modern standpoint [85]. Salicylaldiminato-copper (II) structures have been discovered to catalyze a variety of oxidation reactions, for example, oxidation of essential alcohols, and specific oxidation of essential alcohols with atmospheric oxygen compare to aldehydes [61][62][84]. It has been demonstrated that the synergist changes of alkanes continue through the formation of thermally unstable dynamic mononuclear copper(II)-peroxo (LCuO2) and copper(II)-hydroperoxo (LCuII-OOH) intermediateswhich uses salicyaldimine compounds [61]. As a result, salicyaldimine ligands were combined with the goal of balancing out the resulting copper (II) structures in reactant cycles. Furthermore, it has been demonstrated that endowing the chelating phenolate ligands with cumbersome *tert*-butyl substituents at the *ortho*- and *para*-positions improves the stability of the resulting phenoxyl radical complexes [62][69].

12

These Schiff base is a class of ligands known to be very efficient. As previously discussed in the mechanisms, Schiff base ligands contain a lone pair of electrons in the nitrogen atom of the amine bond, which can then be donated to a suitable metal ion. Several Schiff bases have a second or even third functional group that can include OH (salicylaldehyde or its derivatives), a nitrogen atom from a heterocyclic ring, imidazole rings, or pyridine rings. Electron donation in conjugation with a functional group implies the possibility of preparing a large number of transition metal complexes for various applications. Earlier research indicates that several

Schiff base complexes have been used for catalytic activities [86] [87] [88], biological activities [89] [90], in oxidations, polymer-supported [91], and many more. However, in this work, an overview of Cu(II) coordination in Schiff base ligands with a preliminary application in catalysis will be investigated further.

1.2 Copper

Copper, along with Silver and Gold, are transition metals that are found in group 11 of the periodic table of elements. Copper typically forms compounds with oxidation states +1 and +2, which are commonly referred to as cuprous and cupric, respectively [92] [93]. The oxidation states +1 with electronic configuration $3d^{10}$ form the complexes which are diamagnetic. On the other hand, there is also an unusual/least common case of +3 and +4 [92]. In this work, the focus is on the most stable and common coordination of Cu^{2+} ion with an electronic configuration of $3d^9$.

Table 1.2 Experimental values for selected physical properties of copper

Property	Cu
Atomic number	29
Naturally occurring isotopes	2
Atomic weight	63.546
Electronic configuration	$[Ar]3d^{10}4s^1$
Electronegativity	1.9
metal radius / pm	128

13

	2nd	20.28
(eV)		
3rd		37.07

The Cu(II) d^9 electron configuration favours the coordination with different ligands which adopt the square planner or distorted octahedral geometry.

This effect implies that molecules must adopt geometries that do not result in valence level orbital degeneracy [92] [94] [95] [96] [97]. When the Cu^{2+} ion is coordinated to six homoleptic ligands resulting in octahedral complex, it usually exhibits a distorted octahedral geometry because of Jahn Teller distortion.

Schiff base copper (II) complexes could exhibit a coordinated of 4 or 5 ligands. The octahedral complexes of these Cu(II) Schiff base are typically found in situations where the axial group is coordinating solvent or counter ions. The five-coordinate complexes and the axial phenomenon are mostly similar of course with an exception of the Cu(II) diphosenolate complex [98] [99]. A work which was reported by Franks and co-workers [100] showed that Cu(II) complexes which contain pentadentate N_3O_2 Schiff base ligand with Cu(II) ion have trigonal bipyramidal geometry. It is clearly seen that the Schiff base ligands and their complexes have been widely investigated in the field of chemistry. They are found to be very much effective in the preparation of various useful analytical reagents, industrial catalysts, medicine, agrochemicals, and other industrial products [73][101][102]. Furthermore, Cu(II)-Schiff base complexes based on salicylaldehyde ligands are popular due to a plethora of applications as found in the literature [100][102]. These types of complexes are mostly used in the Catalysis applications [103][104] [105] [106] as well as some biological fields such as the antimicrobial activity.

1.3 Catalysis

Cu (II) Schiff base complexes are frequently used as oxidation catalysts. They are known to be effective and selective in a variety of organic reactions. They are relatively inexpensive, stable, and simple to prepare [107] [108]. The Schiff base ligands have a high electron-donating ability which makes them help to increase the rate of electron transfer. In other words, these ligands can boost an imine functionalized composite's overall catalytic activity [107]. The oxidation of

14

alcohols to their carbonyl, aldehyde, and ketone groups is a fundamental reaction that occurs occasionally in organic amalgamation. Researcher Adams and co-workers [109] reported a suitable catalytic oxidation scheme 1. 14 (PhIO/cat, CH_2Cl_2, ca. 20 °C) of primary and secondary alcohol with allylically and benzylically activated C-H bond [109].
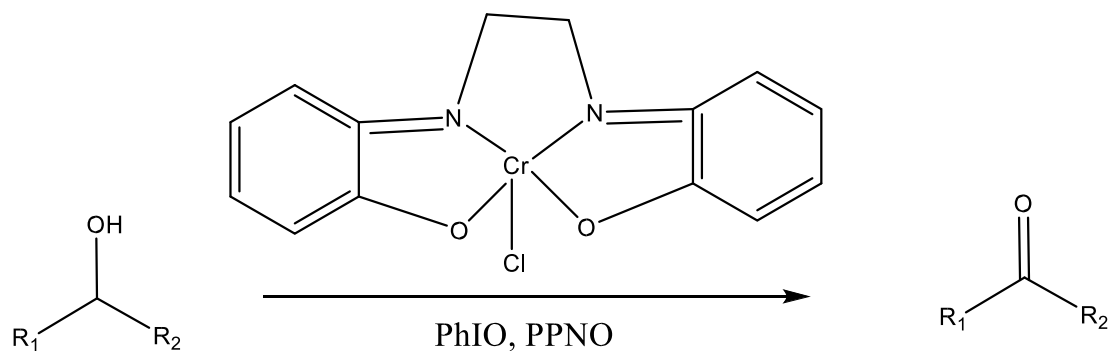
R_1, R_2 = H, Alkyl, Aryl

Scheme 1.14 Catalytic activity of Cr (III) salen Schiff base complex in oxidation reaction [70].

The oxidation of alcohols to aldehydes, ketones, and carboxylic acids is perhaps the most widely utilized class of oxidation responses in natural science [110]. Numerous reagents and impetuses exist for these changes. Yet, for prudent and natural reasons, the improvement of effective and specific impetus for oxidation of alcohols into their relating carbonyl mixes is a fundamental essential in the substrate [111]. Change metal catalysed oxidation of natural substrates is of current intrigue [112]. Efferent reactant techniques dependent on change metals have been developed [113]. However, synergist oxidation was inspired first by the need to understand the capacity of conventional catalysts, and later by its importance in the compound [114][115] thus, exquisite advancement metal structures have been blended, and their synergist properties in oxidation, epoxidation, carboxylation, hydrogenation, and other useful gathering changes have all been accounted for [113].

Copper is a significant metal biologically. It exists in different metalloproteins especially for catalysis [116], Galactose oxidase (GO), laccases, hemocyanin, cytochrome C oxidase, and

superoxide dismutase are a few examples. These catalysts assume a significant role in various bio– oxidation responses. In this way copper has attracted specific consideration as an impetus structure and energizing exploration exercises in the domain of coordination science with little sub-atomic model edifices which have been accounted for [117]. These model buildings offer a profitable stage for the advancement of Cu based homogeneous scaffolds. They can oxidize a range of natural substrates. Be that as it may, from the mechanical perspective, basic and reasonable copper catalysts, which can enact sub-atomic oxygen or hydrogen peroxide with high reactant action and selectivity, are attracting choices for ordinary stoichiometric oxidation strategies.

Atomic oxygen is a non-poisonous and modest oxidant for the oxidation of alcohols. It is currently used in a few large– scale oxidation reactions, which are catalysed by stoichiometric reactions of heterogeneous catalysts such as chromium (VI) [113]. These reagents are unsafe and produce overwhelming metal waste which currently counter their usage as far as the green chemistry and UN sustainable development number 12 are concerned [124]. Likewise, these oxidation responses are carried out at raised temperatures. The heterogeneous oxidation strategies, in any case, are inappropriate for the responses required in the fine chemical industry, where an exceedingly effective oxidation framework under gentle response conditions are required as a result of the efficient and ecological requirements [118].

In another instance, the conjugated nitroxyl radicals, for instance the diphenylnitroxyl radical have been known for a century [119]. Stable non-conjugated free radicals particularly TEMPO (2,2,6,6–tetramethyl– piperidinyloxyl) detailed during the 1960s have discovered significant applications as amazing inhibitors of free extreme chain procedures, for example, autooxidations and polymerizations [120] [121]. Furthermore, TEMPO and its subordinates are outstanding as probably the best middle precursors in oxidation responses and they have a wide– scope of uses in natural reactions [27]. They can be used to catalyze the oxidation of alcohols to their corresponding aldehydes and ketones in particular by an assortment of oxidants and impetuses [122]; including ruthenium [4] and copper [123].

1.4 Problem statement

The advancement of new or improved catalysts is highly involving, including their characterization and broad testing. Since the scope of the factors necessary for producing them is regularly enormous, and the connections between changes in these factors and catalyst executions are frequently obscured, the catalyst development can be a monotonous and costly exercise. Researchers have to consider the nature of new catalysts and their reactions to evaluate their after effects which is of prime importance. These properties are largely controlled by the attached ligands.

The transition to greener, more sustainable manufacturing processes that efficiently use raw materials, crash waste, and avoid the use of harmful/toxic and risky materials is the challenge confronting the chemical and related industries in the twenty-first century. It necessitates a shift in perspective from traditional concepts of process efficiency, which focus on chemical yield, to one that provides economic incentives for replacing fossil resources with renewable raw materials, eliminating waste, and avoiding the use of toxic as well as hazardous substances. An understanding of the amount of waste generated per kilogram of product in various areas of the chemical industry demonstrates the need for green chemical manufacturing.

The development of metal catalysts with unrivalled performance is the ultimate quest. Vast amounts of the most useful soluble and solid catalysts, such as the PGM metals; rhodium, palladium, platinum, and ruthenium, are used to produce highly active catalysts, however, these metals are costly and their supply is limited even in a mineral rich country such as South Africa. Valuable metals must be used more effectively and sparingly if not avoided altogether, alternatively, we need to turn to non-valuable metal catalysts such as copper catalysts, which must be developed as replacements. Consequently, the focus of this work was to develop new Copper (II) complexes that will be chelated by a salophen ligand endowed with different electron donating and withdrawing groups purposely for the ease of the oxidation of primary alcohols. The addition of sterically demanding substituents to the salicylaldimine moiety, such as tert-butyl groups, alters the resulting electronic and chemical properties of the metal complexes for a better activity.

17

1.5 Aims and Objectives

Aim

The general aim of this study is to synthesize salicylaldimines Schiff base ligands and their salicylaldiminato-copper complexes that are endowed with different substituents at the *ortho*- and *para*-position that possess a pendant hemilabile thiophenyl/ furfuryl amine moiety.

The complexes have the potential to act as efficient and selective catalysts in the mild oxidation of alcohols.

Objectives

- Synthesis and characterization of salicylaldimine ligands using standard spectroscopic techniques (FT-IR, NMR, Mass Spec., UV-VIS) and elemental analysis.

- Synthesis and characterization of salicylaldiminato-copper (II) complexes using standard spectroscopy (FT-IR, UV-Vis,), elemental analysis and Electrochemical studies using cyclic voltammetry.

- Preliminary evaluation of catalytic activity and selectivity for mild oxidation of alcohols.

1.6 Thesis Organization

This thesis is organized as follows:

Chapter 1, gives a brief introduction to the concept of Schiff base ligands and their copper (ii) complexes, Catalysis and challenges that have been encountered in the industry catalytic. The literature review of the work aims and objectives of this work.

Chapter 2, focuses on the methods that were used to synthesize the ligands and their complexes, and the characterization techniques that were used to characterize the compounds.

Chapter 3, delves into results from various characterization techniques used and discussion of these results in relation to the properties of the newly synthesized ligands and complexes. A preliminary application is also given here.

Chapter 4, focuses on the conclusions that were drawn from the work and highlights recommendations for future work.

1.7 References

[1]   Götzke, L., Schaper, G., März, J., Kaden, P., Huittinen, N., Stumpf, T., Kammerlander, K.K., Brunner, E., Hahn, P., Mehnert, A. and Kersting, B., 2019. Coordination chemistry of f-block metal ions with ligands bearing bio-relevant functional groups. *Coordination Chemistry Reviews*, *386*, pp.267-309.

[2]   Green, M.L. and Parkin, G., 2014. Application of the covalent bond classification method for the teaching of inorganic chemistry. *Journal of Chemical Education*, *91*(6), pp.807-816.

[3]   Kantchev, E.A.B., O'Brien, C.J. and Organ, M.G., 2007. Palladium complexes of N-heterocyclic carbenes as catalysts for cross-coupling reactions—A synthetic chemist's perspective. *Angewandte Chemie International Edition*, *46*(16), pp.2768-2813.

[4]   Ahmad, J.U., 2012. Copper Catalysts for Alcohol Oxidation.

[5]   Korpi, H., 2005. Copper di-imine complexes: Structures and catalytic activity in the oxidation of alcohols by dioxygen.

[6]   .   Kitajima, N., 1992. Synthetic approach to the structure and function of copper proteins. *Advances in inorganic chemistry*, *39*, pp.1-77.

[7]   Tidwell, T.T., 2008. Hugo (Ugo) Schiff, Schiff bases, and a century of β-lactam synthesis. *Angewandte Chemie International Edition*, *47*(6), pp.1016-1020.

[8]   Fabbrizzi, L., 2020. Beauty in Chemistry: Making Artistic Molecules with Schiff Bases. *The Journal of Organic Chemistry*, *85*(19), pp.12212-12226.

[9]   Dalia, S.A., Afsan, F., Hossain, M.S., Khan, M.N., Zakaria, C., Zahan, M.K.E. and Ali, M., 2018. A short review on chemistry of schiff base metal complexes and their catalytic application. *International journal of chemical studies*, *6*(3), pp.2859-2866.

[10]   Hameed, A., Al-Rashida, M., Uroos, M., Abid Ali, S. and Khan, K.M., 2017. Schiff bases in medicinal chemistry: a patent review (2010-2015). *Expert opinion on therapeutic patents*, *27*(1), pp.63-79.

[11]   Bikas, R., Mirzakhani, P., Noshiranzadeh, N., Sanchiz, J., Krawczyk, M.S., Kalofolias, D.A. and Lis, T., 2020. Synthesis, crystal structure and magnetic properties of a

pentanuclear Mn (III) cluster with 1, 2, 4-triazole based Schiff base ligand. *Inorganica Chimica Acta*, *505*, p.119461.

[12]   Dufera, T.E., Tafesse, S. and Duraisamy, R., 2019. Synthesis and Characterization of Tin (II) and Lead (II) complexes with Benzylidene Aniline Ligand. *International Research Journal of Science and Technology*, *1*(1), pp.56-65.

[13]   Petrini, M., 2005. α-Amido sulfones as stable precursors of reactive N-acylimino derivatives. *Chemical reviews*, *105*(11), pp.3949-3977.

[14]   Cornel, V.M., 2002. Recent Reviews. 63. *The Journal of organic chemistry*, *67*(1), pp.319-326.

[15]   Samani, Z.R. and Mehranpour, A., 2021. Synthesis of new allylidene amino phenol-containing Schiff bases and metal complex formation using trimethinium salts. *RSC Advances*, *11*(35), pp.21695-21701.

[16]   Raczuk, E., Dmochowska, B., Samaszko-Fiertek, J. and Madaj, J., 2022. Different Schiff Bases—Structure, Importance and Classification. *Molecules*, *27*(3), p.787.

[17]   Audebert, P., Sadki, S., Miomandre, F., Clavier, G., Vernières, M.C., Saoud, M. and Hapiot, P., 2004. Synthesis of new substituted tetrazines: electrochemical and spectroscopic properties. *New journal of chemistry*, *28*(3), pp.387-392.

[18]   Pluczyk, S., Zassowski, P., Galmiche, L., Audebert, P. and Lapkowski, M., 2016. Tuning properties of 3, 6-disubstituted-s-tetrazine by changing the chemical nature of substituents. *Electrochimica Acta*, *212*, pp.856-863.

[19]   Pliego Jr, J.R., Alcântara, A.F.D.C., Veloso, D.P. and Almeida, W.B.D., 1999. Theoretical and experimental investigation of the formation of E-and Z-aldimines from the reaction of methylamine with acetaldehyde. *Journal of the Brazilian Chemical Society*, *10*, pp.381-388.

[20]   Silva, P.J., 2020. New insights into the mechanism of Schiff base synthesis from aromatic amines in the absence of acid catalyst or polar solvents. *PeerJ Organic Chemistry*, *2*, p.e4.

[21]   Palomero, O.E., Cunningham, A.L., Davies, B.W. and Jones, R.A., 2021. Antibacterial thiamine inspired silver (I) and gold (I) N-heterocyclic carbene compounds. *Inorganica chimica acta*, *517*, p.120152.

[22]   Mannisto, J.K., Pavlovic, L., Tiainen, T., Nieger, M., Sahari, A., Hopmann, K.H. and Repo, T., 2021. Mechanistic insights into carbamate formation from CO_2 and amines: the role of guanidine–CO_2 adducts. *Catalysis science & technology*, *11*(20), pp.6877-6886.

[23]   Tekamo, I.A., 2019. *Evaluation of schiff bases and its metal complexes with potential therapeutic applications* (Doctoral dissertation).

[24]   Lobana, T.S., Kaushal, M., Bala, R., Garcia-Santos, I. and Jasinski, J.P., 2022. Copper (I) derivatives of 4-benzoylpyridine thiosemicarbazone and 3-formylpyridine-N-methylthiosemicarbazone with triphenylphosphine as a co-ligand. *Journal of the Indian Chemical Society*, *99*(1), p.100298.

[25]   Baumeister, J.E., Mitchell, A.W., Kelley, S.P., Barnes, C.L. and Jurisson, S.S., 2019. Steric influence of salicylaldehyde-based Schiff base ligands on the formation of trans-[Re (PR 3) 2 (Schiff base)]+ complexes. *Dalton Transactions*, *48*(34), pp.12943-12955.

[26]   Aliev, A.E. and Motherwell, W.B., 2019. Some Recent Advances in the Design and Use of Molecular Balances for the Experimental Quantification of Intramolecular Noncovalent Interactions of π Systems. *Chemistry–A European Journal*, *25*(45), pp.10516-10530.

[27]   da Silveira, V.C., Benezra, H., Luz, J.S., Georg, R.C., Oliveira, C.C. and da Costa Ferreira, A.M., 2011. Binding of oxindole-Schiff base copper (II) complexes to DNA and its modulation by the ligand. *Journal of Inorganic Biochemistry*, *105*(12), pp.1692-1703.

[28]   Tsantis, S.T., Tzimopoulos, D.I., Holynska, M. and Perlepes, S.P., 2020. Oligonuclear actinoid complexes with Schiff bases as ligands—older achievements and recent progress. *International Journal of Molecular Sciences*, *21*(2), p.555.

[29]   Ciaccia, M. and Di Stefano, S., 2015. Mechanisms of imine exchange reactions in organic solvents. *Organic & Biomolecular Chemistry*, *13*(3), pp.646-654.

[30]   Mir, J.M., Majid, S.A. and Shalla, A.H., 2021. Enhancement of Schiff base biological efficacy by metal coordination and introduction of metallic compounds as anticovid candidates: a simple overview. *Reviews in Inorganic Chemistry*.

[31]   Hossain, M.S., Roy, P.K., Ali, R., Zakaria, C.M. and Kudrat-E-Zahan, M., 2017. Selected Pharmacological Applications of 1 st Row Transition Metal Complexes: A review. *Clinical Medicine Research*, *6*, pp.177-191.

[32]   Polyakov, V.A., Nelen, M.I., Nazarpack-Kandlousy, N., Ryabov, A.D. and Eliseev, A.V., 1999. Imine exchange in O-aryl and O-alkyl oximes as a base reaction for aqueous

'dynamic'combinatorial libraries. A kinetic and thermodynamic study. *Journal of physical organic chemistry*, *12*(5), pp.357-363.

[33]   Wang, P., Xue, T., Sheng, A., Cheng, L. and Zhang, J., 2022. Application of Chemoselective Ligation in Biosensing. *Critical Reviews in Analytical Chemistry*, *52*(1), pp.170-193.

[34]   Majors, R.E., 2013. Sample preparation fundamentals for chromatography. *Agilent Technologies, Mississauga, Canada*.

[35]   Vigato, P.A. and Tamburini, S., 2004. The challenge of cyclic and acyclic Schiff bases and related derivatives. *Coordination Chemistry Reviews*, *248*(17-20), pp.1717-2128.

[36]   Souza, P., Garcia-Vázquez, J.A. and Masaguer, J.R., 1985. Synthesis and characterization of copper (II) and nickel (II) complexes of the Schiff base derived from 2-(2-aminophenyl) benzimidazole and salicylaldehyde. *Transition Metal Chemistry*, *10*(11), pp.410-412.

[37]   Drozdzak, R., Allaert, B., Ledoux, N., Dragutan, I., Dragutan, V. and Verpoort, F., 2005. Ruthenium complexes bearing bidentate Schiff base ligands as efficient catalysts for organic and polymer syntheses. *Coordination Chemistry Reviews*, *249*(24), pp.3055-3074.

[38]   Sobola, A.O., Watkins, G.M. and Van Brecht, B., 2014. Synthesis, characterization and antimicrobial activity of copper (II) complexes of some ortho-substituted aniline Schiff bases; crystal structure of bis (2-methoxy-6-imino) methylphenol copper (II) complex. *South African Journal of Chemistry*, *67*, pp.45-51.

[39]   Xu, X., Xi, Z., Chen, W. and Wang, D., 2007. Synthesis and structural characterization of copper (II) complexes of pincer ligands derived from benzimidazole. *Journal of Coordination Chemistry*, *60*(21), pp.2297-2308.

[40]   Biswas, R., Giri, S., Saha, S.K. and Ghosh, A., 2012. One Ferromagnetic and Two Antiferromagnetic Dinuclear Nickel (II) Complexes Derived from a Tridentate N, N, O-Donor Schiff Base Ligand: A Density Functional Study of Magnetic Coupling. *European Journal of Inorganic Chemistry*, *2012*(17), pp.2916-2927.

[41]   Yadav, R.J., Vyas, K.M. and Jadeja, R.N., 2010. Synthesis and spectral characterization of Cu (II) complexes of some thio-Schiff bases of acyl pyrazolone analogues. *Journal of Coordination Chemistry*, *63*(10), pp.1820-1831.

[42]   Pahonțu, E., Ilieș, D.C., Shova, S., Paraschivescu, C., Badea, M., Gulea, A. and Roșu, T., 2015. Synthesis, characterization, crystal structure and antimicrobial activity of copper (II)

complexes with the Schiff base derived from 2-hydroxy-4-methoxybenzaldehyde. *Molecules*, *20*(4), pp.5771-5792.

[43] Kannappan, R., Tanase, S., Mutikainen, I., Turpeinen, U. and Reedijk, J., 2006. Low-spin iron (III) Schiff-base complexes with symmetric hexadentate ligands: Synthesis, crystal structure, spectroscopic and magnetic properties. *Polyhedron*, *25*(7), pp.1646-1654.

[44] Nowack, B. and VanBriesen, J.M., 2005. Chelating agents in the environment.

[45] Belcher, R., 1973. The application of chelate compounds in analytical chemistry. In *Analytical Chemistry–4* (pp. 13-27). Butterworth-Heinemann.

[46] Sayes, C.M., Liang, F., Hudson, J.L., Mendez, J., Guo, W., Beach, J.M., Moore, V.C., Doyle, C.D., West, J.L., Billups, W.E. and Ausman, K.D., 2006. Functionalization density dependence of single-walled carbon nanotubes cytotoxicity in vitro. *Toxicology letters*, *161*(2), pp.135-142.

[47] Zhang, W., Loebach, J.L., Wilson, S.R. and Jacobsen, E.N., 1990. Enantioselective epoxidation of unfunctionalized olefins catalyzed by salen manganese complexes. *Journal of the American Chemical Society*, *112*(7), pp.2801-2803.

[48] Raman, N., Kulandaisamy, A., Shunmugasundaram, A. and Jeyasubramanian, K., 2001. Synthesis, spectral, redox and antimicrobial activities of Schiff base complexes derived from 1-phenyl-2, 3-dimethyl-4-aminopyrazol-5-one and acetoacetanilide. *Transition Metal Chemistry*, *26*(1), pp.131-135.

[49] Raman, N., Kulandaisamy, A. and Jeyasubramanian, K., 2002. Synthesis, spectral, redox, and antimicrobial activity of Schiff base transition metal (II) complexes derived from 4-aminoantipyrine and benzil. *Synthesis and reactivity in inorganic and metal-organic chemistry*, *32*(9), pp.1583-1610.

[50] Sayes, C.M., Liang, F., Hudson, J.L., Mendez, J., Guo, W., Beach, J.M., Moore, V.C., Doyle, C.D., West, J.L., Billups, W.E. and Ausman, K.D., 2006. Functionalization density dependence of single-walled carbon nanotubes cytotoxicity in vitro. *Toxicology letters*, *161*(2), pp.135-142.

[51] Patel, R.N., Singh, N. and Gundla, V.L.N., 2006. Synthesis, structure and properties of ternary copper (II) complexes of ONO donor Schiff base, imidazole, 2, 2′-bipyridine and 1, 10-phenanthroline. *Polyhedron*, *25*(17), pp.3312-3318.

[52]   Xavier, A. and Srividhya, N., 2014. Synthesis and study of Schiff base ligands. *IOSR Journal of Applied Chemistry*, *7*(11), pp.06-15.

[53]   Ilieş, D.C., Pahonţu, E., Gulea, A., Badea, M., Paraschivescu, C., Shova, S. and Roşu, T., 2015. Synthesis, Characterization, Crystal Structure and Antimicrobial Activity of Copper (II) Complexes with the Schiff Base Derived from 2-Hydroxy-4-Methoxybenzaldehyde.

[54]   Telfer, S.G., Sato, T., Harada, T., Kuroda, R., Lefebvre, J. and Leznoff, D.B., 2004. Mono- and Dinuclear Complexes of Chiral Tri-and Tetradentate Schiff-Base Ligands Derived from 1, 1 '-Binaphthyl-2, 2 '-diamine. *Inorganic chemistry*, *43*(20), pp.6168-6176.

[55]   Keypour, H., Arzhangi, P., Rahpeyma, N., Rezaeivala, M., Elerman, Y., Büyükgüngör, O., Valencia, L. and Khavasi, H.R., 2010. Synthesis and characterization of Ni (II), Cu (II) and Zn (II) complexes with new macrocyclic Schiff base ligands containing piperazine moiety. *Journal of Molecular Structure*, *977*(1-3), pp.6-11.

[56]   Botero-Rodríguez, F., Pantoja-Ruiz, C. and Rosselli, D., 2022. Corruption and its relation to prevalence and death due to noncommunicable diseases and risk factors: a global perspective. *Revista Panamericana de Salud Pública*, *46*.

[57]   Siddiqi, K.S., Kureshy, R.I., Khan, N.H., Tabassum, S. and Zaidi, S., 1988. Schiff base derived from sulfane thoxazole and salicylaldehyde or thiophene-2-aldehydes. *Inorg Chem Acta*, *151*, pp.95-100.

[58]   Young, R.J. and Cooper, G.W., 1983. Dissociation of intermolecular linkages of the sperm head and tail by primary amines, aldehydes, sulphydryl reagents and detergents. *Reproduction*, *69*(1), pp.1-10.

[59]   Yang, G., Xia, X., Tu, H. and Zhao, C., 1995. Synthesis and antitumor activity of Schiff base coordination compounds. *Chinese Journal of Applied Chemistry*, (2), p.13.

[60]   Qin, W., Long, S., Panunzio, M. and Biondi, S., 2013. Schiff bases: A short survey on an evergreen chemistry tool. *Molecules*, *18*(10), pp.12264-12289.

[61]   Abbas, S.Y., Basyouni, W.M. and El-Bayouki, K.A., 2013. Synthesis of new tridentate 5-(arylazo) salicylaldimine ligands and their Cu (II) complexes. *Journal of Molecular Structure*, *1050*, pp.192-196.

[62]   Gamez, P., Arends, I.W., Reedijk, J. and Sheldon, R.A., 2003. Copper (II)-catalysed aerobic oxidation of primary alcohols to aldehydes. *Chemical communications*, (19), pp.2414-2415.

[63]   Hathaway, B.J., Wilkinson, G., Gillard, R.D. and McCleverty, J.A., 1987. Comprehensive coordination chemistry. *The synthesis, reactions, properties and applications of coordination compounds*, *5*, pp.533-774.

[64]   Campbell, K.N., Sommers, A.H. and Campbell, B.K., 1944. The Preparation of Unsymmetrical Secondary Aliphatic Amines1. *Journal of the American Chemical Society*, *66*(1), pp.82-84.

[65]   Hine, J. and Yeh, C.Y., 1967. Equilibrium in formation and conformational isomerization of imines derived from isobutyraldehyde and saturated aliphatic primary amines. *Journal of the American Chemical Society*, *89*(11), pp.2669-2676.

[66]   Munir, C., AHMAD, N. and YOUSAF, S., 2011. Synthesis, characterization and pharmacological properties of a cobalt (ii) complex of antibiotic ampicillin. *Journal of the Chemical Society of Pakistan*, *7*(4), p.301.

[67]   Mohammed, M.Q., 2011. Synthesis and characterization of new Schiff bases and evaluation as Corrosion inhibitors. *Journal of Basrah Researches*, *37*(4), pp.116-130.

[68]   Busa, A.V., 2016. Synthesis, characterization, and molecular docking of novel 4-Aminoquinolines and Salicylaldimine complexes: evaluation as antimalarial and antitumor agents.

[69]   . Busa, A.V., Lalancette, R., Nordlander, E. and Onani, M., 2018. New copper (II) salicylaldimine derivatives for mild oxidation of cyclohexane. *Journal of Chemical Sciences*, *130*(6), pp.1-10.

[70]   Troschke, E., Oschatz, M. and Ilic, I.K., 2021, December. Schiff-bases for sustainable battery and supercapacitor electrodes. In *Exploration* (Vol. 1, No. 3, p. 20210128).

[71]   Yimer, A.M., 2015. Review on preparation and description of some first series divalent transition metal complexes with novel Schiff's base ligands. *Review of Catalysts*, *2*(1), pp.14-25.

[72]   Lindoy, L.F., 1971. Metal-ion control in the synthesis of Schiff base complexes. *Quarterly Reviews, Chemical Society*, *25*(3), pp.379-391.

[73] Dalia, S.A., Afsan, F., Hossain, M.S., Khan, M.N., Zakaria, C., Zahan, M.K.E. and Ali, M., 2018. A short review on chemistry of schiff base metal complexes and their catalytic application. *International journal of chemical studies*, *6*(3), pp.2859-2866.

[74] Rubin, Y. and Diederich, F., 2000. From fullerenes to novel carbon allotropes: Exciting prospects for organic synthesis. *Stimulating Concepts in Chemistry*, pp.161-186.

[75] Gimeno, N. and Vilar, R., 2006. Anions as templates in coordination and supramolecular chemistry. *Coordination chemistry reviews*, *250*(23-24), pp.3161-3189.

[76] Vickers, M.S. and Beer, P.D., 2007. Anion templated assembly of mechanically interlocked structures. *Chemical Society Reviews*, *36*(2), pp.211-225.

[77] Dalia, S.A., Afsan, F., Hossain, M.S., Khan, M.N., Zakaria, C., Zahan, M.K.E. and Ali, M., 2018. A short review on chemistry of schiff base metal complexes and their catalytic application. *International journal of chemical studies*, *6*(3), pp.2859-2866.

[78] Schiff, H., 1869. Untersuchungen über salicinderivate. *Justus Liebigs Annalen der Chemie*, *150*(2), pp.193-200.

[79] Soliman, A.A. and Linert, W., 2007. Structural features of ONS-donor salicylidene Schiff base complexes. *Monatshefte für Chemie-Chemical Monthly*, *138*(3), pp.175-189.

[80] Kim, E., Chufán, E.E., Kamaraj, K. and Karlin, K.D., 2004. Synthetic models for heme−copper oxidases. *Chemical reviews*, *104*(2), pp.1077-1134.

[81] Duatti, A., Marchi, A., Rossi, R., Magon, L., Deutsch, E., Bertolasi, V. and Bellucci, F., 1988. Reactivity of 2-(2-hydroxyphenyl) benzothiazoline with the oxotetrahalometalate (V) complexes [MOX4]-(M= technetium, rhenium; X= Cl, Br). Synthesis and characterization of new oxo-M (V) complexes containing 2-(2-hydroxyphenyl) benzothiazole. Crystal structure of tetraphenylarsonium oxotrichloro [2-(2-hydroxyphenyl) benzothiazolato] technetate (V). *Inorganic Chemistry*, *27*(23), pp.4208-4213.

[82] Das, P. and Linert, W., 2016. Schiff base-derived homogeneous and heterogeneous palladium catalysts for the Suzuki–Miyaura reaction. *Coordination Chemistry Reviews*, *311*, pp.1-23.

[83] Atwood, D.A. and Harvey, M.J., 2001. Group 13 compounds incorporating salen ligands. *Chemical reviews*, *101*(1), pp.37-52.

[84] Dick, A.R., Hull, K.L. and Sanford, M.S., 2004. A highly selective catalytic method for the oxidative functionalization of C− H bonds. *Journal of the American Chemical Society*, *126*(8), pp.2300-2301.

[85] Agnihotri, S., Rood, M.J. and Rostam-Abadi, M., 2005. Adsorption equilibrium of organic vapors on single-walled carbon nanotubes. *Carbon*, *43*(11), pp.2379-2388.

[86] Kusumaningrum, V.A., Hanapi, A., Ningsih, R., Ani, S. and Nafiah, A.N., 2021, April. Synthesis, Characterization, and Antioxidant Activity of 2-methoxy-4-((4-methoxy phenyl imino)-methyl) phenol compounds. In *International Conference on Engineering, Technology and Social Science (ICONETOS 2020)* (pp. 292-296). Atlantis Press.

[87] Zolezzi, S., Spodine, E. and Decinti, A., 2002. Electrochemical studies of copper (II) complexes with Schiff-base ligands. *Polyhedron*, *21*(1), pp.55-59.

[88] Lakshmi, S.S., Saranya, J. And Priyadharsini, R.B., 2021. Synthesis, Characterization and biological activities of Schiff base metal (Ii) complexes Derived From L-Methionine And Cuminaldehyde. *Journal Of Advanced Scientific Research*, *12*(01 Suppl 2), Pp.71-77.

[89] Arulmurugan, S., Kavitha, H.P. and Venkatraman, B.R., 2010. Biological activities of Schiff base and its complexes: a review. *Rasayan J Chem*, *3*(3), pp.385-410.

[90] Gupta, C.K. and Sutar, A.K., 2008. Catalytic activities of Schiff base transition metal complexes. *Coordination Chemistry Reviews*, *252*(12-14), pp.1420-1450.

[91] Gupta, K.C., Sutar, A.K. and Lin, C.C., 2009. Polymer-supported Schiff base complexes in oxidation reactions. *Coordination Chemistry Reviews*, *253*(13-14), pp.1926-1946.

[92] Auvert, G., 2017. Difference in Number of Electrons in Inner Shells of Charged or Uncharged Elements in Organic and Inorganic Chemistry: Compatibility with the Even-Odd Rule. *Open Journal of Physical Chemistry*, *7*(02), p.72.

[93] Omoregie, H.O., Eseola, A.O. and Akong, R.A., 2022. Mixed ligand complexes of copper (II) with benzoyltrifluoroacetone, 1, 10-phenanthroline and 2, 2′-bipyridine: Structure, spectroscopic and antimicrobial properties. *Journal of Molecular Structure*, *1250*, p.131826.

[94] Bayeh, Y., Abebe, A., Thomas, M. and Linert, W., 2019. Synthesis, characterization and antimicrobial activities of new mixed ligand complexes of copper (II) with 1, 10-phenanthroline and thymine. *Journal of Transition Metal Complexes*, *2*, pp.1-6.

[95] Gamez, P., Aubel, P.G., Driessen, W.L. and Reedijk, J., 2001. Homogeneous bio-inspired copper-catalyzed oxidation reactions. *Chemical Society Reviews*, *30*(6), pp.376-385.

[96] Poli, R., 1996. Open-shell organometallics as a bridge between Werner-type and low-valent organometallic complexes. The effect of the spin state on the stability, reactivity, and structure. *Chemical reviews*, *96*(6), pp.2135-2204.

[97] Hoffmann, R., Alvarez, S., Mealli, C., Falceto, A., Cahill III, T.J., Zeng, T. and Manca, G., 2016. From widely accepted concepts in coordination chemistry to inverted ligand fields. *Chemical Reviews*, *116*(14), pp.8173-8192.

[98] Mandal, S., Layek, M., Saha, R., Rizzoli, C. and Bandyopadhyay, D., 2021. Synthesis, crystal structure and antibacterial activity of four mononuclear Schiff base complexes of copper (II) and nickel (II). *Transition Metal Chemistry*, *46*(1), pp.9-16.

[99] Franks, M., Gadzhieva, A., Ghandhi, L., Murrell, D., Blake, A.J., Davies, E.S., Lewis, W., Moro, F., McMaster, J. and Schröder, M., 2013. Five coordinate M (II)-diphenolate [M= Zn (II), Ni (II), and Cu (II)] Schiff base complexes exhibiting metal-and ligand-based redox chemistry. *Inorganic Chemistry*, *52*(2), pp.660-670.

[100] Franks, M., Gadzhieva, A., Ghandhi, L., Murrell, D., Blake, A.J., Davies, E.S., Lewis, W., Moro, F., McMaster, J. and Schröder, M., 2013. Five coordinate M (II)-diphenolate [M= Zn (II), Ni (II), and Cu (II)] Schiff base complexes exhibiting metal-and ligand-based redox chemistry. *Inorganic Chemistry*, *52*(2), pp.660-670.

[101] More, M.S., Joshi, P.G., Mishra, Y.K. and Khanna, P.K., 2019. Metal complexes driven from Schiff bases and semicarbazones for biomedical and allied applications: a review. *Materials Today Chemistry*, *14*, p.100195.

[102] Borase, J.N., Mahale, R.G., Rajput, S.S. and Shirsath, D.S., 2021. Design, synthesis and biological evaluation of heterocyclic methyl substituted pyridine Schiff base transition metal complexes. *SN Applied Sciences*, *3*(2), pp.1-13.

[103] Srinivas, M., Vijayakumar, G.R., Mahadevan, K.M., Nagabhushana, H. and Naik, H.B., 2017. Synthesis, photoluminescence and forensic applications of blue light emitting azomethine-zinc (II) complexes of bis (salicylidene) cyclohexyl-1, 2-diamino based organic ligands. *Journal of Science: Advanced Materials and Devices*, *2*(2), pp.156-164.

[104] Zhang, J., Xu, L. and Wong, W.Y., 2018. Energy materials based on metal Schiff base complexes. *Coordination Chemistry Reviews*, *355*, pp.180-198.

[105] Liu, H.J., Yi, R., Chen, D.M., Huang, C. and Zhu, B.X., 2020. Self-Assembly by Tridentate or Bidentate Ligand: Synthesis and Vapor Adsorption Properties of Cu (II), Zn (II), Hg (II) and Cd (II) Complexes Derived from a Bis (pyridylhydrazone) Compound. *Molecules*, *26*(1), p.109.

[106] Devi, N., Sarma, K., Rahaman, R. and Barman, P., 2018. Synthesis of a new series of Ni (II), Cu (II), Co (II) and Pd (II) complexes with an ONS donor Schiff base: crystal structure, DFT study and catalytic investigation of palladium and nickel complexes towards deacylative sulfenylation of active methylenes and regioselective 3-sulfenylation of indoles via thiouronium salt formation. *Dalton Transactions*, *47*(13), pp.4583-4595.

[107] Yan, N., Ma, C., Cao, Y., Liu, X., Cao, L., Guo, P., Tian, P. and Liu, Z., 2020. Rational Design of a Novel Catalyst Cu-SAPO-42 for NH3-SCR Reaction. *Small*, *16*(33), p.2000902.

[108] Peng, D.L., 2018. Crystal Structure and Catalytic Property of an Oxidomolybdenum (VI) Complex Derived from N′-(2-Hydroxy-3, 5-Di-Tert-Butylbenzylidene)-4-Methylbenzohydrazide. *Journal of Structural Chemistry*, *59*(3), pp.589-594.

[109] Gao, H., 2013. *Synthesis, characterisation and transition metal ion complexation studies of "pocket-like" imine and amide derivatives*. National University of Ireland, Maynooth (Ireland).

[110] Porcheddu, A., Colacino, E., Cravotto, G., Delogu, F. and De Luca, L., 2017. Mechanically induced oxidation of alcohols to aldehydes and ketones in ambient air: Revisiting TEMPO-assisted oxidations. *Beilstein journal of organic chemistry*, *13*(1), pp.2049-2055.

[111]   Geng, Y., Huang, L., Wu, S. and Wang, F., 2010. Kumada chain-growth polycondensation as a universal method for synthesis of well-defined conjugated polymers. *Science China Chemistry*, *53*(8), pp.1620-1633.

[112]   Vinod, C.P., Wilson, K. and Lee, A.F., 2011. Recent advances in the heterogeneously catalysed aerobic selective oxidation of alcohols. *Journal of Chemical Technology & Biotechnology*, *86*(2), pp.161-171.

[113]   Ye, W. and Li, Y., 2022. Performance Characteristics of Digital Media Art Design Relying on Computer Technology. *Mobile Information Systems*, *2022*.

[114]   Saeednia, S., Ardakani, M.H., Parizi, Z.P. and Hafshejani, M.T., 2016. Synthesis and characterization of a magnetically recoverable molybdenum (VI) nanocatalyst for eco-friendly oxidation of alcohols. *Transition Metal Chemistry*, *41*(7), pp.767-774.

[115]   Dwulet, G.E. and Gin, D.L., 2018. Ordered nanoporous lyotropic liquid crystal polymer resin for heterogeneous catalytic aerobic oxidation of alcohols. *Chemical Communications*, *54*(85), pp.12053-12056.

[116]   Costas, M., Chen, K. and Que Jr, L., 2000. Biomimetic nonheme iron catalysts for alkane hydroxylation. *Coordination Chemistry Reviews*, *200*, pp.517-544.

[117]   Mahapatra, S., Halfen, J.A., Wilkinson, E.C., Que Jr, L. and Tolman, W.B., 1994. Modeling copper-dioxygen reactivity in proteins: aliphatic CH bond activation by a new dicopper (II)-peroxo complex. *Journal of the American Chemical Society*, *116*(21), pp.9785-9786.

[118]   Chen, T., Xiao, W., Wang, Z., Xie, T., Yi, C. and Xu, Z., 2022. Design and engineering of heterogeneous nitroxide-mediated catalytic systems for selective oxidation: Efficiency and sustainability. *Materials Today Chemistry*, *24*, p.100872.

[119]   Markó, I.E., Giles, P.R., Tsukazaki, M., Brown, S.M. and Urch, C.J., 1996. Copper-catalyzed oxidation of alcohols to aldehydes and ketones: an efficient, aerobic alternative. *Science*, *274*(5295), pp.2044-2046.

[120]   Wieland, H. and Offenbächer, M., 1914. Diphenylstickstoffoxyd, ein neues organisches Radikal mit vierwertigem Stickstoff. *Berichte der deutschen chemischen Gesellschaft*, *47*(2), pp.2111-2115.

[121] Ilieş, D.C., Pahonţu, E., Gulea, A., Badea, M., Paraschivescu, C., Shova, S. and Roşu, T., 2015. Synthesis, Characterization, Crystal Structure and Antimicrobial Activity of Copper (II) Complexes with the Schiff Base Derived from 2-Hydroxy-4-Methoxybenzaldehyde.

[122] Arends, I.W., Li, Y.X., Ausan, R. and Sheldon, R.A., 2006. Comparison of TEMPO and its derivatives as mediators in laccase catalysed oxidation of alcohols. *Tetrahedron*, *62*(28), pp.6659-6665.

[123] d'Acunzo, F., Baiocco, P., Fabbrini, M., Galli, C. and Gentili, P., 2002. A mechanistic survey of the oxidation of alcohols and ethers with the enzyme laccase and its mediation by TEMPO. *European Journal of Organic Chemistry*, *2002*(24), pp.4195-4201.

UNIVERSITY *of the*
WESTERN CAPE

31

Chapter 2

Methodology and instrumentations

This chapter is mainly focusing on the methodology used for the synthesis and the instrumentation used for the characterization of the Schiff base ligands and their Cu (II) complexes. The methodology of synthesizing the ligands and the complexes was found in the literature by Busa [1]. This chapter entails the chemicals that were used in the study. Furthermore, the details of all the characterization techniques are also explained in detail.

2.1 Experimental Section

2.1.1 General remarks

All experimental manipulations were carefully carried out under inert nitrogen atmosphere using standard dual vacuum/nitrogen lines and Schlenk techniques. All commercial chemicals were purchased from the Sigma-Aldrich and were used as received. The solvents were dried and purified by heating at reflux under nitrogen in the presence of a suitable drying agent; ethanol was dried over magnesium. Ethanol was dried over 3 Å molecular sieves. Reaction progress and product mixtures were monitored by using the IR spectroscopy. The anhydrous magnesium sulphate ($MgSO_4$) was used for drying of the product. The NMR spectra were recorded on Bruker Avance IIIHD 400 MHz (University of the Western Cape, South Africa) spectrometers using the solvent resonance as an internal standard for the ^1H NMR and ^{13}C NMR shifts. Infrared spectra were recorded on a FT-IR spectrometer (University of the Western Cape Chemistry Department). The GC-MS spectra were recorded using an Agilent technology gas chromatograph. Samples of 10 µl were injected into the GC analyser Helium gas was used as the carrier gas.The cyclic voltammetry (CV) experiments were performed using Palmsens PTrace (Sensor lab) electrochemical work station using a three electrode cell. Elemental analysis was conducted at the central analytical facility (CAF). Laboratory (Stellenbosch University).

2.1.2 Chemicals used for all the synthesis

Table 2.1: List of all chemicals used for the synthesis of ligands and complexes

Chemical Name	Chemical Formula	M/W	Purity	Company
Furfurylamine	C_5H_7NO	97.12	99.9%	Sigma
3,5-Di-tert-butyl-2hydroxybenzaldehyde	$HOC_6H_2[C(CH_3)_3]_2CHO$	234.33	99%	Sigma
2-thiopheneethylamine	C_6H_9NS	127.21	96%	Sigma
5-chlorosalicylaldehyde	$ClC_6H_3(OH)CHO$	156.57	98%	Sigma
3-bromo-5chlorosalicylaldehyde	$BrC_6H_2(Cl)-2-(OH)CHO$	235.46	98%	Sigma
2-Hydroxy-5nitrobenzaldehyde	$HOC_6H_3(NO_2)CHO$	167.12	98%	Sigma
2-hydroxy-5methylbenzaldehyde	$HOC_6H_3(CH_3)CHO$	136.15	98%	Sigma
Ethanol	CH_3CH_2OH	46.07	99.9%	DLD
Trimethylamine	$(CH_3)_3N$	59.11	$\geq$99%	Sigma
Copper(II) acetate	$Cu(CO_2CH_3)_2$	181.65	99.99%	Sigma
Dichloromethane	CH_2Cl_2	84.97	$\geq$99.8%	Sigma
2-amino-1-hexadecanol hydrochloride	$C_{16}H_{36}ClNO$	341.92	$\geq$99%	Fluka
Dimethylformamide	C_3H_7NO	73.09	$\geq$99.5%	DLD
Acetonitrile	CH_3CN	41.05	$\geq$99.9%	Sigma
Nitric acid	HNO_3	63.01	$\geq$90%	Sigma
Benzyl alcohol	$C_6H_5CH_2OH$	108.14	99.8%	Sigma
Decane	$CH_3(CH_2)_8CH_3$	142.28	$\geq$99%	Sigma
Dimethyl sulfoxide	C_2H_6OS	78.13	99.5%	KIMIX
TEMPO	2,2,6,6-Tetramethylpiperidine 1oxyl	156.25	98%	Sigma
Benzyldehyde	C_6H_5CHO	106.12	$\geq$99%	Sigma

33

2.1.3 Synthesis of salicylaldimine ligands (HL^1-HL^5)

2.1.3.1 HL^1 : ($^{(}$E)-4-(tert-butyl)-2-(((2-(thiophen-2-yl) ethyl) imino) methyl) phenol

A solution of 2-hydroxy-5-methylbenzaldehyde (1000 mg-, 0.78 mmol) in 10 mL dry ethanol was added to 50 mL round bottomed flask equipped with a a stirrer bar and a condenser. A solution of 2-thiopheneethylamine (0.092 mL, 0.78 mmol) in 10 mL dry ethanol was added to the solution in the round-bottomed flask. Upon addition of the 2-thiopheneethylamine solution, a color change was observed from a clear solution to a bright yellow solution, and there was a formation of a precipitate. The solution was stirred at room temperature under nitrogen gas for 12 hours. The solvent was removed from the product with a rotary vapour followed by the addition of 20 mL of dichloromethane (DCM) to the resulting ligand. The ligand was washed 3 times with 15 mL of deionized water and the product was recovered through separatory funnel. Magnesium sulphate was added to the recovered ligand to remove any water present in the product followed by gravity filtration. Subsequently, the remaining solvent was removed from the filtrate with rotary vapour resulting in a yellow, oily product, which crystallized when left overnight at room temperature. **HL^1** with product mass of 518.4 mg. (91.4%). M.P (109°C). IR data (KBr, v/cm^{-1}): 3688(v_{CO-H}) 1620 ($v_{C=N}$),1432 ($v_{C=C}$), 1361 (v_{C-S-C}), EA: N 4.87, C

70.63,H 7.36, S 11.15 Found N 4.59, C 71.04, H 8.568, S 11.168. ^{1}H NMR data (CDCl$_3$, ppm): δ 1.29 (s, 9H, C(CH$_3$)$_3$), 3.38 (s, 2H, =N-CH$_2$), 6.84 (d, 1H), 7.35 (dd, 1H), 6.80 (dd, 1H), 7.19 (d, 1H), 7.15(d, 1H), 7.35 (d, 1H), 8.30 (s, 1H, H-C=N), 13.07 (s, 1H, C-OH). ^{13}C NMR (CDCl$_3$, ppm): δ 165.90 (HC=N), 165.87 (C-OH), 141.67 (4-C), 141.27 (2-C), 123.11 (11-C), 129.61 (10 C), 127.73 (8-C), 117.9 (7-C), 116.51 (9-C), 110.4 (3-C), 107.9 (1-C), 55.1 (5-C), 33.96 (t-Bu-C).

2.1.3.2 HL^2 : (E)-2, 4-di-tert-butyl-6-(((furan-2-ylmethyl) imino) methyl) phenol

A solution of 3.5-di-tert-butylsalicyladehyde (0.23 g, 0.981 mmol) in 10 mL dry ethanol was added to 50 mL round bottomed flask equipped with a condenser. A solution of furfurylamine (0.1148 mL, 0981 mmol) in 10 mL dry ethanol was added to the solution in the round bottomed flask. Upon addition of the furfurylamine solution, a colour change was observed from a clear solution to a bright yellow solution. The solution was stirred at room temperature under nitrogen gas for 12 hours. The solvent was removed from the product with a rotary vapour followed by the addition of 20 mL of dichloromethane (DCM) to the resulting ligand. The ligand was washed 3 times with 15 mL of deionized water and the product was recovered through separatory funnel. Magnesium sulphate was added to the recovered ligand to remove any water present in the product followed

by gravity filtration. Subsequently, the remaining solvent was removed from the filtrate with rotary vapour resulting in a yellow, oily product, which crystallized when left overnight at room temperature. **HL^2** with product mass of 1087 mg (90.58%). M.P (106°C). IR data

(KBr,/cm^{-1}): 1620 ($\upsilon_{C=N}$), 1460 ($\upsilon_{C=C}$), 1215 (υ_{C-O-C}). EA Calc N 4.47, C 76.3, H 9.984, S 0.1 Found N 4.12, C 76.64, H 8.68, and S 0.389. ^{1}H NMR data (CDCl$_3$, ppm): δ 1.23 (s, 9H, C(CH$_3$)$_3$), 4.68 (s, 2H, =N-CH$_2$), 6.24 (d, 1H), 6.34 (dd, 1H), 6.80 (dd, 1H), 7.07(d, 1H), 7.33 (d, 1H), 7.38 (d, 1H), 8.40 (s, 1H, H-C=N), 13.60 (s, 1H, C-OH). ^{13}C NMR (CDCl$_3$, ppm): δ 166.49 (HC=N), 156.92 (C-OH), 150.50 (4-C),141.36 (2-C), 125.12 (11-C), 126.16 (10-C), 127.73 (8-C), 116.82 (7-C), 116.51 (9-C), 109.78 (3-C), 106.74 (1-C), 54.18 (5-C), 33.99 (tBu-C).

2.1.3.3 HL^3: (E)-4-chloro-2-(((furan-2-ylmethyl) imino) methyl) phenol

A solution of 5-chlorosalicylaldehyde (0.3131 g, 2 mmol) in 10 mL dry ethanol was added to 50 mL round bottomed flask equipped with a condenser. A solution of furfurylamine (0.1176 mL,2 mmol) in 10 mL dry ethanol was added to the solution in the round bottomed flask. Upon addition of the furfurylamine solution, a colour change was observed from a clear solution to a bright yellow solution. The solution was stirred at room temperature under nitrogen gas for 12 hours. The solvent was removed from the product with a rotary vapour followed by the addition of 20 mL of dichloromethane (DCM) to the resulting ligand. The ligand was washed 3 times with 15 mL of deionized water and the product was recovered through separatory funnel. Magnesium sulphate was added to the recovered ligand to remove any water present in the product followed by gravity filtration. Subsequently, the remaining solvent was removed from the filtrate with rotary vapour resulting in a brownish-yellow powder. The brownish-yellow, powder ligand **HL^3** with product mass of 485.1mg (97.02%). M.P (121°C). IR data (KBr,v/cm^{-1}): 1613($\upsilon_{C=N}$), 1480 ($\upsilon_{C=C}$), 1278 (υ_{C-O-C}). EA Calc N 5.27, C 63.27, H 6.07, S 0.1 Found: N 6.4, C 64.9, and H 4.4 S 0.1. ^{1}H NMR: δ 4.78 (2H, s), 6.28 (2H, 6.21 (dd, 1.1 Hz), 6.32 (dd, J = 25 Hz)), 6.90 (1H, dd, J = 4.22), 7.25 (2H, 7.32 (dd, J = 5.32), 7.32 (dd, J = 8.02)),). ^{13}C NMR (CDCl$_3$, ppm) δ 165.16 (HC=N), 159.58 (C-OH), 150.62(4-C), 142.69(2C), 123.42 (11-C), 132.31(10-C), 130.67 (8-C), 119.52(7-C), 118.63 (9-C), 110.50 (3-C),

108.26 (1-C), 54.99 (5-C).

2.1.3.4 HL^4: (E)-2-bromo-4-chloro-6-(((2-(thiophen-2-yl) ethyl) imino) methyl) phenol

A solution of 3-bromo-5-chlorosalicylaldihyde (0.23 g, 0.981 mmol) in 10 mL dry ethanol was added to 50 mL round bottomed flask equipped with a condenser. A solution of 2-

thiopheneethylamine (0.1148 mL, 0981 mmol) in 10 mL dry ethanol was added to the solution in the round bottomed flask. Upon addition of the 2-thiopheneethylamine solution, a colour change was observed from a clear solution to a bright orange-yellow solution, and there was a formation of precipitate. During the stirring the precipitate the turned orange-yellow. The solution was stirred at room temperature under nitrogen gas for 12 hours The solvent was removed from the product with a rotary vapour followed by the addition of 20 mL of dichloromethane (DCM) to the resulting ligand. The ligand was washed 3 times with 15 mL of deionized water and the product was recovered through separatory funnel. Magnesium sulphate was added to the recovered ligand to remove any water present in the product followed by gravity filtration. Subsequently, the remaining solvent was removed from the filtrate with rotary vapour resulting in a orange-yellow powder. The orange-yellow, powder ligand **HL^3** with product mass of 162.3mg (81.15%). M.P (114°C). IR (KBr,/cm^{-1}): 1627($v_{C=N}$), 1439 ($v_{C=C}$), 1355(v_{C-S-C}). EA Calc N 4.06, C 45.30, H 3.22, S 9.30 Found: N 4.2, C 46.1, H 2.6, and S 10.6 ^{1}H NMR: δ 3.24 (2H, t, J = 6.66 Hz), 3.90(2H, t, J = 6.2 Hz), 7.57 (3H,1.22 Hz), 8.06 (dd, J = 5.0, Hz)), 7.54 (1H, d, J = 1.4 Hz), 7.92 (1H, d, J = 1.4 Hz), 8.27 (1H, s). ^{13}C NMR (CDCl$_3$, ppm) 163.95 (HC=N), 157.38 (C-OH), 140.68(4-C), 135.14(2-C), 125.72 (11-C), 129.77(10-C), 139.05 (8-C), 124.33(7-C), 127.05 (9-C), 119.08 (3 C), 112.06 (1-C), 60.01 (5-C).

2.1.3.5 HL^5 : (E)-4-nitro-2-(((2-(thiophen-2-yl) ethyl) imino) methyl) phenol

A solution of 2-hydroxy-5-nitrobenzaldehyde (0.3342 g, 2 mmol) in 10 mL dry ethanol was added to 50 mL round bottomed flask equipped with a condenser. A solution of furfurylamine (0.1767 mL, 2 mmol) in 10 mL dry ethanol was added to the solution in the round bottomed flask. Upon addition of the furfurylamine solution, a colour change was observed from a clear solution to a bright orange-yellow solution. During the stirring the solution then turned bright orange. The solution was stirred at room temperature under nitrogen gas for 12 hours. The solvent was removed from the product with a rotary vapour followed by the addition of 20 mL of dichloromethane (DCM) to the resulting ligand. The ligand was washed 3 times with 15 mL of deionized water and the product was recovered through separatory funnel. Magnesium sulphate was added to the recovered ligand to remove any water present in the product followed by gravity filtration. Subsequently, the remaining solvent was removed from the filtrate with rotary vapour resulting in a oreng-yellow product, The orange-yellow, powder ligand **HL^5** with product mass of 216.5 mg (72.17%). M.P (119°C). IR data (KBr,/cm^{-1}): 1662($v_{C=N}$), 1432 ($v_{C=C}$), 1306 (v_{C-S-C}). EA Calc N 10.14, C 56.51, H 4.38, S 11.60 Found: N 9.56, C 55.94, H 4.597, and S 11.964. ^{1}H NMR: δ 3.27 (2H, t, J = 6.6 Hz), 3.93(2H, t, J = 6.2 Hz), 7.57 (3H,1.22 Hz), 8.06 (dd, J = 5.0, Hz)), 7.36 (1H,

d, $J = 1.29$ Hz), 7.23 (1H, d, $J = 1.29$ Hz), 8.18 (1H, s). ^{13}C NMR (CDCl$_3$, ppm) 168.64 (HC=N), 164.50 (COH), 140.43(4-C), 139.05(2-C), 128.09 (11-C), 129.77(10-C), 128.09 (8-C), 124.31(7-C), 125.82 (9-C), 118.82 (3-C), 112.06 (1-C), 59.67 (5-C).

2.1.4 Synthesis of salicylaldiminato-copper complexes (C^1-C^5)

2.1.4.1 Complex 1: (E)-4-(tert-butyl)-2-(((2-(thiophen-2-yl) ethyl) imino) methyl) phenol and Copper (II) Acetate

Ligand **HL^1** (300 mg, 1.09035 mmol) was stirred with Et$_3$N (151.97 μL, 1090 μmol) in EtOH (10 mL) for 1hr to deprotonate HL^1 followed by addition of Cu (CH$_3$COO)$_2$ (198 mg, 1.09035 mmol) in EtOH (10 mL). The reaction mixture was stirred overnight. Thereafter, the solvent was removed under reduced pressure resulting in a yellow residue, which was the product. There after complexation the solvent volume was then reduced under vacuum to ~3 mL and the complex was precipitated with cold diethyether. The precipitate was filtered and washed with copious (3 times with 30 ml) amount of cold diethyl ether and isolated, the product was left to dry overnight inside fume cabinet. The color of the product was pale yellow with mass of 92.7 mg (32.4%). M.P (205°C). IR data (KBr,/cm^{-1}): 1613 ($v_{C=N}$), 1453 ($v_{C=C}$), 1375 (v_{C-S-C}). EA Calc N 4.40, C 64.17, H 6.34, S 10.0 Found: N 3.61, C 63.65,

H 6.208, and S 10.115.
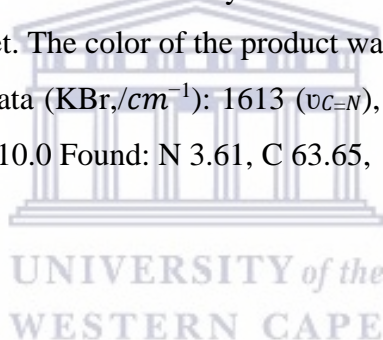
2.1.4.2 Complex 2: (E)-2, 4-di-tert-butyl-6-(((furan-2-ylmethyl) imino) methyl) phenol and copper (II) Acetate

Ligand **HL^2** (400 mg, 1.27616 mmol) was stirred with Et$_3$N (177.69 μL, 1276 μmol) in EtOH (10 mL) for 1hr to deprotonate HL^2 followed by addition of Cu (CH$_3$COO)$_2$ (231.79 mg, 1.27616 mmol) in EtOH (10 mL). The reaction was stirred overnight. Thereafter, the solvent was removed under reduced pressure resulting in a dark brown residue, which was the product.

The complex was allowed to dry overnight then scraped off to obtain salicylaldiminato-copper (II) complex as a black solid with mass product of 348 mg (87%). M.P (198°C). IR data (KBr,/cm^{-1}): 1613($v_{C=N}$), 1425 ($v_{C=C}$), 1271 (v_{C-O-C}). EA Calc 2.07, C 63.79, H 7.61, S 0.1. Found: N 2.72, C 62.78, H 8.626, S 0.24.

### 2.1.4.3 Complex 3: (E)-4-chloro-2-(((furan-2-ylmethyl) imino) methyl) phenol and Copper (II) Acetate

Ligand **HL^3** (50 mg, 0.21216 mmol) was stirred with Et$_3$N (29.6 μL, 212 μmol) in EtOH (10 mL) for 1hr to deprotonate HL^3 followed by addition of Cu (CH$_3$COO)$_2$ (38.6 mg, 0.21216 mmol) in EtOH (10 mL). The reaction was stirred overnight. Thereafter, the solvent was removed under reduced pressure resulting in a yellow residue, which was the product. There after complexation the solvent volume was then reduced under vacuum to ~3 mL and the complex was precipitated with cold diethyether. The precipitate was filtered and washed with copious (3 times with 30 ml) amount of cold diethyl ether and isolated, the product was left to dry overnight inside fume cabinet. The color of the product was pale green with mass of 26.4 mg (52.8%). M.P (247°C). IR data (KBr,/cm^{-1}):1627 ($\upsilon_{C=N}$), 1467 ($\upsilon_{C=C}$),1306 (υ_{C-O-C}). EA Calc N 3.26, C 45.10, H 3.40, S 0.1 Found 3.3, C 44.82, H 3.023, and S 0.82.

2.1.4.4 Complex 4: (E)-2-bromo-4-chloro-6-(((2-(thiophen-2-yl) ethyl) imino) methyl) phenol and Copper (II) Acetate

Ligand **HL^4** (50 mg, 0.14507 mmol) was stirred with Et$_3$N (20.22 μL, 145.07 μmol) in EtOH (10 mL) for 1hr to deprotonate HL^4 followed by addition of Cu (CH$_3$COO)$_2$ (26.35 mg, 0.14507 mmol) in EtOH (10 mL). The reaction was stirred overnight. Thereafter, the solvent was removed under reduced pressure resulting in a yellow residue, which was the product. There after complexation the solvent volume was then reduced under vacuum to ~3 mL and the complex was precipitated with cold diethyether. The precipitate was filtered and washed with copious (3 times with 30 ml) amount of cold diethyl ether and isolated, the product was left to dry overnight inside fume cabinet. The color of the product was pale green with mass of 23.8 mg (47.6%). M.P (200°C). IR data (KBr,/cm^{-1}): 1606 ($\upsilon_{C=N}$), 1453($\upsilon_{C=C}$), 1327 (υ_{C-S-C}). EA Calc N 3.73, C 41.59, H 2.68, S 8.54 Found: N 3.4, C 40.3, H 1.7, and S 7.3**.**

2.1.4.5 Complex 5: (E)-4-nitro-2-(((2-(thiophen-2-yl) ethyl) imino) methyl) phenol and Copper (II) Acetate

Ligand **HL^5** (40 mg, 0.16256 mmol) was stirred with Et$_3$N (29.53 μL, 162.56 μmol) in EtOH (10 mL) for 1hr to deprotonate HL^5 followed by addition of Cu (CH$_3$COO)$_2$ (22.66 mg, 0.16256 mmol) in EtOH (10 mL). The reaction was stirred overnight. Thereafter, the solvent was removed under reduced pressure resulting in a yellow residue, which was the product. There

after complexation the solvent volume was then reduced under vacuum to ~3 mL and the complex was precipitated with cold diethyether. The precipitate was filtered and washed with copious (3 times with 30 ml) amount of cold diethyl ether and isolated, the product was left to dry overnight <u>inside</u> fume cabinet. The color of the product was pale green with mass of 37 mg (92.5%) and was kept in sealed vile and covered with foil to avoid any decomposition .M.P (246°C). IR data (KBr,/cm^{-1}): 1627($v_{C=N}$), 1453 ($v_{C=C}$), 1327 (v_{C-S-C}). EA Calc N 6.12, C 43.84, H 3.61, S 8.44 Found: N 6.32, C 42.46, H 3.694, and S 7.88

Method for catalysis

The solution of complex 1 (2mg, 3.14 µL) was dissolved in 5mL dry MeCN, H_2O_2 (81.26 µL, 2.70mmol) and Tempo (421.88mg, 2.7mmol) was added and stir for a short time. Benzyl alcohol (172.64 µL, 0.17mmol) was added subsequently and the reaction was started. The reaction was then allowed to stir for 36 h at room temperature. 100µL were aliquoted from the reaction mixture at specific time intervals during the reaction. Decane (9µL, internal standard) 90 µL of ether was added from the aliquots to extract the substrate and products. An appropriate volume was sampled from the mixture and injected into a GC. Retention times from the catalytic mixture was compared with commercial standards.
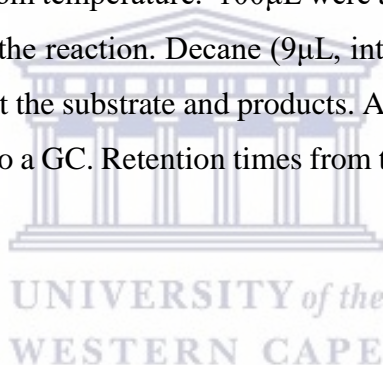
2.2 Instruments

2.2.1 Fourier transform infrared (FTIR) spectroscopy.

The FTIR or Fourier transform infrared, is the most preferable method of measuring the vibration bands of a molecule. In the FTIR spectroscopy, the infrared radiation is passed through a sample. Some of the radiations is absorbed by the sample and some of it is passed through (transmitted). The resulting spectrum represents the molecular absorption and transmission, creating a molecular fingerprint of the sample. As two fingerprints never match, similarly no two unique molecular structures produce the same IR spectrum. This makes IR spectroscopy useful for several types of analysis. IR spectroscopy has been a workhorse technique for materials analysis in the laboratory for over 70 years. An IR spectrum represents the fingerprint of a sample, with absorption peaks that correspond to the frequencies of vibrations between the bonds of the atoms making up the material [2]. Infrared Spectroscopy is the evaluation of the interaction of infrared light with matter. Analysis of infrared spectra can

reveal what molecules are present in a sample and at what amounts; this is why infrared spectroscopy is useful [3].

Figure 2.1   Example of a FT-IR.

2.2.2 Ultraviolet-visible spectroscopy

The Ultraviolet-visible spectroscopy or ultraviolet-visible spectrophotometry (UV-Vis or UV/Vis**)** involves the use of light in the visible and adjacent (near ultraviolet (UV) and near infrared (NIR)) ranges in a molecule. The absorption in the visible ranges directly affects the color of the compounds involved. In this region of the electromagnetic spectrum, molecules undergo electronic transitions. This technique is complementary to fluorescence spectroscopy, in that fluorescence deals with transitions from the excited state to the ground state, while absorption measures transitions from the ground state to the excited state [3]. UV/Vis spectroscopy is routinely used in the quantitative determination of solutions of transition metal ions and highly conjugated organic compounds [3]. • Solutions of transition metal ions can be colored (i.e., absorb visible light) because d electrons within the metal atoms can be excited from one electronic state to another. The color of metal ion solutions is strongly affected by the presence of other species, such as certain anions or ligands. For instance, the color of a dilute solution of copper sulfate is a very light blue; adding ammonia intensifies the color and changes the wavelength of maximum absorption (λmax) [3].

• Organic compounds, especially those with a high degree of conjugation, also absorb light in the UV or visible regions of the electromagnetic spectrum. The solvents for these determinations are often water for water soluble compounds, or ethanol for organic-soluble compounds. (Organic solvents may have significant UV absorption; not all solvents are suitable for use in UV spectroscopy. Ethanol absorbs very weakly at most wavelengths.) Solvent polarity and pH can affect the absorption spectrum of an organic compound.

• While charge transfer complexes also give rise to colors, the colors are often too intense to be used for quantitative measurement. The Beer-Lambert law states that the absorbance of a solution is directly proportional to the concentration of the absorbing species in the solution and the path length. Thus, for a fixed path length, UV/VIS spectroscopy can be used to determine the 18 concentration of the absorber in a solution. It is necessary to know how quickly the absorbance changes with concentration.

2.2.3 NMR spectroscopy

Nuclear magnetic resonance spectroscopy (NMR) is a technique which exploits the magnetic properties of certain nuclei to produce desired results. It's most important utilization is found in the organic chemistry in the proton NMR and carbon-13 NMR experiments. In principle, the NMR is applicable to any nucleus possessing spin [4]. A lot of information can be obtained from an NMR spectrum. Much unlike using infrared spectroscopy to identify all the groups and not just the functional groups. The analysis of a 1D NMR spectrum provides information on the number and type of chemical entities in a molecule. It is seen that the NMR provides much more information than IR. The impact of NMR spectroscopy on the natural sciences has been substantial. It can, among other things, be used to study mixtures of analyses, to understand dynamic effects such as change in temperature and reaction mechanisms, and is an invaluable tool in understanding protein and nucleic acid structure and function. It can be applied to a wide variety of samples, both in the solution and the solid state. When placed in a magnetic field, NMR active nuclei (such as ^{1}H or ^{13}C) absorb at a frequency characteristic of the isotope [3]. The resonant frequency, energy of the absorption and the intensity of the signal are proportional to the strength of the magnetic field. Depending on the local chemical environment, different protons in a molecule resonate at slightly different frequencies. Since both this frequency shift and the fundamental resonant frequency are directly proportional to the strength of the magnetic field, the shift is converted into a field-independent dimensionless value known as the chemical shift. The chemical shift is reported as a relative measure from some reference resonance frequency. For the

41

nuclei ^{1}H and ^{13}C, are commonly used as a reference. This difference between the frequency of the signal and 15 the frequency of the reference is divided by frequency of the reference signal to give the chemical shift. The frequency shifts are extremely small in comparison to the fundamental NMR frequency. A typical frequency shift might be 100 Hz, compared to a fundamental NMR frequency of 100 MHz, so the chemical shift is generally expressed in parts per million (ppm). By understanding different chemical environments, the chemical shift can be used to obtain some structural information about the molecule in a sample.

The conversion of the raw data to this information is called assigning the spectrum. For example, for the ^{1}H NMR spectrum for ethanol (CH_3CH_2OH), one would expect three specific signals at three specific chemical shifts: one for the CH_3 group, one for the CH_2 group and one for the OH group. A typical CH_3 group has a shift around 1 ppm, a CH_2 attached to an OH has a shift of around 4 ppm and an OH has a shift around 2–3 ppm depending on the solvent used. Because of molecular motion at room temperature, the three methyl protons average out during the course of the NMR experiment (which typically requires a few ms). These protons become degenerate and form a peak at the same chemical shift which is difficult to interpret in more complicated NMR experiments. The shape and size of peaks are indicators of chemical structure too. In the example above—the proton spectrum of ethanol—the CH_3 peak would be three times as large as the OH. Similarly the CH_2 peak would be twice the size of the OH peak but only 2/3 the size of the CH_3 peak. The analyst must integrate the peak and not measure its height because the peaks also have width—and thus its size is dependent on its area not its height. However, it should be mentioned that the number of protons, or any other observed nucleus, is only proportional to the intensity, or the integral, of the NMR signal, in the very simplest one-dimensional NMR experiments. In more elaborate experiments, for instance, experiments typically used to obtain carbon-13 NMR spectra, the integral of the signals depends on the relaxation rate of the nucleus, and its scalar and dipolar coupling constants. Very often these factors are poorly understood - therefore, the integral of the NMR signal is very difficult to interpret in more complicated NMR experiments [4][5].

2.2.4 Elemental analysis

Elemental analysis (E.A) is used determine the precise amounts of elements (carbon, hydrogen, nitrogen, sulphur) present in an unknown substance, a quantitative analysis is required. Commercially available elemental analyzers are capable of determining simultaneously the percentages of carbon, hydrogen and nitrogen in a compound. In these

42

instruments the sample is burned in a stream of oxygen. The gaseous products are converted to carbon dioxide, water, and nitrogen, which can be detected via gas chromatography, using thermal conductivity detectors. The precise amount of each gas produced in the combustion is determined by integration of the corresponding gas chromatography peaks.

Gas chromatography/mass spectrometry

Gas chromatography (GC is an analytical technique used to analyze complex mixtures of volatile compounds in the gas phase. The main components of a gas chromatograph are an injector, a capillary column housed in an oven (Figure 1.8) and a detector. A sample is injected, volatilized and carried through the column by a carrier gas, typically helium or nitrogen, where the mixture is separated by a substituted polysiloxane stationary phase based on volatility and structure. In a typical GC experiment, temperature is increased at a certain rate to elute analytes. The temperature ramp determines analyte retention times and separation efficiency. The detector used throughout this dissertation was a mass spectrometer. Mass spectrometry (MS) coupled to a gas chromatograph not only provides sensitivity, but it allows for structural elucidation. A mass spectrometer analyzes ions based on size and charge. Mass spectrometers are comprised of three main components: an ionization source, mass analyzer and a detector. Gas chromatography/mass spectrometry (GC/MS) techniques have two common ionization techniques, electron ionization (EI) and chemical ionization (CI).
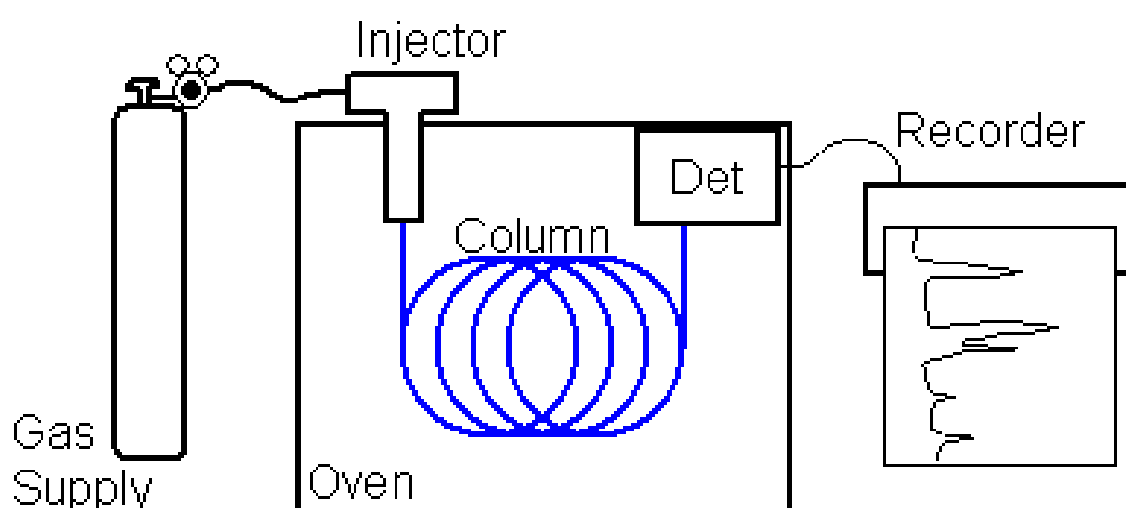
Figure 2.2 Gas Chromatography.

2.2.5 Cyclic voltammetry

Cyclic Voltemmetry (CV) is the basic electrochemical material test. In this, the current is detected by sweeping the potential back backwards and forwards (from positive to negative and from negative to positive) between the chosen limits. Information collected from CV can be used to learn about the electrochemical activity of the material. The graphical analysis of the cyclic voltammogram shows redox peaks (Figure 2.4), which are reduction and oxidation peaks of the material, predicting the capacitive behaviour of the electrode. Therefore, the potential to oxidize and reduce the material can be deduced.
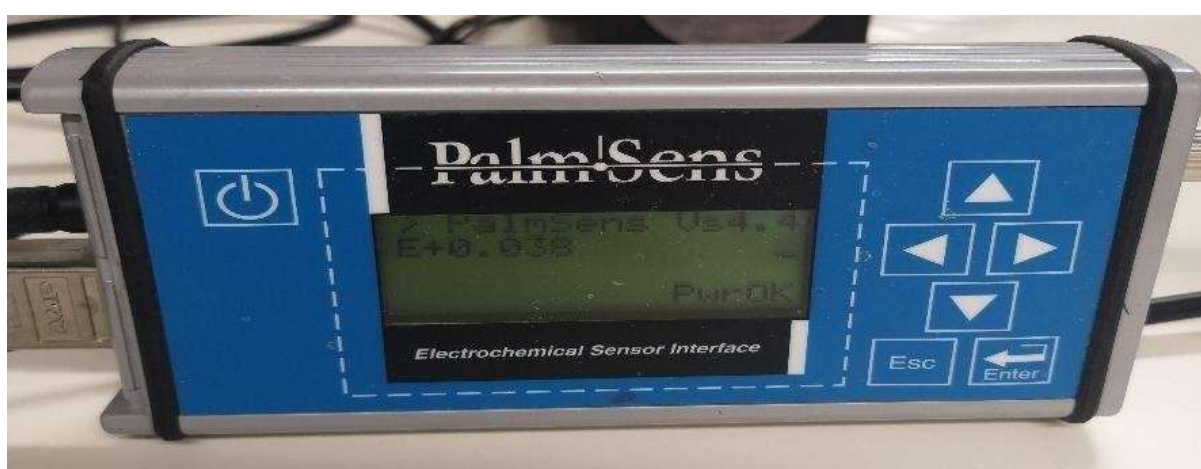
Figure 2.3 PalmSens Potentiostat.
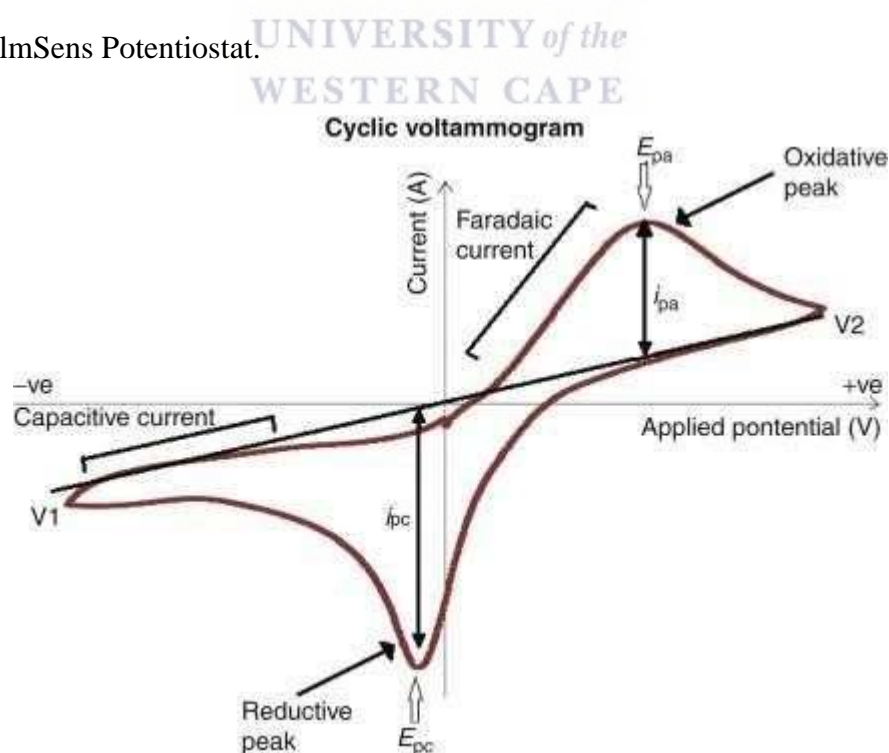
Figure 2.4 Example of a reversible cyclic voltammegram. Image extracted from the internet.

44

Experimental setup:

An electrochemical setup for voltammetry studies is usually made up a potentiostat and three electrodes, Figure 6. A potentiostat is an electronic instrument that is used to control the voltage difference between the working electrode and the reference electrode. The set up includes three electrodes reference electrode, working electrode and counter electrode. At the working electrode the potential is controlled, the current is measured and the chemical reaction takes place at the surface of the working electrode [6] Examples of working electrodes are, glassy carbon electrode, gold electrode, platinum electrode etc. The working electrode potential is measured at the reference electrode. The counter electrode carries the current flow through the electrochemical cell and it passes the same current as the working electrode [6] [7].

Figure 2.5 Example of a three-electrode system.

2.3 References

[1]   Busa, A.V., Lalancette, R., Nordlander, E. and Onani, M., 2018. New copper (II) salicylaldimine derivatives for mild oxidation of cyclohexane. *Journal of Chemical Sciences*, *130*(6), pp.1-10.

[2]   Ganzoury M. A., Allam N. K.,. Nicolet T., and C. All,   2015. "Introduction to Fourier Transform Infrared Spectrometry," *Renew. Sustain. Energy Rev.*, vol. 50, pp. 1–8,

[3]   Engel, R.G., George, S., Kriz, G.M.L. and Pavia, D.L., 2010. Introduction to organic laboratory techniques: a small-scale approach. *Chem. Listy*, *104*, pp.950-953.

[4]   Emwas, A.H., Roy, R., McKay, R.T., Tenori, L., Saccenti, E., Gowda, G.A., Raftery, D., Alahmari, F., Jaremko, L., Jaremko, M. and Wishart, D.S., 2019. NMR spectroscopy for metabolomics research. *Metabolites*, *9*(7), p.123.

[5]   Chaffin, M., Hecht, D., Bard, D., Silovsky, J.F. and Beasley, W.H., 2012. A statewide trial of the SafeCare home-based services model with parents in Child Protective Services. *Pediatrics*, *129*(3), pp.509-515.

[6]   Bard, A.J., Faulkner, L.R. and White, H.S., 2022. *Electrochemical methods: fundamentals and applications*. John Wiley & Sons.

[7]   Elgrishi, N., Rountree, K.J., McCarthy, B.D., Rountree, E.S., Eisenhart, T.T. and Dempsey, J.L., 2018. A practical beginner's guide to cyclic voltammetry. *Journal of chemical education*, *95*(2), pp.197-206.

Chapter 3

Results and discussion

This chapter focuses on the results and discussion of the synthesized ligands and their copper (II) complexes. The first part of the chapter gives the results while the second part discusses them.

3.1 Synthesis of salicylaldimine ligands (HL^1-HL^5)

The ligands, HL^1–HL^5, reported herein were synthesized by reacting the commercially available3-*tert*-butyl-2-hydroxybenzaldehyde,3,5-di-*tert*-2-hydroxybenzaldehyde,5-chlorosalicylaldehyde, 3-bromo-5-chloro-salicyaldehyde and 2hydroxy-5-nitrobenzaldehyde with either 2-thiopheneethylamine or 2-furfurylmethylamine, respectively. The reactions mixtures were stirred at room temperature for 12 hours. The solvent was removed from the product with a rotary vapour followed by the addition of dichloromethane (DCM) to the resulting ligand. The ligands were washed with deionized water and the product was recovered through separatory funnel. Magnesium sulphate was added to the recovered ligand to remove any water present in the product followed by gravity filtration. Subsequently, the remaining solvent was removed from the filtrate with rotary vapour and obtaining the product. The ligands were isolated as stable yellow solids (fig 3.1) with yields ranging from 70% - 97 %. The ligands were soluble in most organic solvents such as dichloromethane, chloroform, acetonitrile and dimethylsulfoxide which was very favourable for their characterization.

Figure 3.1. Schiff Base Ligands (HL^1-HL^5).

The ligands were all prepared as shown in Scheme 3.1 and described in details in experimental section 3.3 to .3.7.
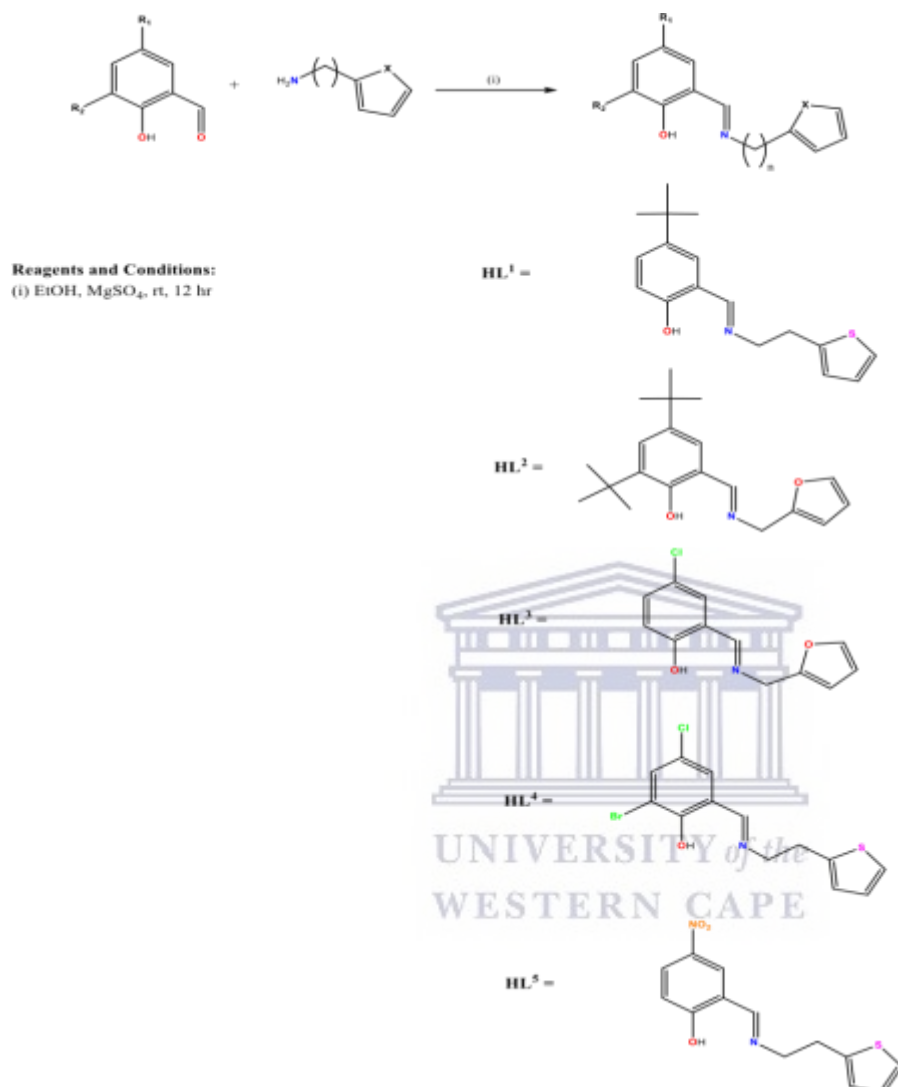
Scheme 3.1. General outline for the synthesis of salicylaldimine ligands (HL[1]-HL[5]).

3.2. Synthesis of salicylaldiminato-copper complexes (C[1]-C[5])

The ligands HL[1]-HL[5] obtained in Scheme 3.1 above were used for the preparation of respective copper complexes C[1]-C[5] (fig 3.2) giving a total of 10 new compounds. The complexes ranged from yellow to green and black coloured products.

The complexes were prepared by reacting copper acetate with appropriate ligand in ethanol solvent. The reaction was catalysed by triethyl amine. The products which were obtained in moderate to high yields are shown in fig 3.2 below.

Figure 3.2. Salicylaldiminato-copper (II) complexes (C^1-C^5)
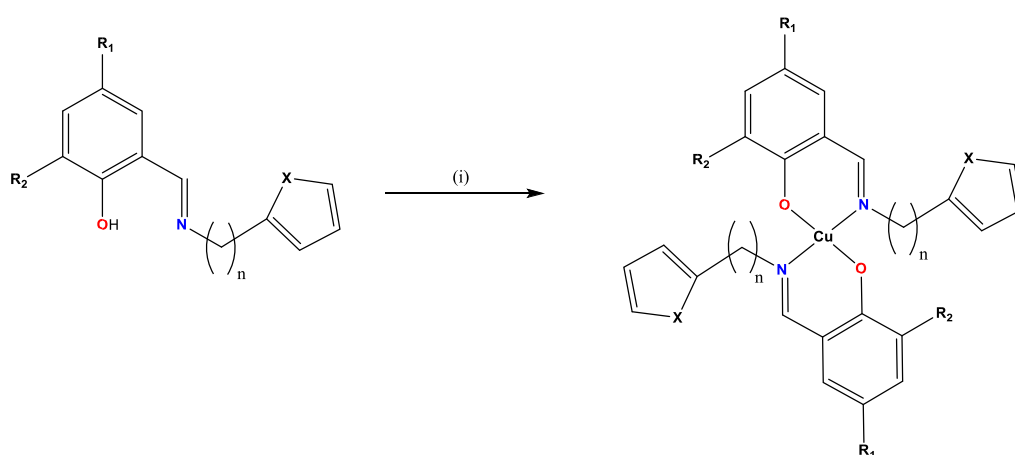
Reagent and conditions:

(i) EtOH, $Cu(CH_3COO)_2$, Et_3N, rt, overnight

49
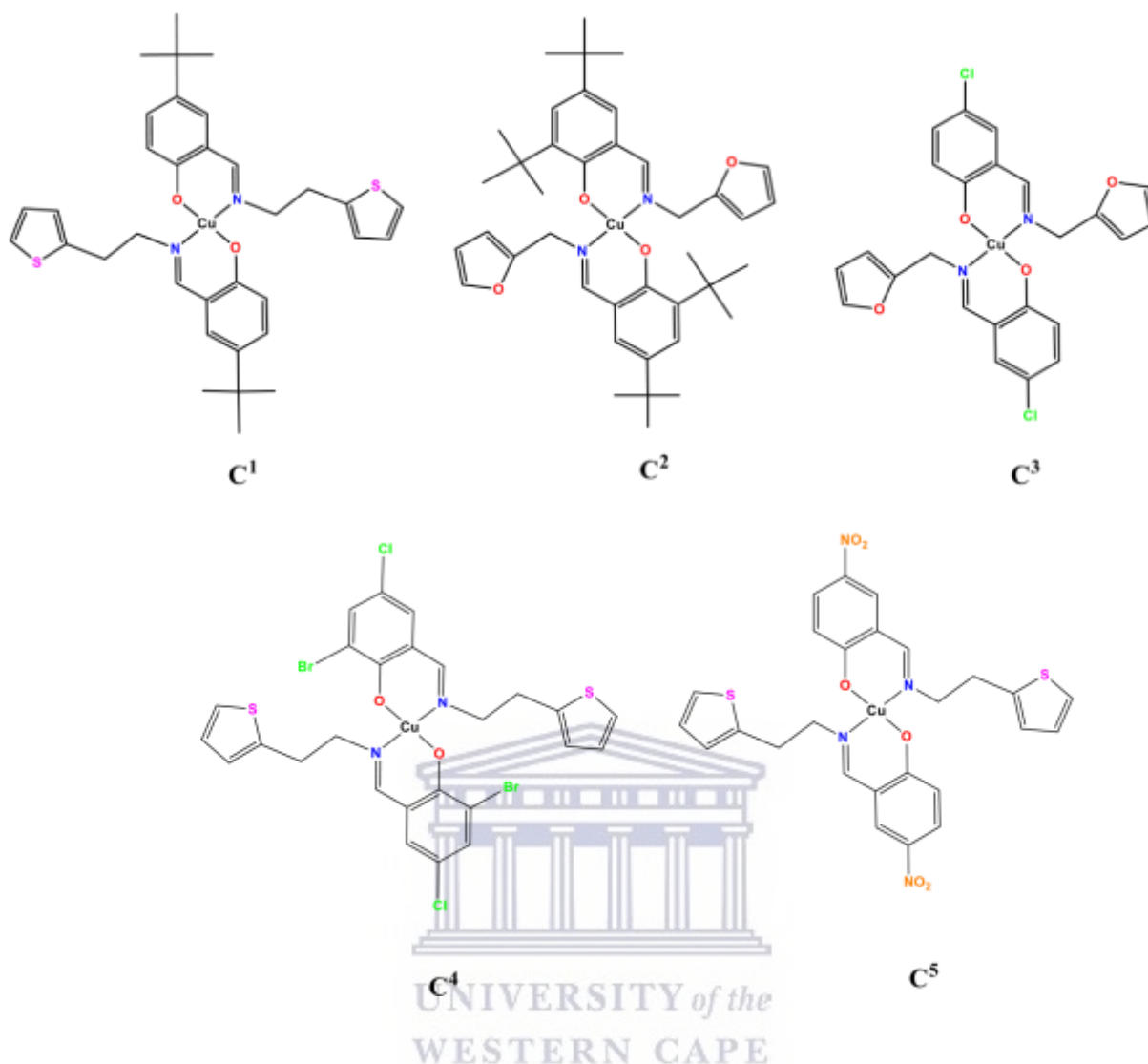
Scheme 3.2. General outline for the synthesis of salicylaldiminato-copper complexes (C[1]-C[5]).

3.3 Physical properties of the prepared ligands and complexes

The physical properties of the Schiff base ligands and their copper (II) complexes were obtained using appropriate instruments and recorded as shown in Table 3.1 below.

Table 3.1. Physical properties of salicylaldehyde ligands and their copper(II) complexes.

Compound	Color	Yields (%)	Melting Point (°C)	Texture
SB-HL[1]	Yellow	91.4	109	Crystals
SB-HL[2]	Yellow	90.58	106	Crystals
SB-HL[3]	Brownishyellow	97.02	114	Powder
SB-HL[4]	Orange-yellow	81.15	121	Powder
SB-HL[5]	Orange-yellow	72.17	119	Powder
Complex [1]	Yellow	32.4	205	Powder
Complex [2]	Black	87	198	Powder
Complex [3]	Pale green	52.8	220	Powder
Complex [4]	Pale green	47.6	238	Powder
Complex [5]	Pale green	92.5	235	Powder

The ligands and the complexes were all obtained as solids either in the form of crystals but most were powdery. This is the nature in which these compounds are usually obtained [1]. The ligands displayed yellow colour as expected because they generally absorb in the UV-Vis region thereby reflecting in the yellowish region [480*-590* nm] [2]. Different solvents were used to test the solubility of the complexes, and they were found to be soluble in the common solvents such as the DCM, Chloroform, and ethanol. However, a few of them required heating and thus were regarded as poor in solubility rather than insoluble. Due to the variability in their solubility, unfortunately the the highly desired crystals for X-ray diffraction studies were unattainable.

51

The melting point of ligands were determined and the results were given in the Table 3.1 above. It can be seen that the melting point of the ligand depends upon the attached group to the nitrogen atom of C=N [3]. Kamellia Nejati *et al* had made similar observation from their thermogravimetric studies. Ligand HL[1] and HL[2] melting points were found to be lower compared to those of the other ligands with a difference of only 3°C. The two ligands show similarities which could be arising from the fact that both HL[1] and HL[2] are *para* substituted with *tert*-butyl substituent although the latter is both *ortho* and *para* substituted. It may be envisaged that the bulky groups could be contributing to uneven packing of the molecules within the unit cells of the compound's arrangement. The m.p of the compounds HL[4]-HL[5] are found to be in slightly closer 121 and 119°C respectively, looking at the structures of the compound it can be observed HL[4] and HL[5] contain ethyl arm just after the azomethine group which could suggest that there is similarity in their packing.

3.4 Infrared (IR) spectroscopy

The functional groups of the prepared Schiff's bases were confirmed by infrared spectroscopy. To probe the presence of the functional groups and to validate the formation of the ligands and their complexes HL[1]–HL[5] and C[1]-C[5], Infrared spectroscopy was employed which confirmed the presence of a new iminic bond on all the ligands. The absorption bands of the ligands namely **HL[1] – HL[5]** were obtained as KBr pellets which showed the presence of the important functional groups. The FT-IR spectra showed the expected heterocyclic ring absorption bands (C-O-C) for **HL[2]**, and **HL[3]** in the range 1242 cm^{-1} and 1263 cm^{-1}, however for **HL[1]**, **HL[4]** and **HL[5]** the heterocyclic ring absorption bands differed (C-S-C) for the ligands and were observed in the range 1302 to 1395 cm^{-1} respectively. Motswainyana *et al* observed similar results [4] [5]. There was a very strong band observed in all the ligands in the region 1619 to 1640 cm^{−1}, which was assigned for the azomethine (C=N) group and is in agreement with the literature [6]. A close observation showed that there were other bands in the region 1432 cm^{-1} to 1464 cm^{-1} which could be assigned to the C=C stretching frequency. An absorption band at 3137 to 3456 cm^{-1} was attributed to the stretching frequency of the phenolic OH bond present as a substituent for all the ligands HL[1] to HL[5] [7] [8].

In the FTIR spectra of the complexes, four major bands were observed ν(C=N), ν(C−O), ν(Cu−O), and ν(Cu−N) [1]. The imine reduction was confirmed by the appearances of strong absorption bands observed in the region between 1605 -1633 cm⁻¹. This observation was in agreement with the reported values by Santos *et al* [8]. The evidence of coordination of the ligands to the metal center was observed by the imine absorption bands being shifted to lower frequencies by 27 cm⁻¹ compared to the corresponding free ligands, an observation well documented in the literature [1]. However, other reports, for example, Busa et al. attributed this to a co-coordination of N,O-donor atoms which partially supports the argument [9].
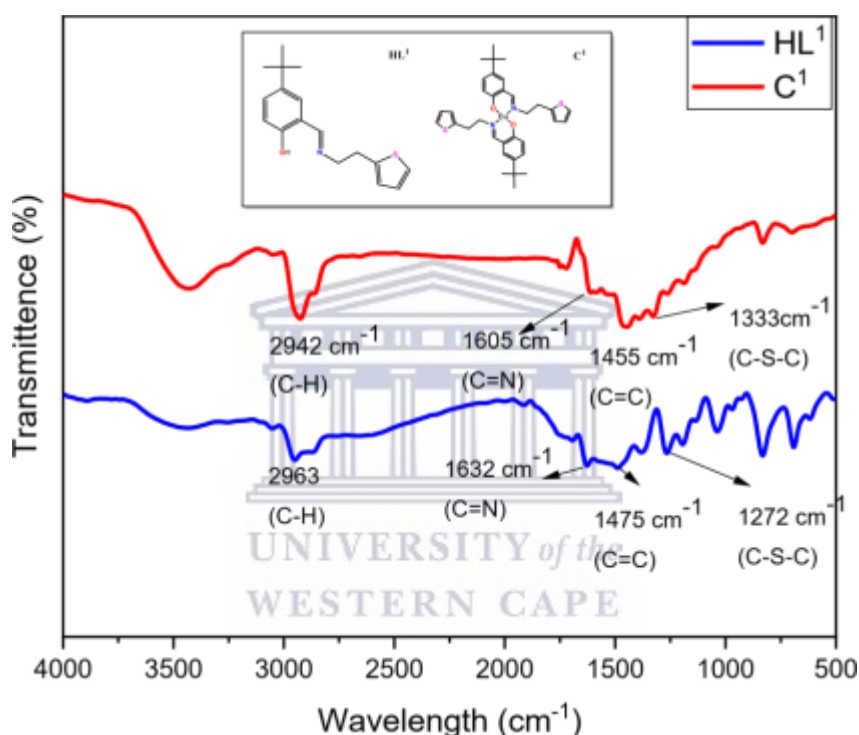
Figure 3.3. FTIR spectra of **HL¹** and **C¹**.

The absorption bands arising from (C-O) for the complexes were lowered to 1157 cm⁻¹ from corresponding ligand 1171 cm⁻¹. Cemal *et al.* reported similar results where they observed the ligand stretching frequency lowered from 1189 cm-¹, to that of the complex 1167 cm-¹ . The lowering shift was attributed to the coordination via the phenolic oxygens [10]. The observed absorption bands at 1615 cm⁻¹ for the complex confirmed the presence of the C=N group which is in agreement with the reported literature values for salicylaldimine complexes with a heterocyclic pendant arm [11]. The shift that was observed for C=N from that of the ligand of 1619 cm⁻¹ to 1615 cm⁻¹, a lower shift value of 4 cm⁻¹ may have be intrinsic from a weakening occurring in the C═N bond after complexation [9] [12]. Chemically, this could be a result of

53

the donation of an electron from the imine nitrogen to the copper metal void d-orbital [10] [13]. This is also an evidence of the participation of the N, O-donor atoms in the coordination which was observed by other researchers.
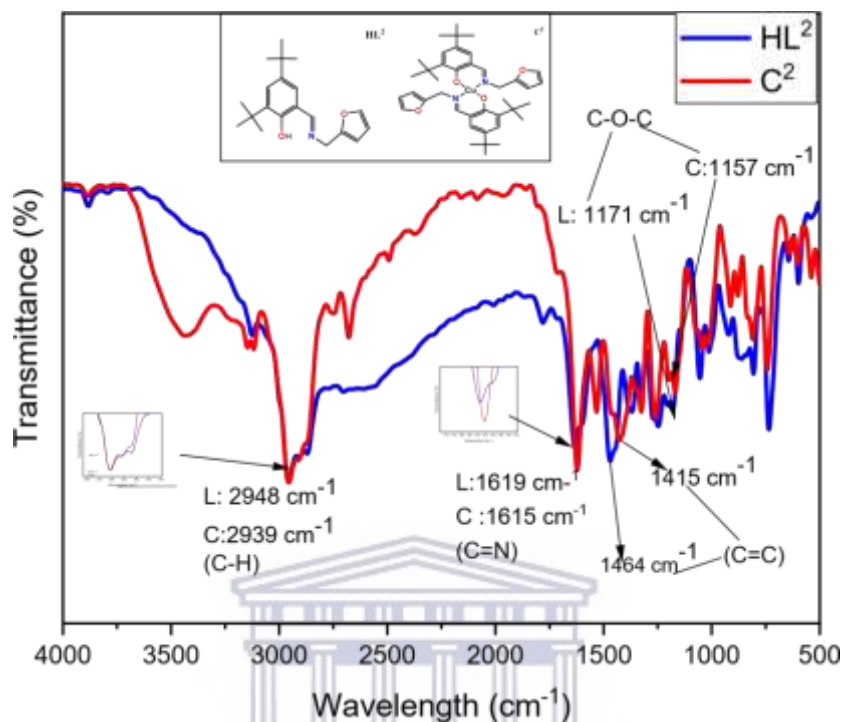
Figure 3.4. FTIR spectra of **HL²** and **C²**.

The infrared spectra of the copper (II) complex showed the presence of a sharp intense peak of v(C=N) at 1622 cm⁻¹. Again, this indicates the participation of nitrogen atoms in the coordination with Cu(II). Kasumov e*t al.* demonstrate similar findings and confirmed that the band of the ligands undergoes small shift to lower frequencies upon coordination by the imine nitrogen atoms [14]. Other researchers observed absorptions of auxiliary bonds such as C=C. Samposion and co-workers reported that the peak they observed at 1596 cm⁻¹ in their complex spectrum indicated the presence of the C=C. Equally, we observed v (C=C) vibrational stretch for similar bond between 1475 and 1462 cm⁻¹ [15][16].
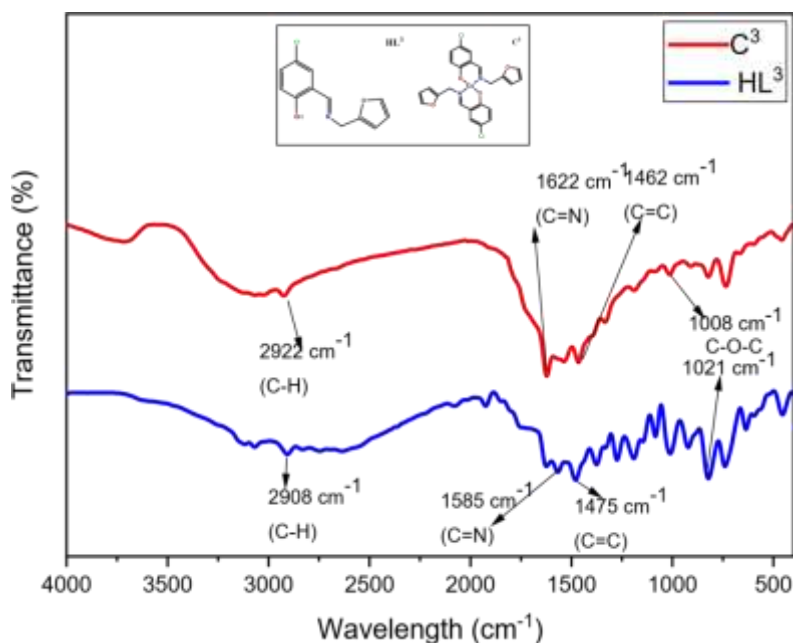
Figure 3.5. FTIR spectra of **HL³** and **C³**.

In the FT-IR spectrum of C⁴, the v(C=N) vibration was 1632 cm⁻¹ having shifted from 1629 cm⁻¹ of the ligand reported above. The lowering of this band shifting to a lower frequency.

Such an observation is reported by Fatima *et.al* [17]. The v(C=C) was recorded at region 1489-1428 cm-¹ [16] . In this complex, an absorption bond (C-S) was observed at 1388cm¹ compared to 1374 cm⁻¹ of the ligand. The absence of the phenolic group bands in the Cu(II) complex indicates that the hydroxyl groups are deprotonated during coordination [18][19][20].
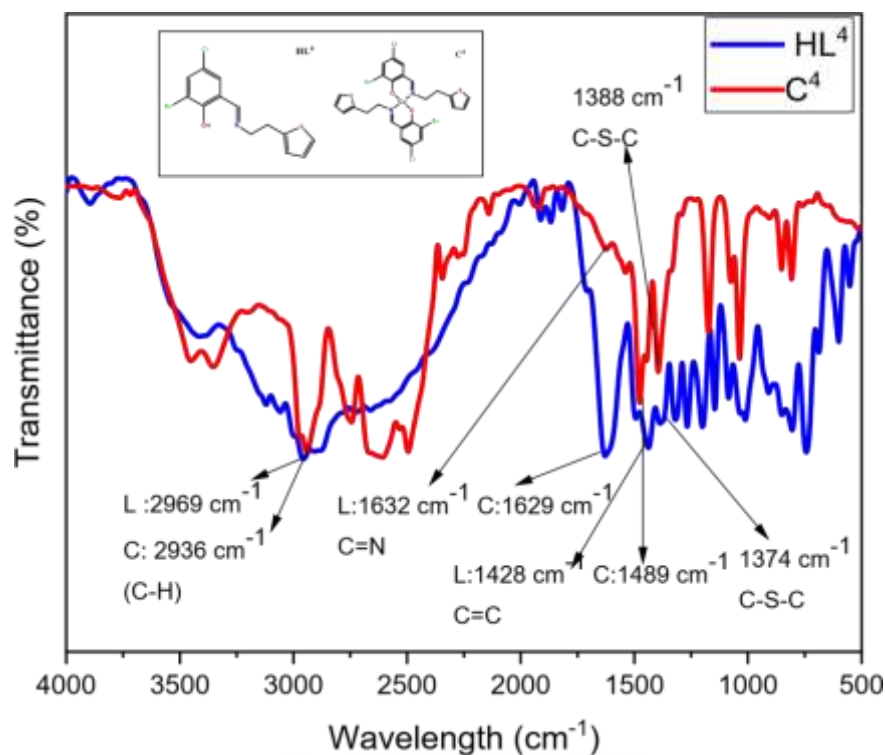
Figure 3.6. FTIR spectra of **HL⁴** and **C⁴**.

The IR spectra of the complexes, when compared with that of the free ligands, show noteworthy differences. Agata Bartyzel as well as Kasumov V *et al* among others indicated that in the Schiff base complexes, the C=N band is more intense and occurs in the same or lower frequencies confirming the participation of nitrogen atoms in coordination of Cu(II) metal [14] [21].

Figure 3.7. FTIR spectra of **HL⁵** and **C⁵**.

56
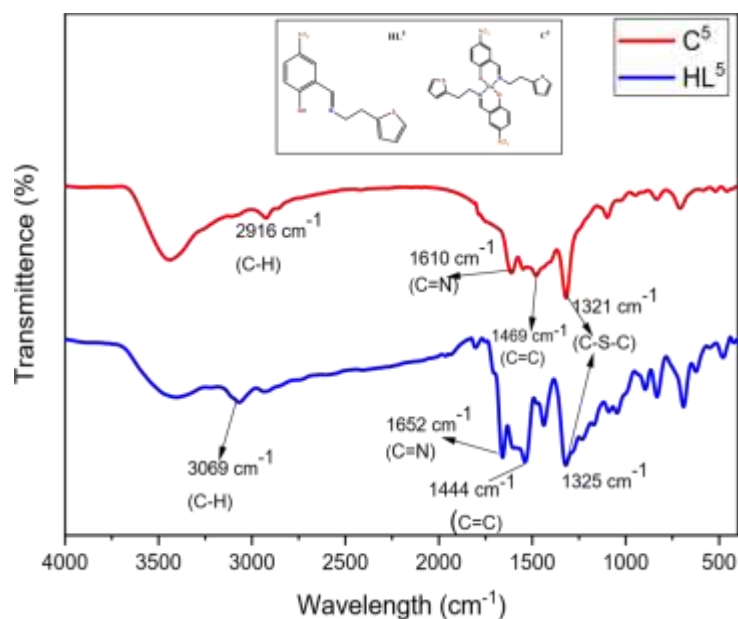
3.5 UV–Vis Spectroscopic Results

The electronic absorption spectra of HL[1] – HL[5] and their complexes C[1]-C[5] were experimentally determined and their results recorded in the region of 250 - 500 nm using DMSO at standard conditions.

Electronic spectra of ligand **HL[1]** and its Cu(II) complexes shown in Fig 3.8 below. It can be seen that there is are intense absorptions in the visible and ultraviolet. he spectrum shows two moderately intense absorption bands at 263 nm and 323 nm. The bands are assigned to π - π * transition of the aromatic ring and n - π * transition of the azomethine chromophores, respectively. These values are in agreement with other similar Schiff base compounds reported in the literature. [22] [23]. On the other hand, when comparing the spectrum of the complex to that of the ligand, we observe that there are 3 peaks and a shoulder. It is notable that the bond that were previously assigned to π - π * and n - π * transitions of the ligand appear with a shift in the complex 255 nm and 302 nm respectively. The presence of the new peak at 371 nm is as a result of the ligand-to-metal charge transfer (LMCT) which indicates the formation of the complex, Asma A *et al*, in the literature, reported similar findings with similar conclusions [24] [21]. However, Yaning G. and co-workers reported that regardless of the metal ion, the energy band of the complex becomes lower in comparison to the ligand due to the π - π* transition [22].
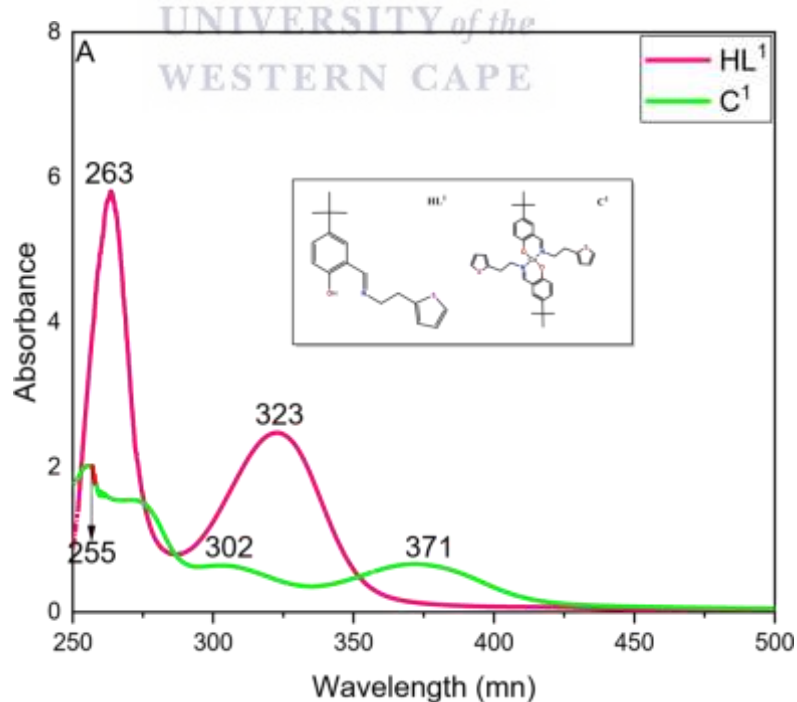
Figure 3.8. UV-vis spectra of **HL[1]** and **C[1]** in **DMSO.**

Tomczyk *et al.* in the literature reported that the ligand UV-Vis absorption is always lower in energy compared to that of the complex. They explained that this observation arose from the π → π* transition, which is an intramolecular charge transfer (CT transition) involving the entire molecule and the azomethine (CH=N) chromophore ground state. Their reported results were 262 for the HL^2 ligand and 265 nm for its complex the Cu(II) complex certainly due to the n → π* transitions[25]. Similarly, from the electronic spectrum of **HL^2**, displays two prominent peaks at around 266 nm, and 329 nm (Fig 3.9). These are the characteristic peaks of

Schiff base ligands due to n–π* and π–π* transitions of the phenyl ring, and a peak attributed

to the C=N group. Remarkably so the absorption corresponds to π − π and n− π for the complex shifted to 256 nm and 277 nm respectively [16][25]. Moreover, the intermolecular charge transfers of the ligand disappeared and the appearance of the new peak at 384 nm is due to the LMCT transition of the complex. Asma *et al.* and others also made similar observations and reported in the literature [24] [26] [27] [28].
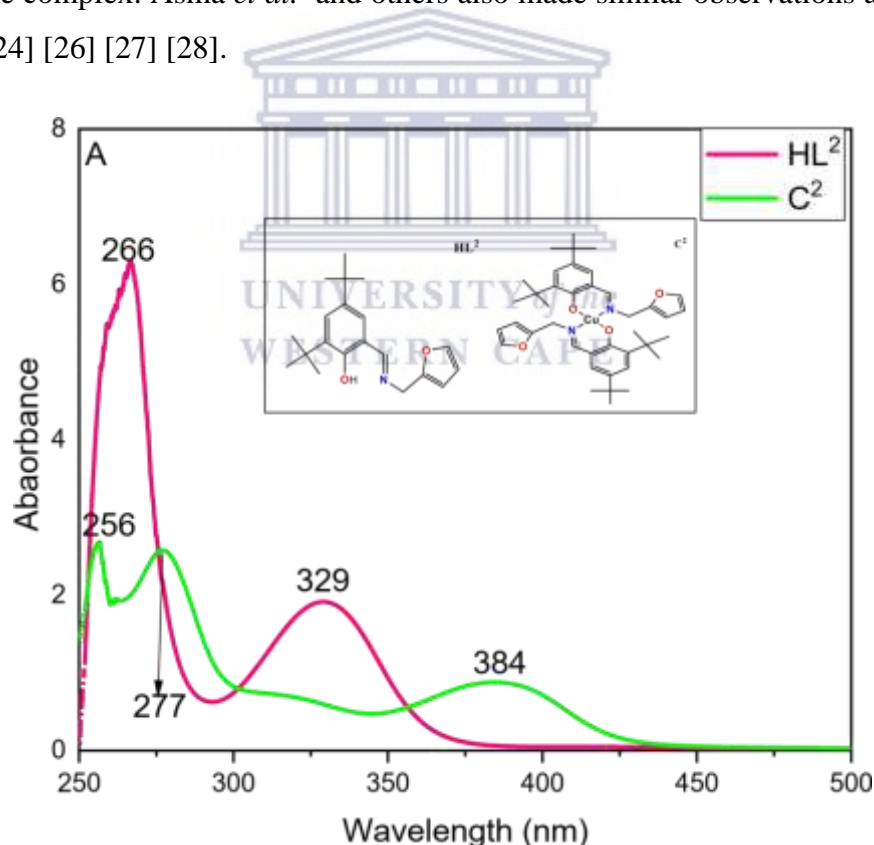
Figure 3.9. UV-Vis spectra of **HL^2** and **C^2** in **DMSO.**

The spectrum of the ligand **HL^3** exhibited 2 bands at 257 nm and 326 nm assignable to π→π∗ and n→π transitions, respectively. These bands are attributed to π→ π* transitions, the first to the

benzene ring and the second to the azomethine group [22] [29]. For the complex, we observed two peaks but the 256 nm and 376 nm were due to the $\pi \to \pi^*$ transition and comparatively, they shifted to a shorter wavelength by 1 nm in the complex. This observation is as a result of the coordination when binding with the metal thus confirming the formation of Schiff base metal complex. [30].
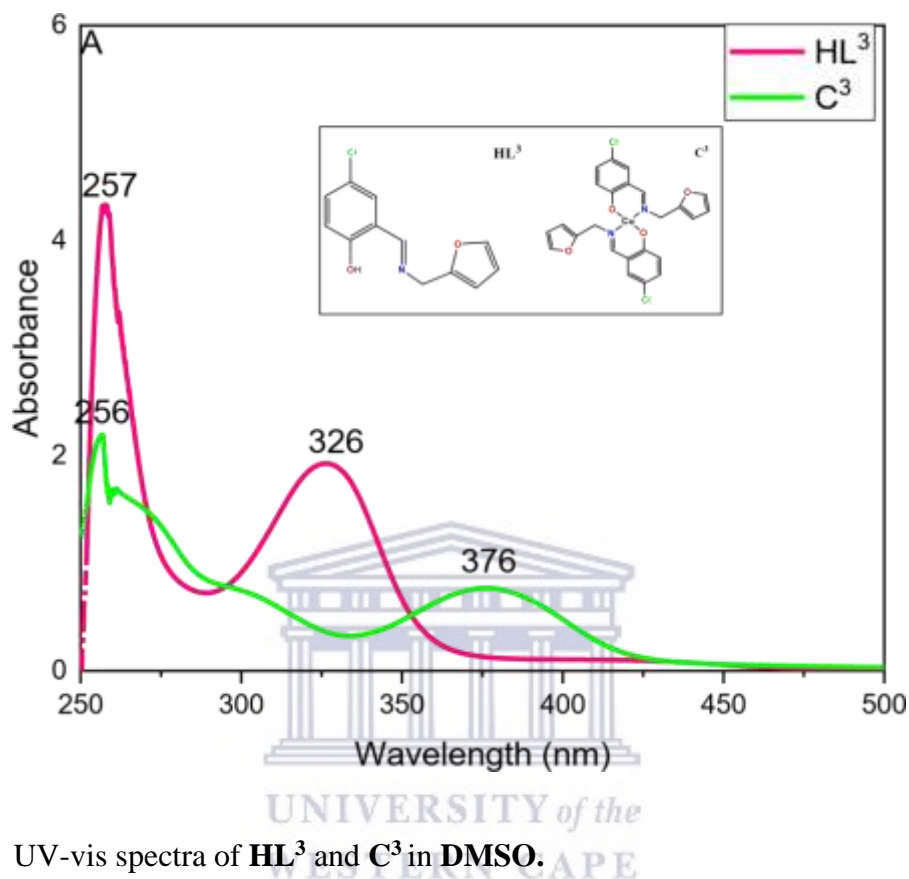
Figure 3.10. UV-vis spectra of **HL³** and **C³** in **DMSO.**

The spectrum of the ligand **HL⁴** showed two intense absorption bands at 238 nm and 320 nm, respectively. The first band which appears at higher energy with a strong intensity may be assigned to the $\pi-\pi^*$ electronic transition of the benzene ring, Karakaya *et al.* in their work; "Novel Metal(II) Complexes with Bidentate Schiff Base Ligand" had similar observation where the 295 nm peak attributed to $\pi-\pi^*$ electronic transition was assigned to benzene ring. The second, being weaker band, is attributed $n-\pi^*$ transition of the (C=N) azomethine group and that is in agreement with literature [9] [29]. For the complex, now we observe two peaks at 235 nm, 366 nm. The first band in the complex had a slight shift as compared to that of a ligand which could be an exception from the red shift [13]. The band observed at 331 nm is most probably due to $n-\pi^*$ of imine group corresponding to the metal complexes [11] [26].

59
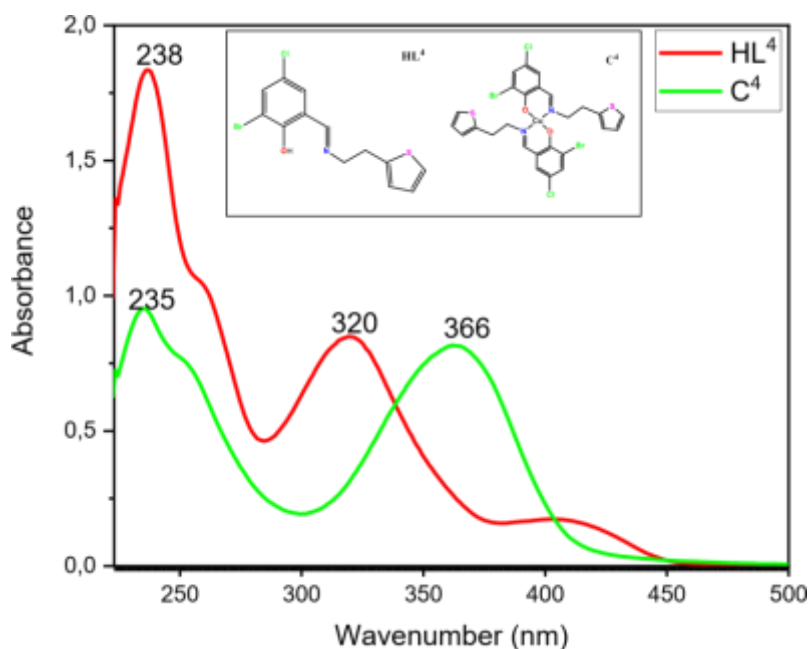
Figure 3.11. UV-vis spectra of **HL⁴** and **C⁴** in **DMSO.**

Karakaya *et al.* in their work, reported that the ligand's UV-vis spectrum contained two major peaks: at position 229 and 335 nm. The first and the second peaks were attributed to benzene and imine group transitions as appropriate, respectively. The ligand's first peak was not affected upon chelation [29]. However, in this work similar observation were obtained, **HL⁵** exhibits 3 bands at 237 nm, 227 nm, and 380 nm, respectively (Fig 3.12). The bands correspond to $\pi \rightarrow \pi*$ (Benzene ring and Imine group) and $n \rightarrow \pi*$ transition respectively. The appearance of a strong band between 380 nm is assigned to charge transfer bands which could be due to LMCT of the complex. The $\pi - \pi$ and $n-\pi*$ of the complex were recorded at 237 nm. The latter observation is supported by literature reports where Asma *et al*. indicated that their new bands appeared in the region of 380–455 nm and were due to LMCT transitions of complexes[24].
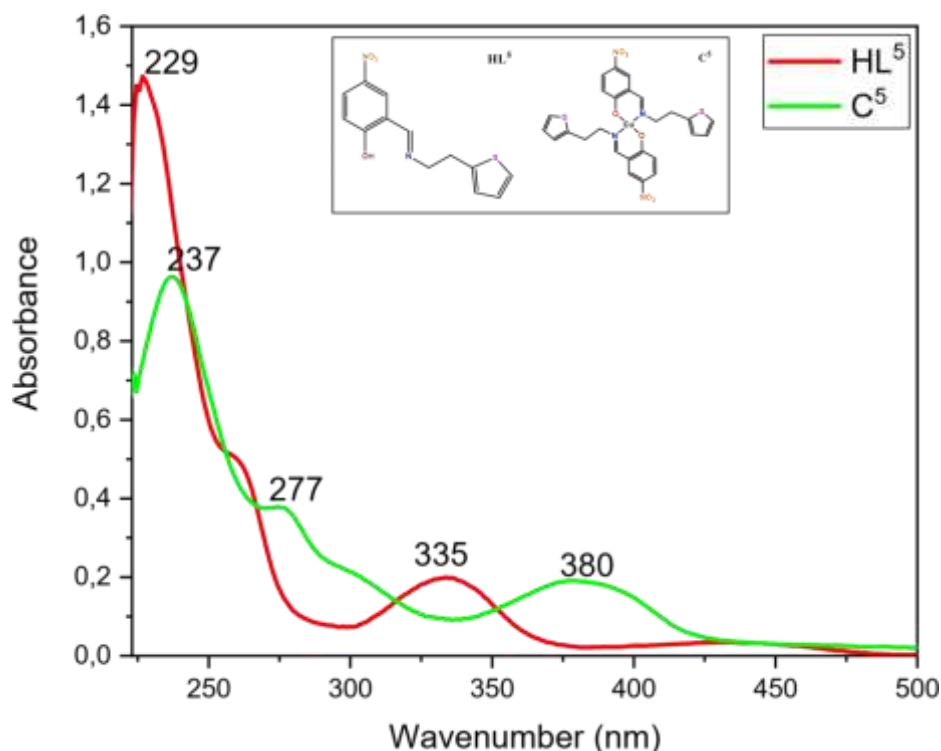
Figure 3.12. UV-vis spectra of **HL^5** and **C^5** in **DMSO.**

3.6 1 H-NMR and 13C-{1H}-NMR spectroscopy

The salicylaldimine ligands HL^1–HL^5 were characterized by the ^{1}H-and ^{13}C-NMR spectroscopy. Confirmation of the condensation reaction is clearly reflected in the ^{1}H NMR spectrum of all the ligands HL^1–HL^5, which showed the disappearance of the NH$_2$ singlet (CH)$_{imine}$. The example of the ^{1}H- and ^{13}C {^{1}H}-NMR spectra are given in Fig 3.11 and 3.12 respectively. Their discussions are given thereafter.

The ^{1}H NMR spectra of all the ligands and seen in a selected example, HL^1, exhibited a characteristic azomethine (HC=N) resonance. The success of the Schiff-base condensation reaction was confirmed by the appearance a singlet peak observed at 8.302 ppm, which was due to the presence of this azomethine functionality. This is well reported in the literature where the signal is mostly indicated to be a singlet at about 8.00 ppm, [31] [32] [33]. The hydroxyl (OH) protons were observed downfield around 13.00 ppm for the ligands. This downfield appearance of the –OH protons can be attributed to the present intramolecular hydrogen bonding (OH-N). This phenomenon has been observed to govern the appearance of downfield hydroxyl signals in similar salicylaldimine ligands reported in the literature [34]. The two triplets observed at 3.21-3.24 ppm and 3.85-3.88 ppm in HL^1 confirmed the presence of an ethylene arm (=N-CH$_2$CH$_2$) in the ligand.

The triplet's signals underwent the vicinal proton coupling. Kifah and co-workers had similar observations but recorded their readings at 3.67 ppm [35].

In the ^{13}C NMR analysis, Gokulnath *et al.* reported in the literature their observations of phenolic carbon C-O at the region 165.29-167.26 ppm and azomethine CH=N at at 160.76160.62 ppm. This was the exact replica of our results where we found the phenolic carbon at the region 165.92-165.88 ppm [36]. The signals for the azomethine carbons were recorded around 158.00 ppm. This was an upfield shift compared to the unreacted aldehyde carbon [36]. The two signals for the ethylene arm in HL[1] appeared at 61.11 ppm and the others further upfield at about 31.43-31.52 ppm. The two carbon signals in HL[1] appear at different regions due to their proximity to the dishielding nitrogen atom which becomes less pronounced as the length of the alkyl chain increases. These observations are consistent with those of similar compounds where the ethyl linker was reported to have a similar influence for a ferrocenylimine and salicylaldimine moieties [37][38]. The carbon 13 spectrum analysis is given in Figure 3.13 below. Each of the five ligands had their proton NMR spectra discussed because of the significant differences which were observed.
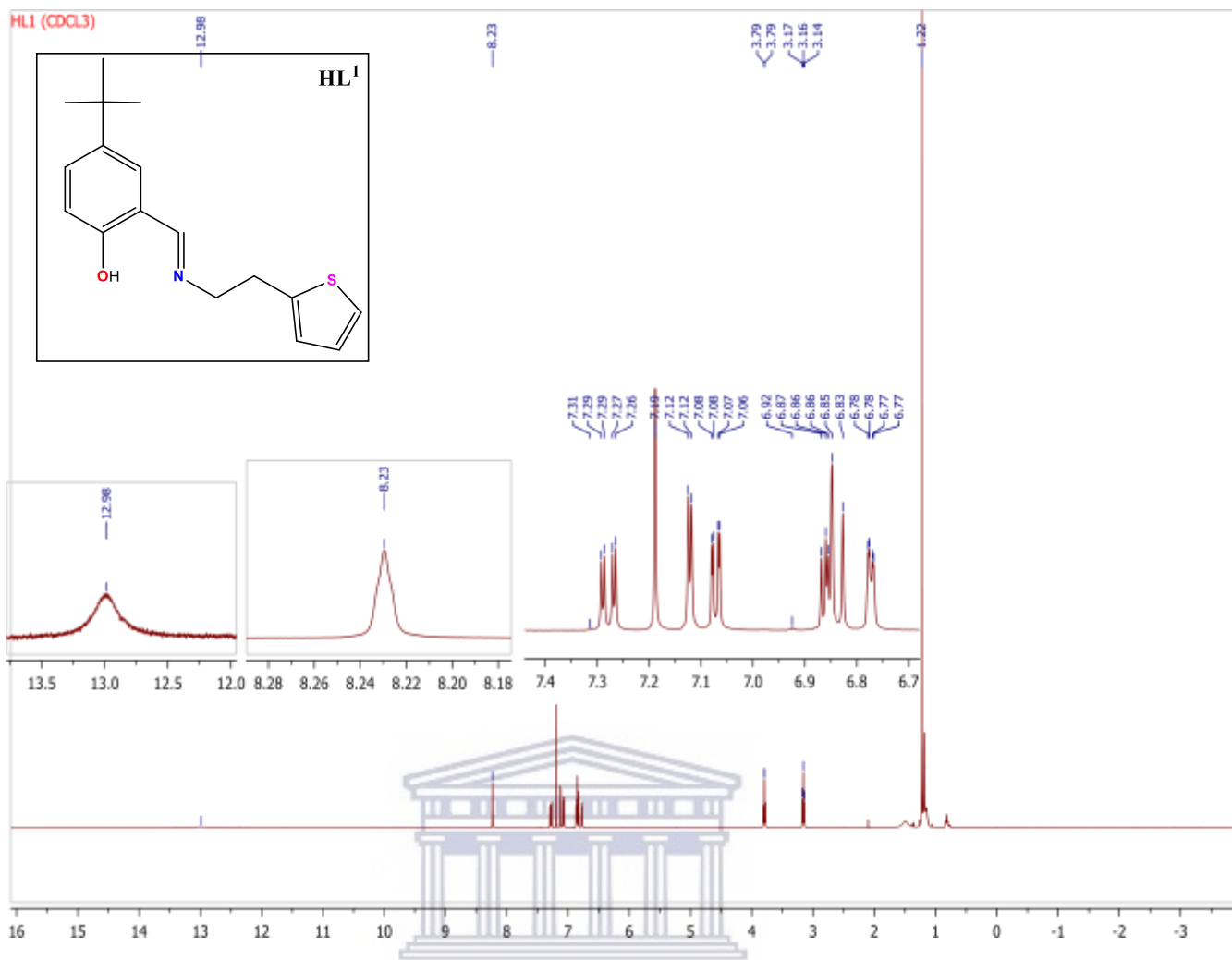
Figure 3.13. ^{1}H NMR spectrum of ligand **HL^1** in CDCl$_3$.
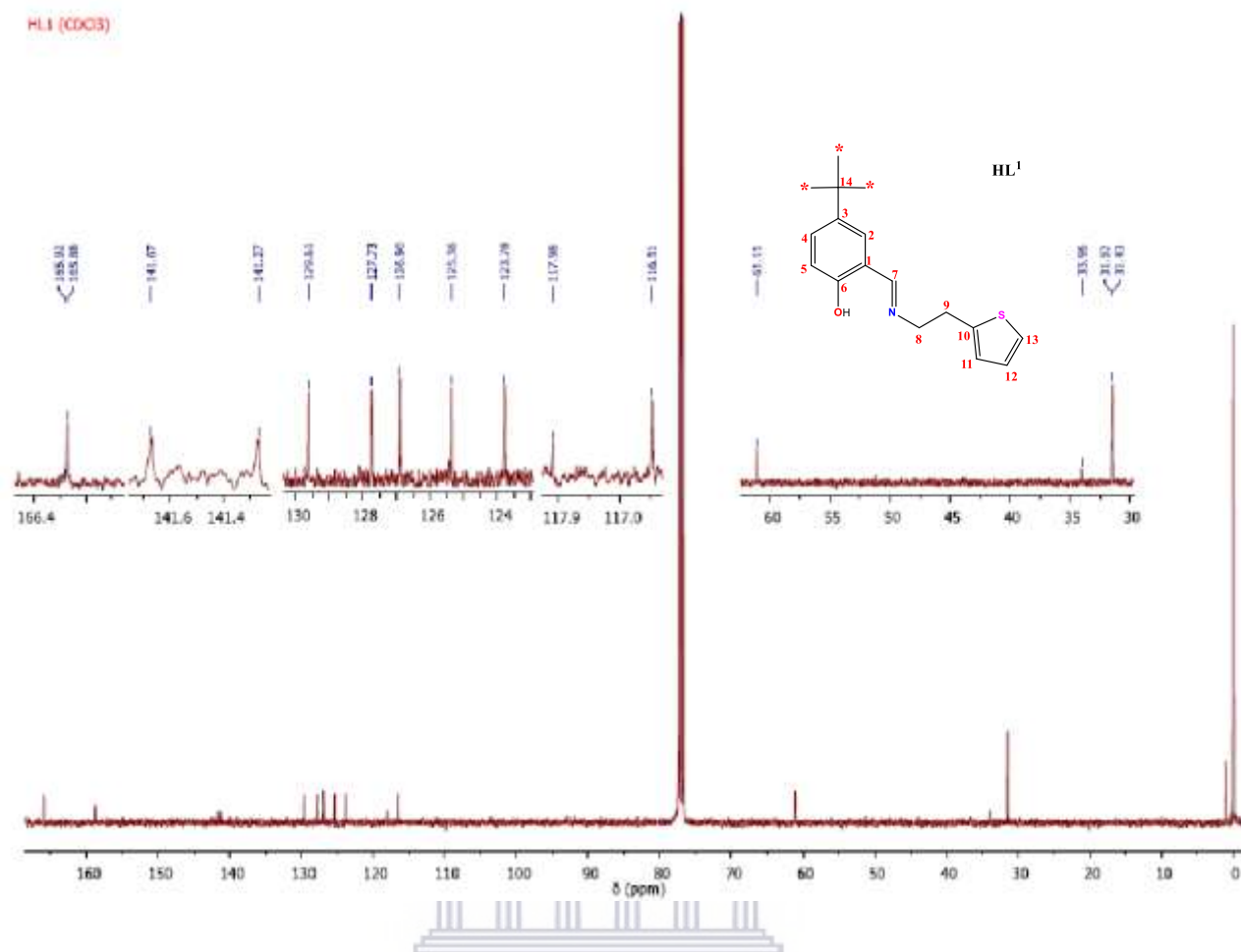
Figure 3.14. ^{13}C NMR spectrum of ligand **HL^1** in CDCl$_3$.

The ligand **HL²** were prepared according to the literature procedures [9] and were confirmed by ^{1}H NMR and ^{13}C NMR. The ^{1}H NMR spectum of the ligand HL[2], similar to HL[1] exhibited a characteristic HC=N resonances and the appearance of a singlet chemical shift around 8.40 ppm as shown in fig.3.15, just as was confirmed by Sumrra, *et al.* Their observations were recorded in the region 7.18-8.85 ppm [39]. Other literature reports had similar observations, a singlet in the region 8.31-8.38 ppm [40][36]. This chemical shift for the hydroxyl (-OH) protons were observed downfield in the range 13.53 – 13.60 ppm, also similar to the ligands reported by Asma A. *et al* [24]. The chemical shifts of the methylene arm (=N-CH$_2$) for HL[2] appeared as singlets at 4.73 ppm, compared to the 4.00 ppm signal of the heterocyclic amines reported in literature. We observe a downfield shift in the alkyl protons upon successful condensation reaction. Other two singlets were observed at 1.30 ppm and 1.43 ppm which indicated the presence of the two *tert*-butyl groups of the ligands. Figure 3.16 shows the carbon-13 spectrum for the ligand HL[2]. The chemical shift for the phenolic carbon (CO) and azomethine (CH=N) carbon were observed at 165.29 - 67.26 p pm and 160.76-160.62 ppm, respectively. As seen above and similar to work by Gokulnath *et al.* the iminic carbons (HC=N) showed similar signals [36].
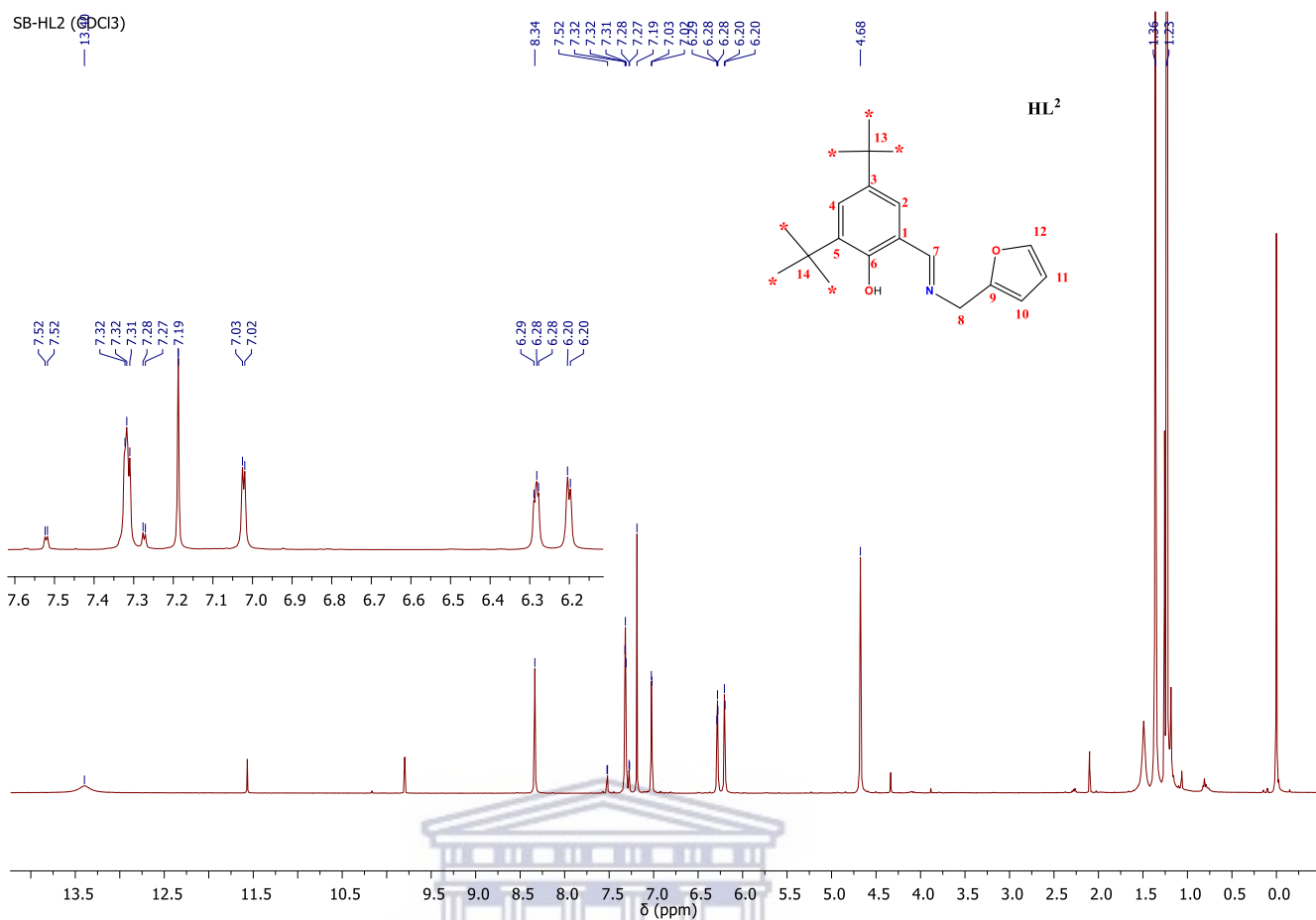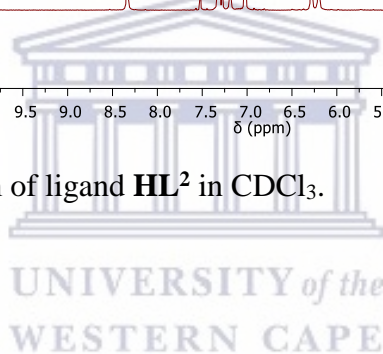
Figure 3.15. ^{1}H NMR spectrum of ligand **HL^2** in CDCl$_3$.
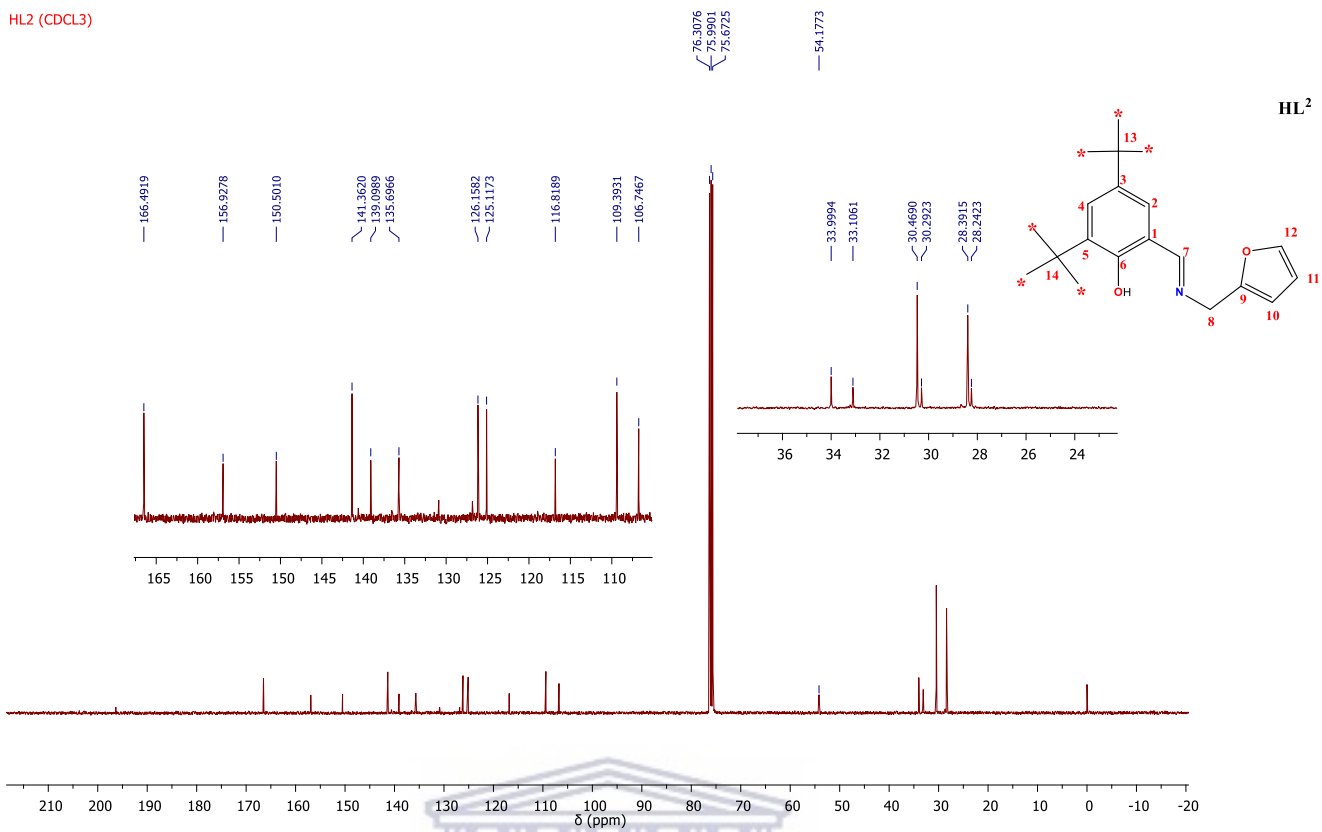
Figure 3.16. ^{13}C NMR spectrum of ligand **HL^2** in CDCl$_3$.
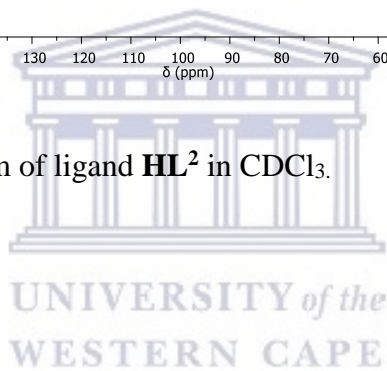
The ligand **HL³** was equally prepared in the similar manner to HL¹ and HL². The ¹H NMR spectrum of the ligand, HL³(fig 3.17), exhibited a characteristic HC=N NMR singlet resonances signal at 8.30 ppm. This observation was attributed to the presence of this functional group and the success of the condensation reaction. This chemical shift value is in good agreement with those reported for similar Schiff base ligands which were in the range of 8.708.73 ppm [41]. The hydroxyl (-OH) proton was observed downfield in the range 13.14 ppm for our ligand. In the literature reports, researchers Hamid Khanmohammadi and Maryam Darvishpour observed a broad signal at region 13.90-14.05 ppm [42]. The chemical shifts of the methylene arm (=N-CH₂) for the ligands appeared as singlet at 4.78 ppm, rather downfield when compared to the 4.00 ppm signal of the heterocyclic amines reported in literature by Motswainyana *et al.* where their methyl arm was a singlet at the region 4.68 - 4.81 ppm [5].

In the ¹³C NMR analysis of the ligand, fig.3.18, the characteristic signals for the iminic carbons (HC=N) appeared at 165.16 ppm for HL³, again very similar to the work by Motswainyana *et al.* [5]. The signals for the carbons attached to the hydroxyl group were observed at 159.58 ppm. This was very close to the chemical shifts of 160.76-160.62 ppm reported by Gokulnath. *et al.* [36]. Kumaran and co-workers reported that at 55.9 ppm, a peak for carbon (CO). Similarly, our findings observed a peak at 54.99 ppm confirming this carbon-oxygen bond [43].
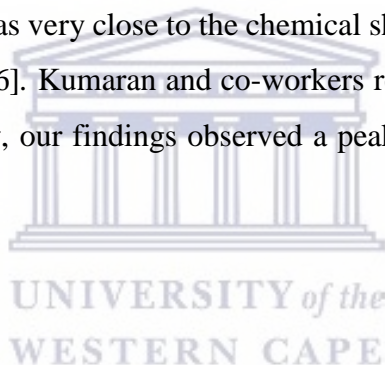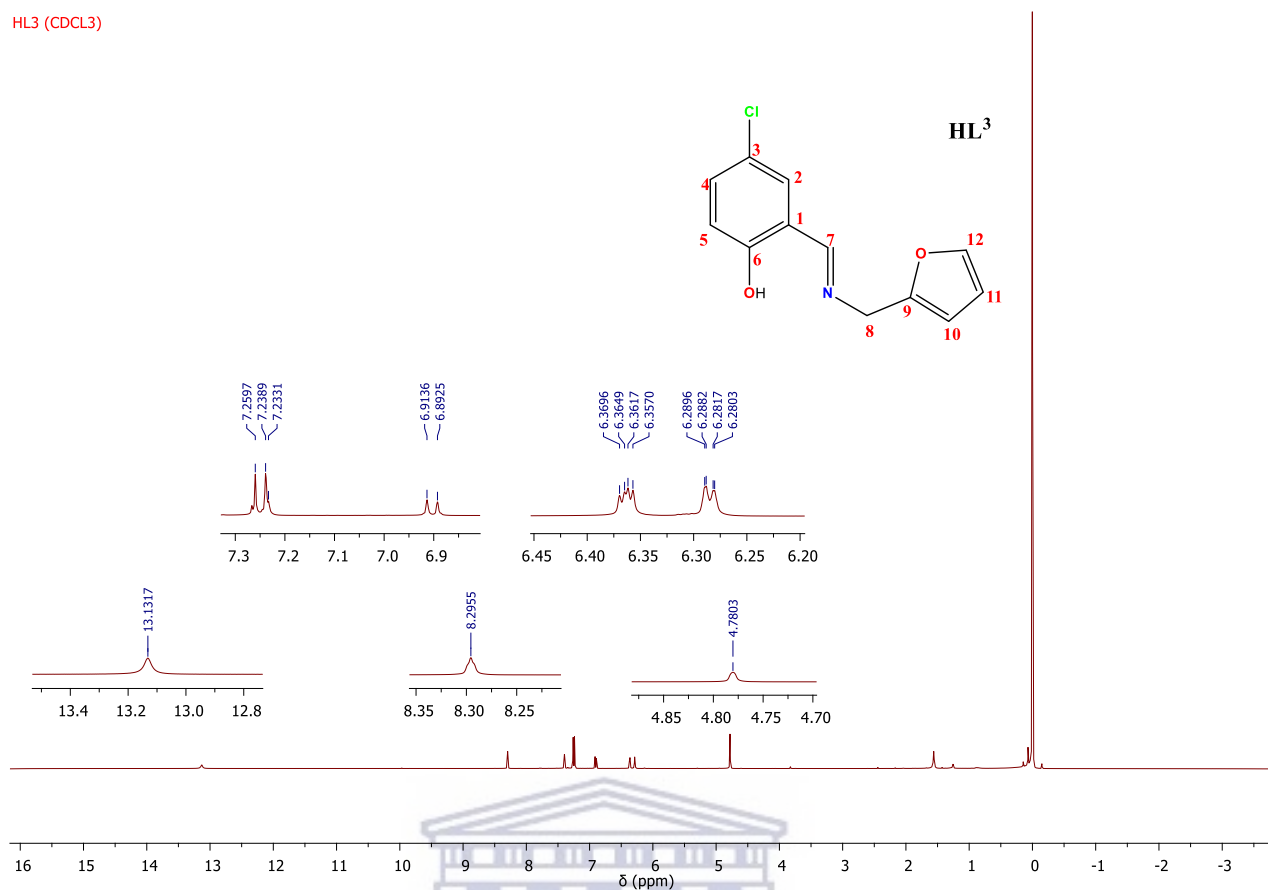
Figure 3.17. ^{1}H NMR spectrum of ligand **HL³** in CDCl₃.
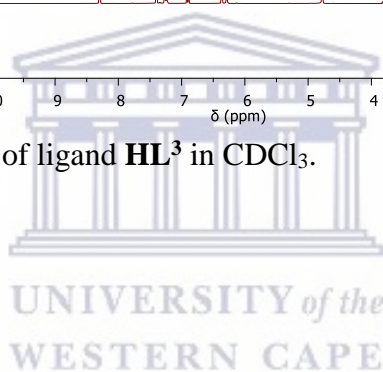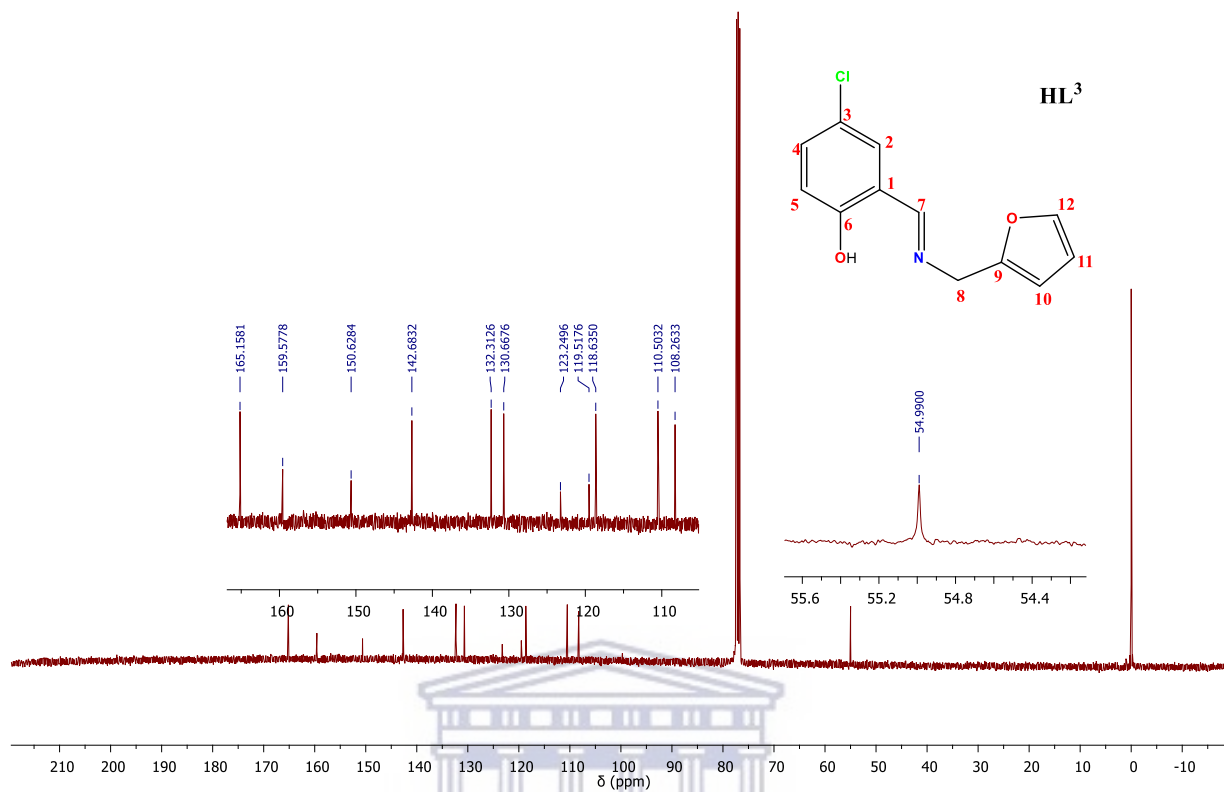
69

Figure 3.18. ^{13}C NMR spectum of ligand **HL^3** in CDCl$_3$.

Literature show the following observation, a singlet at 8.92 ppm which is associated with azomethine group and confirmation of formation of Schiff base ligand, the literature further discusses the presence of a single peak at 12.44 ppm and that peak is associated with phenolic group –OH [31]. In this work the ^{1}H NMR spectra of all the ligands, **HL^4**, exhibited a similar peak with that one observed by Selma which is characteristic azomethine (HC=N) resonance. The success of the Schiff-base condensation reaction was confirmed by the appearance of a singlet peak observed within at 8.0364 ppm which was due to the presence of the azomethine functionality. Furthermore, the phenolic (OH) protons was observed downfield at 14.427 ppm for the ligands reported herein. This downfield appearance of the –OH protons for the ligands can be attributed to the intramolecular hydrogen bonding (OH-N), that has been observed to govern the appearance of downfield hydroxyl signals in similar salicylaldimine ligands [9] [38]. The two triplets observed at the range of 3.2274-3.2607 ppm and 3.8862-3.9193 ppm in the ligand confirmed the presence of an ethylene arm (=N-CH$_2$CH$_2$) in the ligand, and the appearance of triplets indicated vicinal proton-proton coupling. Salih and collegues also had similar observations where they observed at the 3.67 ppm, and also according to the rules of the functional group of NMR they agree with the findings [35].

In the ^{13}C NMR analysis of the ligand, fig.3.19, the characteristic signals for the iminic carbons (HC=N) appeared at 163.96 ppm for HL^4, again very similar to the work by Motswainyana *et al* [13]. The two signals for the ethylene arm in the ligand appeared at 60.0186 ppm and further upfield at 31.0617 ppm. The two carbon signals in L^4 differ greatly due to the dishielding effect of the nitrogen atom which becomes less pronounced as the length of the alkyl chain increases. These observations are consistent with those of similar compounds where the ethyl linker was reported to have a similar influence for ferrocenylimine and salicylaldimine ligands with an appended heterocyclic moiety [44].
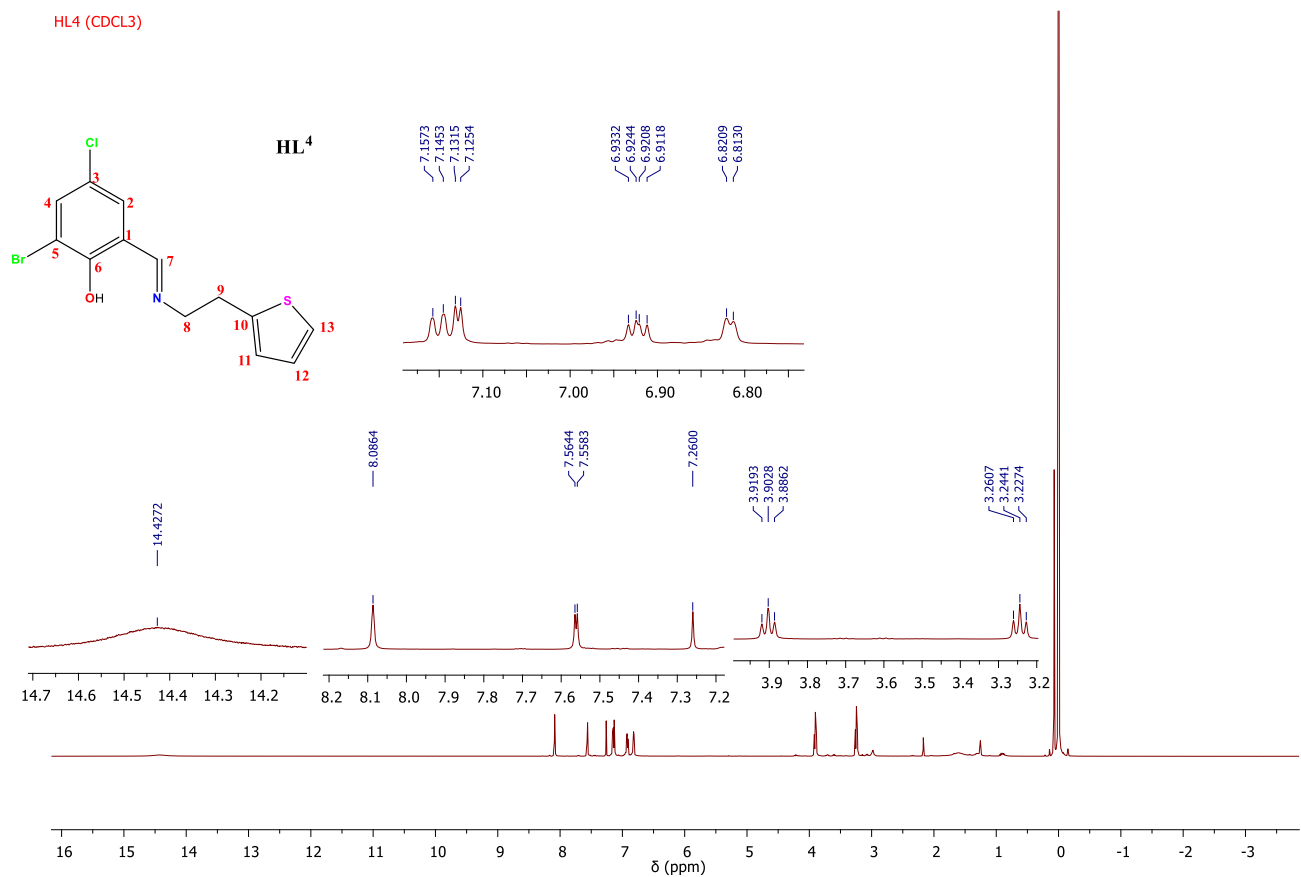
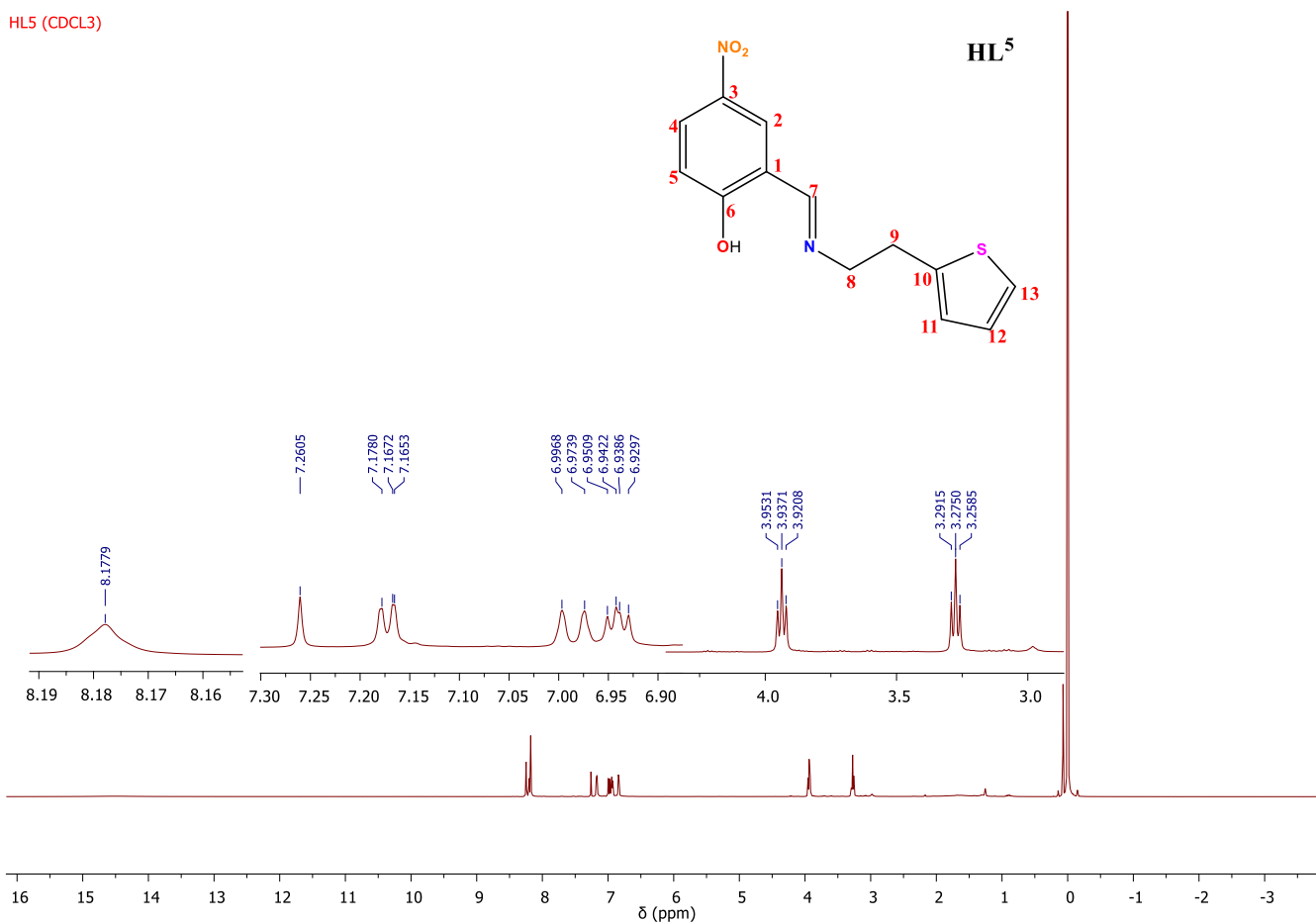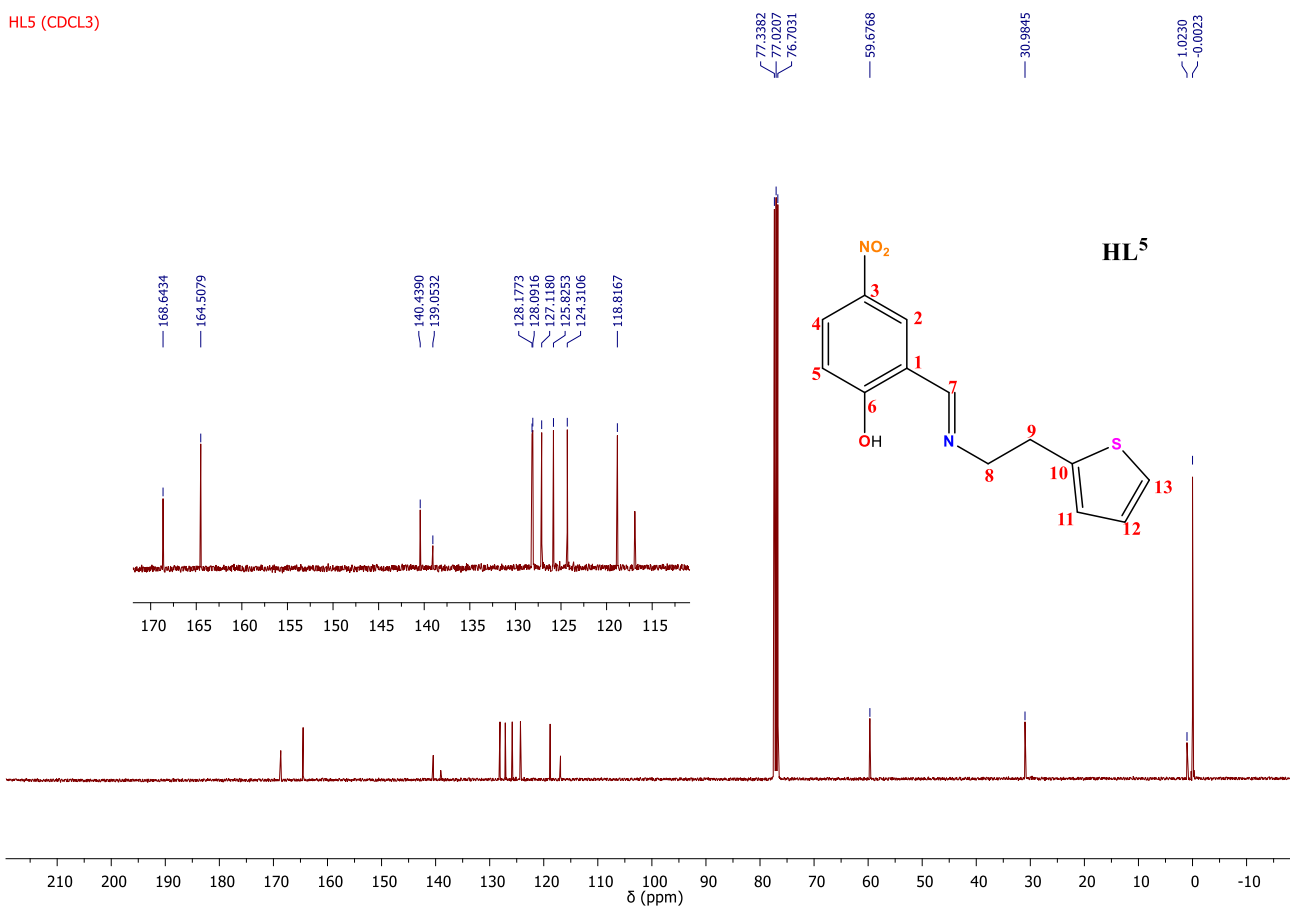**Figure 3.19.** ¹H NMR spectrum of ligand **HL⁴** in CDCl₃.
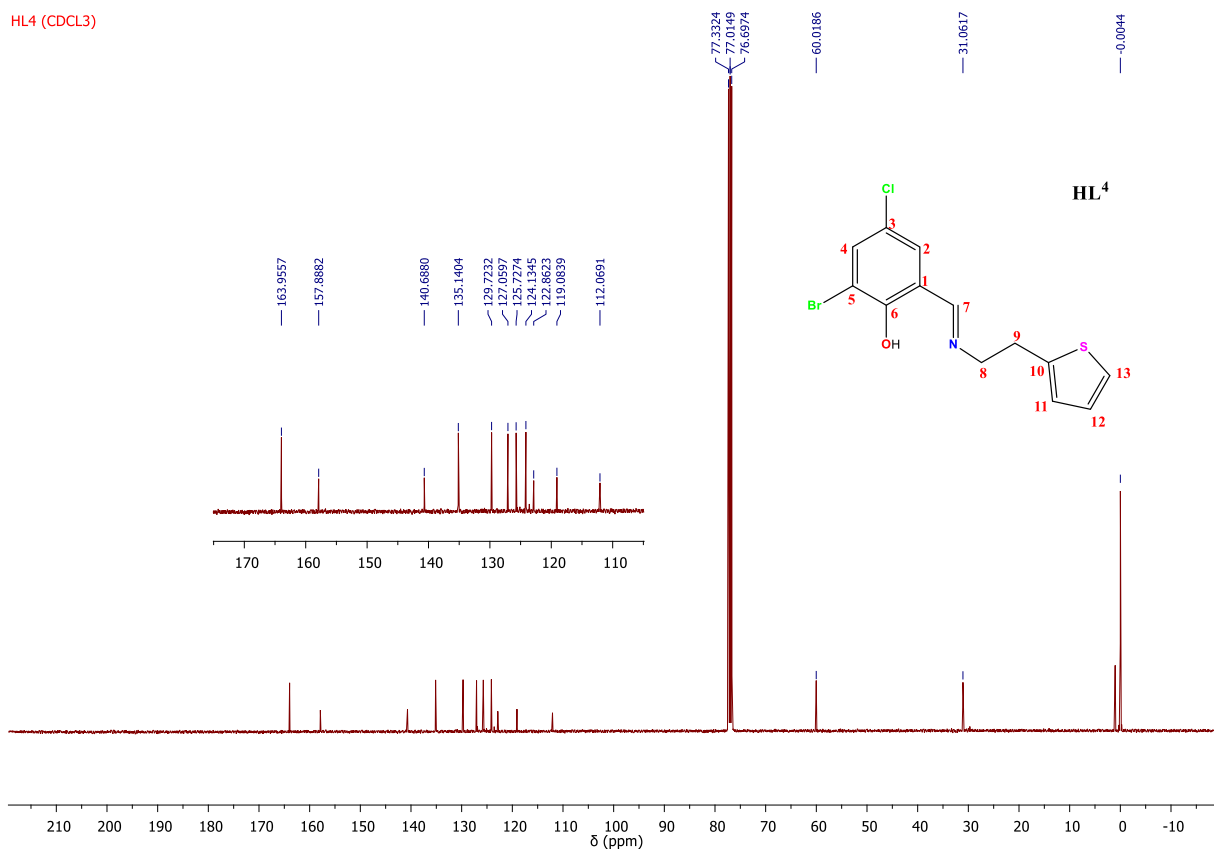
Figure 3.20. ^{13}C NMR spectrum of ligand **HL^4** in CDCl$_3$.

The ^{1}H spectrum of the ligands, **HL^5**, exhibited a characteristic azomethine (HC=N) resonance. The success of the Schiff-base condensation reaction was confirmed by the appearance of a singlet peak observed at 8.1779 ppm, which was due to the presence of the azomethine functionality. Asma *et al.* also agrees in their literature reported that the singlet is due to formation of the ligand which is a characteristic of the Schiff base [24]. The two triplets observed at the range of 3.2585-3.2915 ppm and 3.9208-3.9531 ppm in the ligand confirmed the presence of an ethylene arm (=N-CH$_2$CH$_2$) in the ligand [4] and the appearance of triplets indicated vicinal proton-proton coupling. The findings are similar to what William M. Motswainyana *et al.* observed in their work [5].

In the ^{13}C NMR spectrum of the ligand, the characteristic signal for the azomethine at appeared at 164.50 ppm according to the literature reported by Ahmad Ali Dehghani and Firouzabadi Sakineh Firouzmandi also observed similar peak at 162.5 ppm [45]. The two signals for the ethylene arm in HL^5 appeared at 59.6768 ppm and further upfield at 30.9845 ppm. Similar observation were observed by William M. Motswainyana *et al* in their literature [4]. The two carbon signals in the ligand differ greatly due to the dishielding effect of the nitrogen atom which becomes less pronounced as the length of the alkyl chain increases. These observations are consistent with those of similar compounds where the ethyl linker was reported to have similar influence for ferrocenylimine and salicylaldimine ligands with an appended heterocyclic moiety [37][38].

Figure 3.21. ^{1}H NMR spectrum of ligand **HL^5** in CDCl$_3$.

Figure 3.22. ^{13}C NMR spectrum of ligand **HL^5** in CDCl$_3$.

3.7 Mass Spectroscopy

The mass spectrometer is a versatile equipment which is quite helpful in providing the measure of the difference in mass-to charge ratio (m/z or m/e) of ionized atoms, molecules, and fragment ions. These charged ions are separated from each other and the mass spectrum records the quantity of ions of particular mass-to charge ratios. All the peak heights recorded on MS are proportional to the number of ions of each mass. In this manner, the readout using mass spectroscopy is used to determine the molecular weight and help support the identity and features of the molecular structure. The ligands synthesized herein were analysed by the GC-MS and the results are discussed below.

The mass spectrum of the compound **HL^1**, is presented in fig. 3.23. The highest mass peak, m/z 287 mu corresponds to the molecular mass of **HL^1** molecule, $C_{17}H_{21}NOS$. Subsequent fragmentation yields smaller fragment ions, which can be identified in the spectrum in as much the is a difference of (0.07) still the results are in line with the findings of Ommenya F.K *et al* where the [M+1] of the calculated compound is the same as the one that is observed in the mass spec [46]
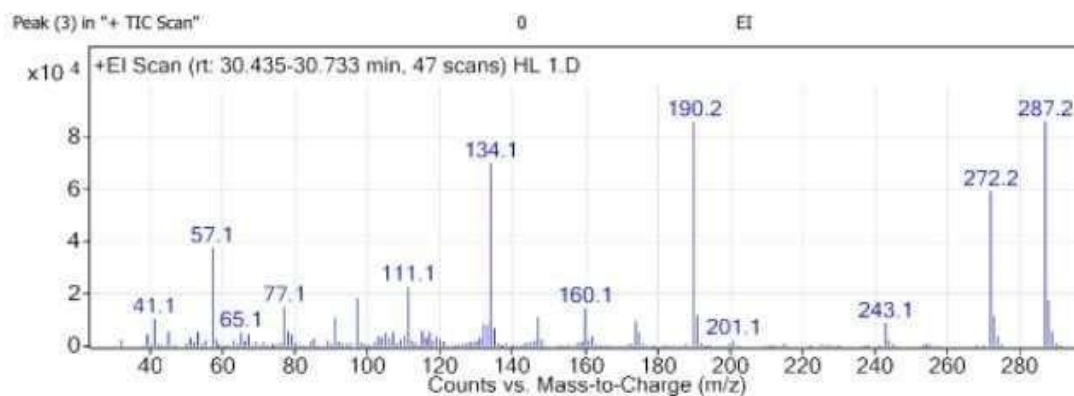
Figure 3.23. GC-MS of **HL^1**.

The proposed molecular formula of compound **HL^2** was $C_{20}H_{27}NO_2$. A peak at 298.2 m/z was identified as the molecular peak though was slightly different by 15 m/z compared to the calculated molecular weight (fig.3.24). This could be due to further fragmentation of the molecular ion peak by probably a CH_3^+. According to a literature report, interpretations of Mass Spectra of illogical peaks, it is accepted to have a difference of 15 between the calculated and obtained results that is said to correspond to elimination of one CH_3 group [47]

77
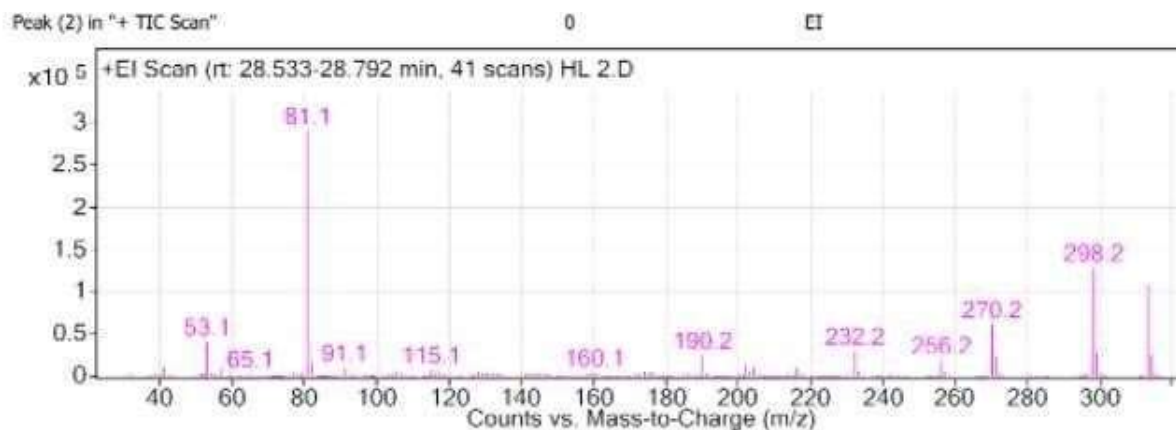
Figure 3.24. GC-MS of **HL²**.

The elemental analysis showed that the compound **HL³** was a pure compound. The compound had a molecular ion peak of 235.04 m/z as obtained in fig.3.25 below. This very much agreed with the calculated molecular weight from the molecular formula of the compound, $C_{12}H_{10}ClNO_2$. Davidson *et al.* reported in their similar work that difference of ±2% is acceptable [48].
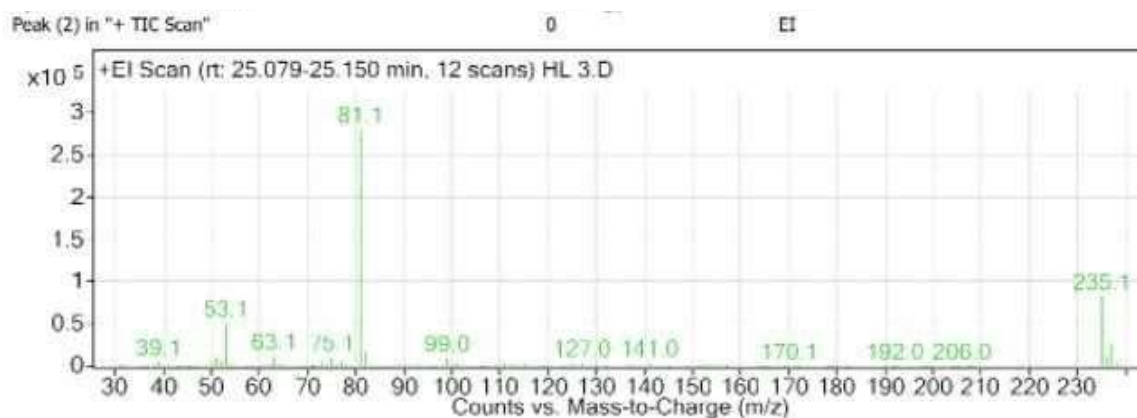
Figure 3.25, GC-MS of **HL³**.

From the mass spectrum for **HL⁴**, fig.3.26, which shows molecular ion peaks of The compound. The molecular ion peak observed was 342.0 m/z. which closely agree with the theoretical molecular weight of the synthesized compound $C_{13}H_{11}NOSBrCl$. The difference could be an addition of H_2, which could be as a result of the hydrogen gas from the instrument.

http://etd.uwc.ac.za/
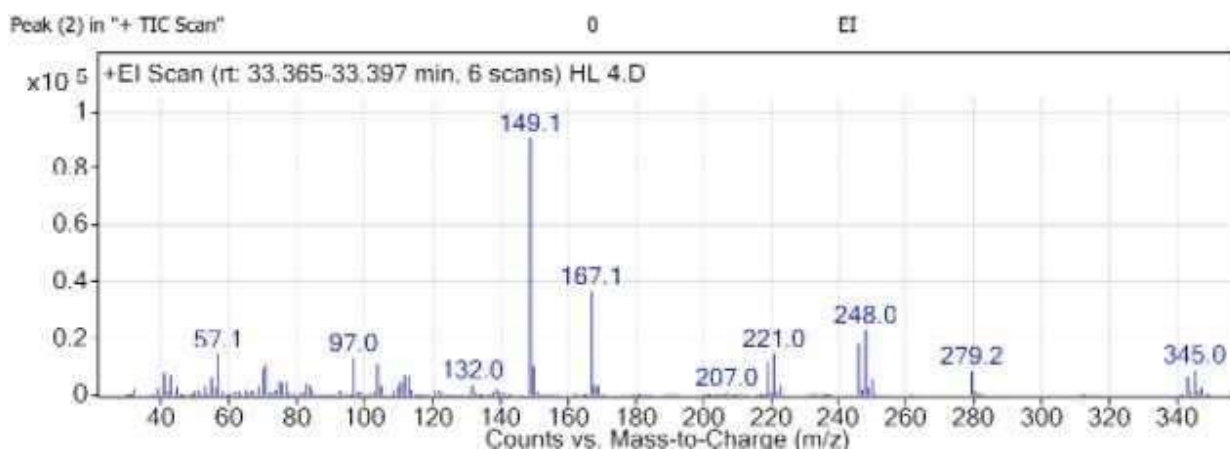
Figure 3.26, GC-MS of **HL**[4]

The compound had the molecular formula of $C_{13}H_{12}N_2O_3$ and the molecular ion peak obtained was 276.1 m/z and completely agreed with the calculated molecular weight. The observation agrees with the literature report [48]. All the ligands were confirmed of their molecular weights by using the MS [48].
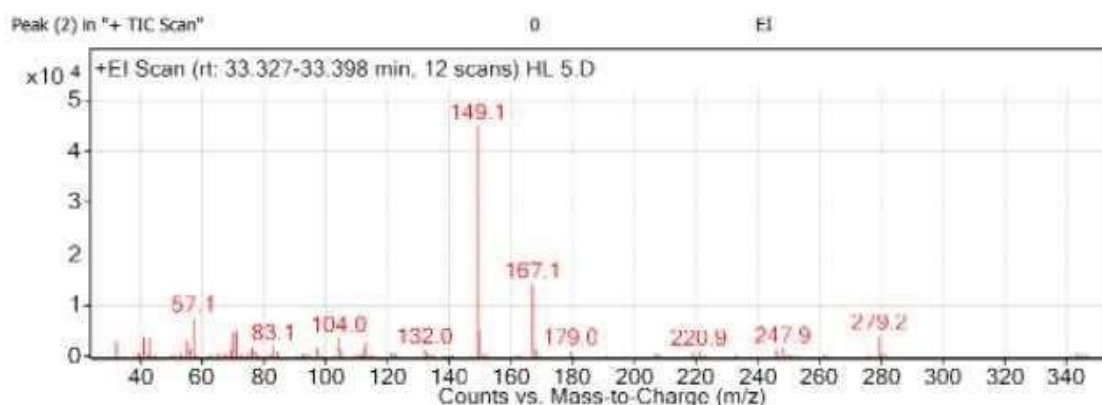
Figure 3.27, GC-MS of **HL**[5]

3.8 Electrochemical characterization

All the CV experiments were carried out using PalmSens Ptrace workstation. All the experimental solutions were purged using Argon. The chemically synthesized copper (II) complexes were dissolved in 0.3 M of TBAP solution. The complexes were sonicated for +/- 15 min until completely dissolved. Three-electrode configurations were often used where the working electrode was GCE, reference electrode Ag/AgCl, and counter electrode platinum wire. The GCE was cleaned by polishing it using alumina powder and sonicated in di-ionized water for 5 min before use. The electrochemical behavior of all the complexes was evaluated

79

by cycling the potential between -1.5 and 2.0 V at different scan rates of 50 and 100 mV/s. The C.V was conducted as a characterization technique to understand the redox behaviour of copper in the synthesized complexes and to further understand the effect of scan rate on copper (II) in the absence/presence of complexes.
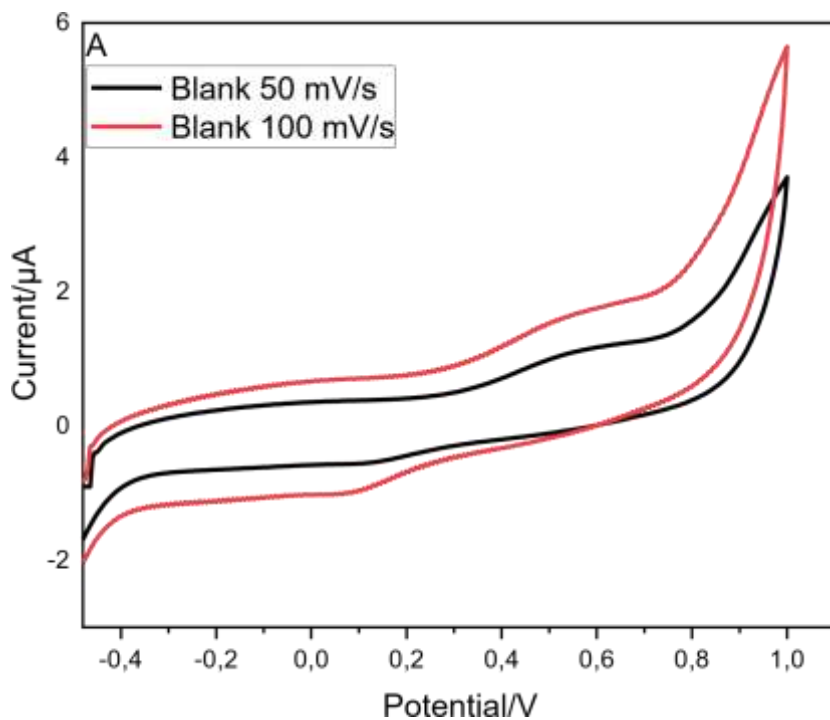
Figure: 3.28. Cyclic voltammogram of unmodified **GCE** in at scan rate of 50 and 100 mV/s.

The redox peaks of the C^1 were identified as Epa and Epc. The peak currents showed an increase with the increasing scan rate indicating good diffusion-controlled electron mobility [49]. The electrochemistry of the complex showed one reversible redox couple at 1.33, -0.74 V and 45.67, -30.70 μA respectively. Noticeably, the anodic peak(E_{pa})at scan rate 100 mV/s shifted towards the negative by -0.03 mV/s from that of scan rate of 50mV/s, while the cathodic peak (E_{pc}) at a scan rate of 100mV/s shifted to the towards positive potential by +0.08 mV/s, this is in agreement with the literature [50] [51]
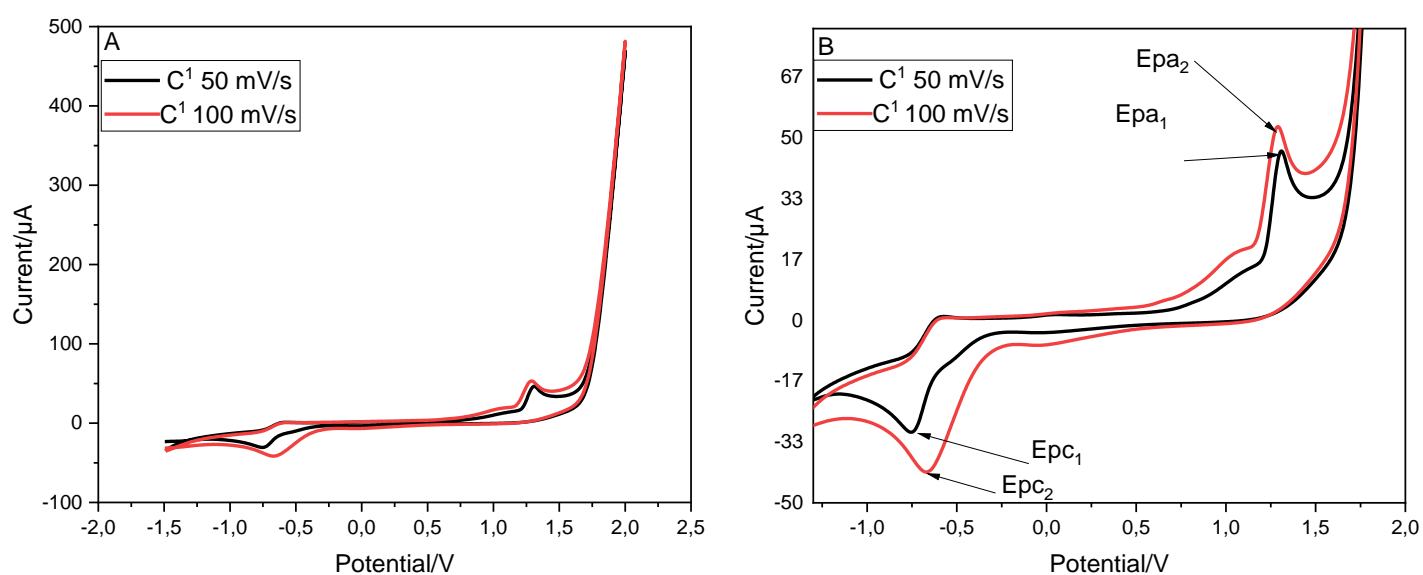
Figure 3.29. (a) Cyclic voltammogram of **Complex 1(C^1)** in 0.3 M of TBAP solution at scan rate of 50 and 100 mV/s. **(b)** zoomed in cyclic voltammogram of **(C^1)**.

81

Cyclic Voltammogram of C^2 obtained at a potential window of -1.5 to -2 mV/s at a scan rate of 50 and 100 mV/s in the presence of 0.3M TBAP solution and supporting electrolyte using the Cu^{2+} ion concentrations $1x10^{-3}$ M showed that the increase in the scan rate also increases the rate of redox reaction [11]. It is known that the more electrons are transferred the more the anodic and cathodic currents increase. As the ions are formed, the anodic and cathodic potential shifts their position to a more positive direction [12] [52]
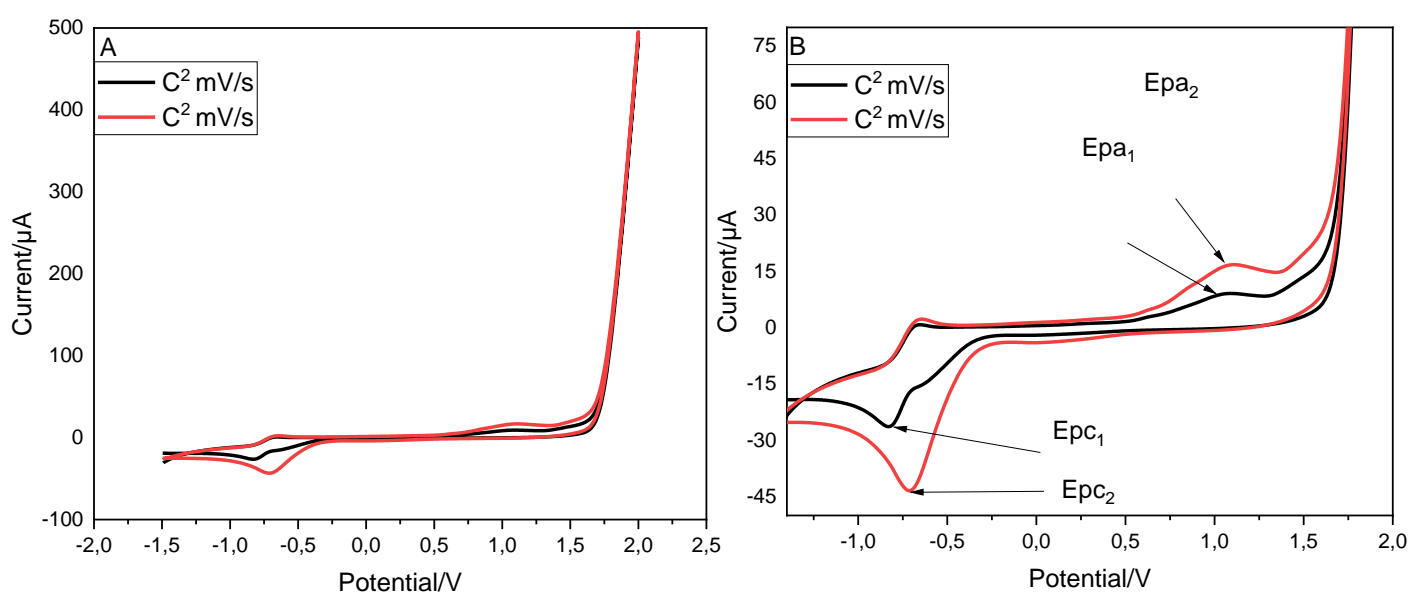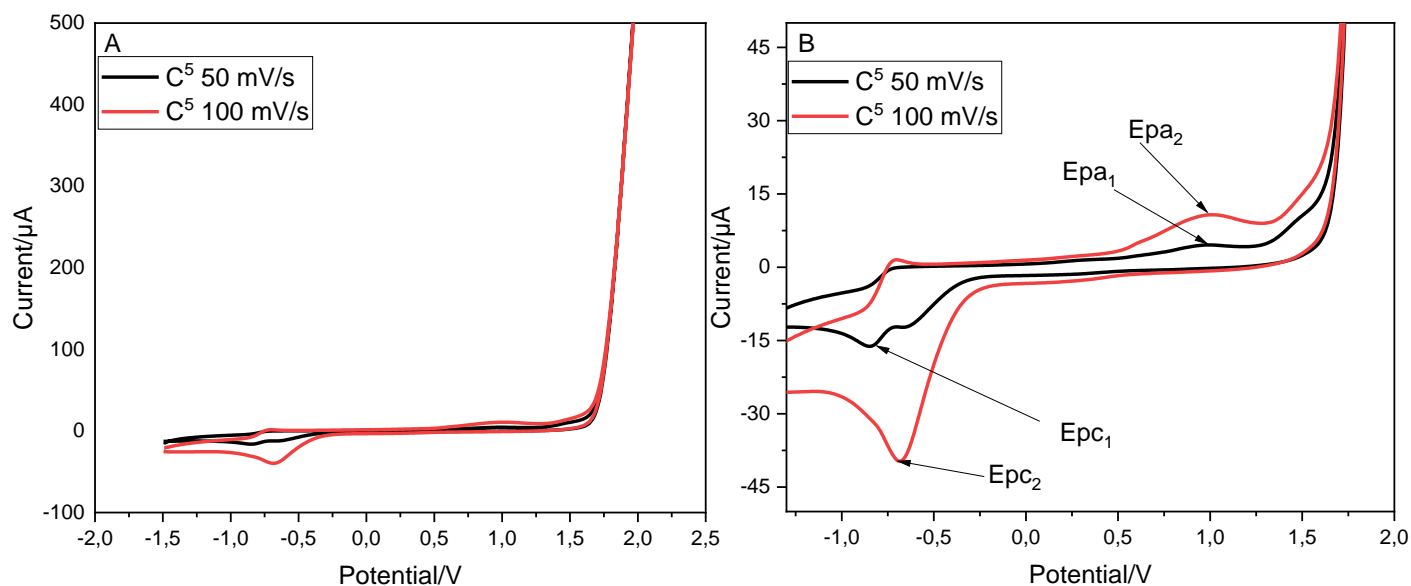

Figure 3.30. (a) Cyclic voltammogram of **complex 2 (C^2)** in 0.3 M of TBAP solution at scan rate of 50 and 100 mV/s. (**b**) zoomed in cyclic voltammogram of **(C^2).**

The cyclic voltammogram of **C³** exhibits a reversible redox peak. The ratio of anodic peak current to cathodic peak current (Ipa/Ipc) decreased at faster scan rates and the separation between peak potentials gradually increased with increasing scan rates. This is characteristic of a quasireversible one-electron redox process corresponding to the copper (II) couple [53] [54]. Furthermore, literature confirms that the analogous copper (II) compounds undergo diffusion-controlled quasi-reversible one-electron oxidation/reduction electrochemical processes [55].
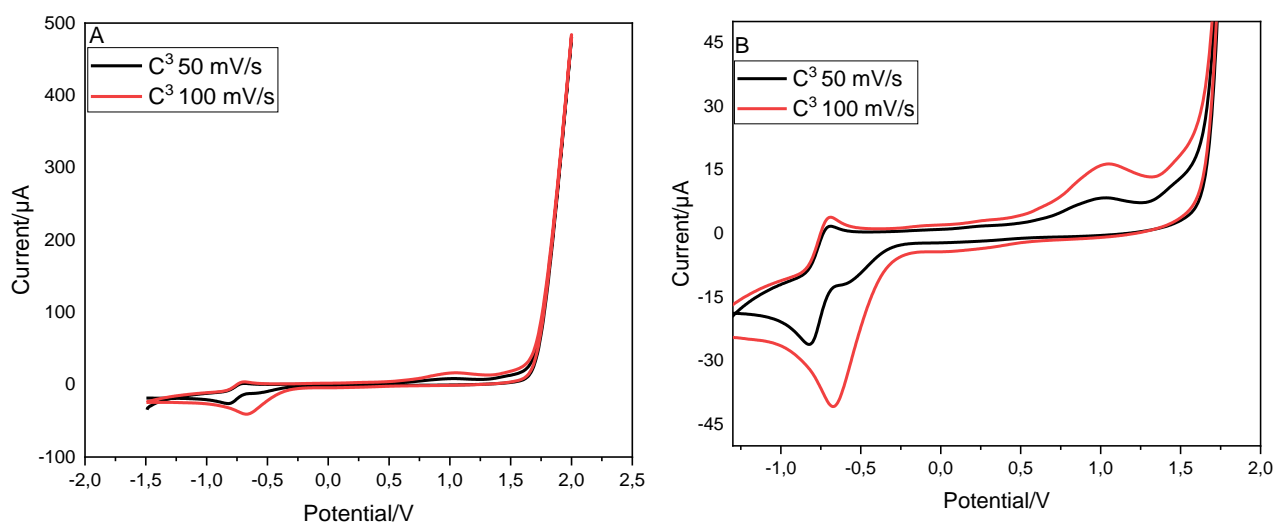
Figure 3.31. (a) Cyclic voltammogram of **complex 3 (C³)** in 0.3 M of TBAP solution at scan rate of 50 and 100 mV/s. **(b)** zoomed in cyclic voltammogram of (**C³**).

The changed scan rate displays a reflective effect on the redox peaks Ipa, and Ipc, which regularly enhances with increment in the scan rate i.e., from 50 to 100 mV/s and proportional to each other. The oxidation peaks of the complex were identified as Epa1 and Epa2 with complimentary reduction peaks (Figure 3.36). These peak currents showed an increase with the increasing scan rate indicating good diffusion-controlled electron mobility. The electrochemistry of **C⁴** showed two reversible redox couples. For the scan rate of 50 Mv/s it was observed that the Epa1 showed a potential peck which is at 1.01 mV/s with a current of 5.03 µA whereas at the maximum scan rate 100 mV/s we observe

83

a slight increase in the potential peck by 0.04 mV/s and for the current. It can be concluded that the increase is 8.58 µA which is in agreement with literature reports

indicating that an increase in the scan rate results in an increase in the peak observations [49][11][52].
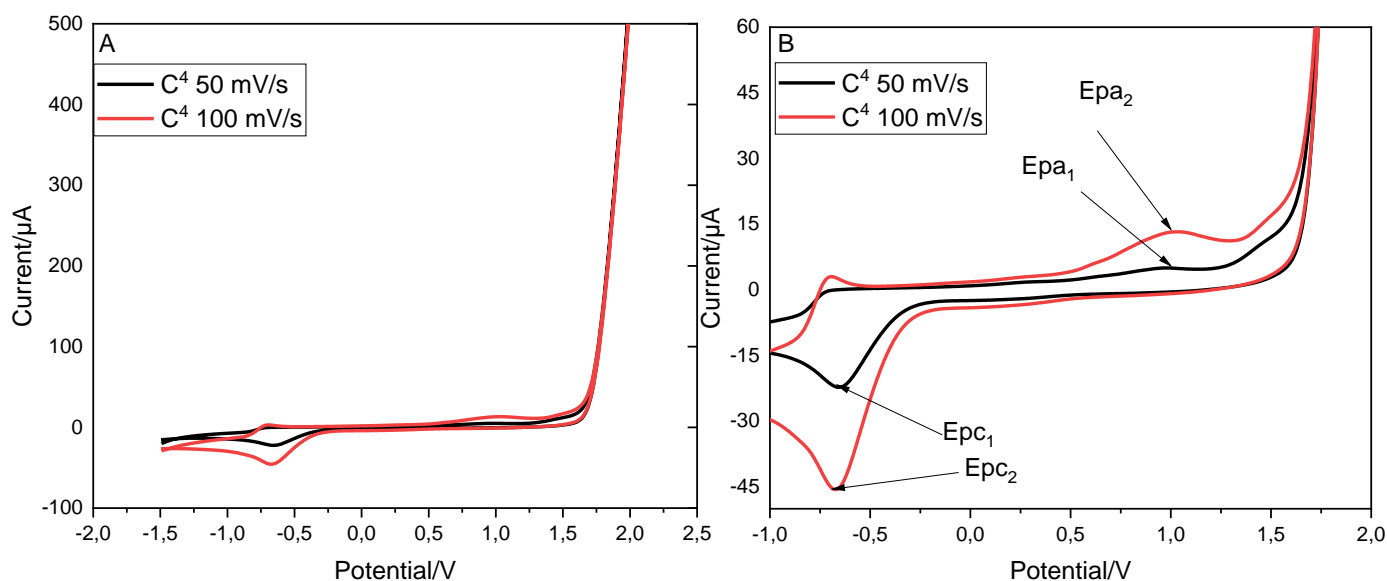
Figure 3.32. (a)Cyclic voltammogram of **complex 4 (C^4)** in 0.3 M of TBAP solution at scan rate of 50 and 100 mV/s. **(b)** Zoomed in cyclic voltammogram of **(C^4).**

Cyclic Voltammogram of **C^5** obtained at potential window of -1.5 to 2 mV/s at scan rate of 50 and 100 mV/s in the presence of 0.3M TBAP solution as supporting electrolyte and different Cu^{2+} ion concentrations 1×10^{-3} M. Again and as above, we observe an increase in the scan rate resulting in an increase in the rate of the redox reaction this is due to a higher scan rates the rate of diffusion is more than the rate of reaction. Hence, more electrolytic ions reach the electrode electrolyte interface whereas very few ions participate in the charge transfer reaction. Therefore, the current at higher scan rate increase. [11]. This indicates that more electrons are transferred from the complex to the electrode and therefore the anodic and cathodic currents have to increase. As the complex is formed the

84

anodic and cathodic potential shifts their position to a more positive direction with a function of scan rate which supports quasireversible process[49] [11] [52].

Figure 3.33. (a) Cyclic voltammogram of **complex 5 (C^5)** in 0.3 M of TBAP solution at scan rate of 50 and 100 mV/s. **(b)** zoomed in cyclic voltammogram of **(C^5).**

Table 3.2 Summary table of the CV studies.

Compound scan rate	Epa		Epc	
	Potential/(V)	Current/(μA)	Potential/(V)	Current/(μA)
C1 (50)	1.33	45.67	-0.74	-30.70
C1 (100)	1.30	52.85	-0.66	-41.21
C2 (50)	1.09	8.18	-0.82	-26.46
C2 (100)	1.11	17.06	-0.70	-43.55
C3 (50)	1.06	7.92	-0.80	-26.46
C3 (100)	1.07	16.10	-0.66	-40.66
C4 (50)	1.01	5.03	-0.65	-23.02
C4 (100)	1.05	13.61	-0.67	-45.25
C5 (50)	1.01	4.56	-0.83	-15.87
C5 (100)	1.03	11.06	-0.67	-40.34

3.9 Evaluation of the complexes as catalysts for alcohol oxidation reaction

The results were submitted for analysis of any products. However, the GC had no helium nor nitrogen to carry out the reactions. The results were stored in the fridge and here, the slow catalysis took place and eventually when the samples were run after over one year, no substantive results were obtained. An attempt to repeat the reaction was stalled by non-delivery of the chemical orders by the suppliers due to what they claimed to be a huge backlog. A sample of the result obtained which gave inadequate interpretation is given in Figure 3.37 below.
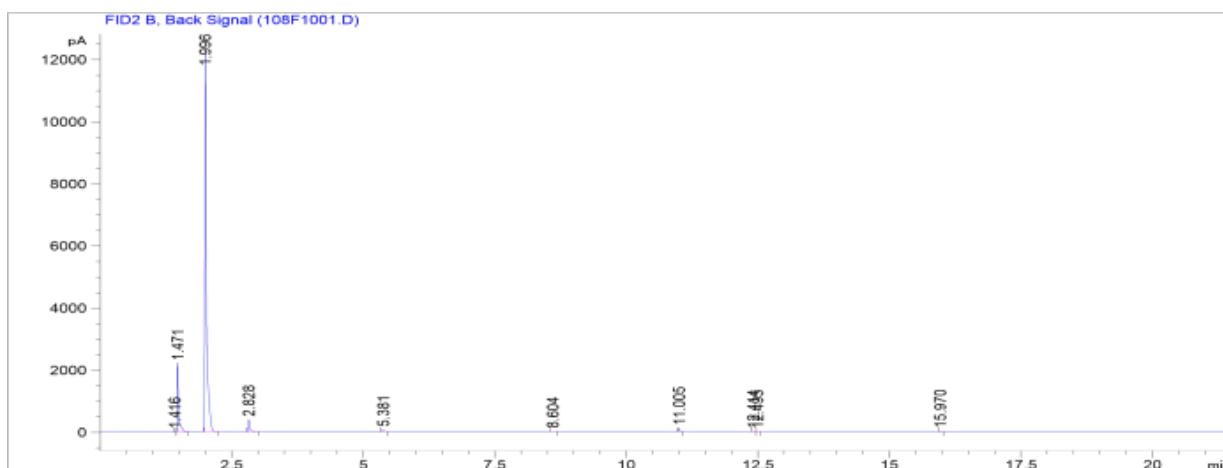
Figure 3.34. Sample of the chromatogram after 12 hours of catalysis reaction.

The solvent peak is very clearly seen however; the desired peaks gave inconclusive results. The GC results are attached to the Appendix for the reference purposes as a proof for the preliminary catalysis.

3.10 References

[1] Salehi, M., Faghani, F., Kubicki, M. and Bayat, M., 2018. New complexes of Ni (II) and Cu (II) with tridentate ONO Schiff base ligand: synthesis, crystal structures, electrochemical and theoretical investigation. *Journal of the Iranian Chemical Society*, *15*(10), pp.2229-2240.

[2] Hussain, Z., Yousif, E., Ahmed, A. and Altaie, A., 2014. Synthesis and characterization of Schiff's bases of sulfamethoxazole. *Organic and medicinal chemistry letters*, *4*(1), pp.1-4.

[3] Nejati, K., Rezvani, Z. and Massoumi, B., 2007. Syntheses and investigation of thermal properties of copper complexes with azo-containing Schiff-base dyes. *Dyes and pigments*, *75*(3), pp.653-657.

[4] Motswainyana, W., Onani, M., Lalancette, R. and Tarus, P., 2014. Hemilabile imino-phosphine palladium (II) complexes: synthesis, molecular structure, and evaluation in Heck reactions. *Chemical Papers*, *68*(7), pp.932-939.

[5] Motswainyana, W.M., Onani, M.O. and Madiehe, A.M., 2012. Bis (ferrocenylimine) palladium (II) and platinum (II) complexes: Synthesis, molecular structures and evaluation as antitumor agents. *Polyhedron*, *41*(1), pp.44-51.

[6] Ramesh, R. and Maheswaran, S., 2003. Synthesis, spectra, dioxygen affinity and antifungal activity of Ru (III) Schiff base complexes. *Journal of inorganic biochemistry*, *96*(4), pp.457-462.

[7] Martins, D.A., Bomfim, L.F., Silva, C.M.D., Fátima, Â.D., Louro, S.R., Batista, D.G., Soeiro, M.D.N.C., Carvalho, J.E.D. and Teixeira, L.R., 2017. Copper (II) nitroaromatic Schiff base complexes: synthesis, biological activity and their interaction with DNA and albumins. *Journal of the Brazilian Chemical Society*, *28*, pp.87-97.

[8] Dos Santos, J.E., Dockal, E.R. and Cavalheiro, É.T., 2005. Synthesis and characterization of Schiff bases from chitosan and salicylaldehyde derivatives. *Carbohydrate polymers*, *60*(3), pp.277-282.

[9] Busa, A.V., Lalancette, R., Nordlander, E. and Onani, M., 2018. New copper (II) salicylaldimine derivatives for mild oxidation of cyclohexane. *Journal of Chemical Sciences*, *130*(6), pp.1-10.

[10] Şenol, C., Hayvali, Z., Dal, H. and Hökelek, T., 2011. Syntheses, characterizations and structures of NO donor Schiff base ligands and nickel (II) and copper (II) complexes. *Journal of Molecular structure*, *997*(1-3), pp.53-59.

[11]   Habib, A., Shireen, T., Islam, A., Begum, N. and Alam, A.S., 2006. Cyclic voltammetric studies of copper and manganese in the presence of L-leucine using glassy carbon electrode. *Pakistan Journal of Analytical & Environmental Chemistry*, *7*(2), p.7.

[12]   Rana, M., Rahman, M.A. and Alam, A.M., 2014. A CV study of copper complexation with guanine using glassy carbon electrode in aqueous medium. *International Scholarly Research Notices*, *2014*.

[13]   Signorini, O., Dockal, E.R., Castellano, G. and Oliva, G., 1996. Synthesis and characterization of aquo [N, N′-ethylenebis (3-ethoxysalicylideneaminato)] dioxouranium (VI). *Polyhedron*, *15*(2), pp.245-255.

[14]   Kasumov, V.T., Bulut, A., Köksal, F., Aslanogˇlu, M., Uçar, İ. and Kazak, C., 2006. Synthesis, structure, spectroscopic and redox properties of copper (II)-N-3, 5-Bu2tphenylsalicylaldinine complexes: Crystal and molecular structure of bis (N-3, 5-Bu2t-phenylsalicylaldininato) copper (II). *Polyhedron*, *25*(5), pp.1133-1141.

[15]   Kyei, S.K., Akaranta, O. and Darko, G., 2020. Synthesis, characterization and antimicrobial activity of peanut skin extract-azo-compounds. *Scientific African*, *8*, p.e00406.

[16]   N. Abdulabbasbahar and H. Thamerghanim, "Synthesis and Characterization of some Heterocyclic Compounds from Indole Derivatives ABSTRACT:," no. 8, pp. 1–16.

[17]   Elantabli, F.M., Radebe, M.P., Motswainyana, W.M., Owaga, B.O., El-Medani, S.M., Ekengard, E., Haukka, M., Nordlander, E. and Onani, M.O., 2017. Thiophene based imino-pyridyl palladium (II) complexes: Synthesis, molecular structures and Heck coupling reactions. *Journal of Organometallic Chemistry*, *843*, pp.40-47.

[18]   Ahmed, A.H., Hassan, A.M., Gumaa, H.A., Mohamed, B.H., Eraky, A.M. and Omran, A.A., 2019. Copper (II)-oxaloyldihydrazone complexes: Physico-chemical studies: Energy band gap and inhibition evaluation of free oxaloyldihydrazones toward the corrosion of copper metal in acidic medium. *Arabian Journal of Chemistry*, *12*(8), pp.4287-4302.

[19]   Bhatia, P. and Nath, M., 2020. Green synthesis of p-NiO/n-ZnO nanocomposites: Excellent adsorbent for removal of congo red and efficient catalyst for reduction of 4-nitrophenol present in wastewater. *Journal of Water Process Engineering*, *33*, p.101017.

[20]   El-Gammal, O.A., El-Reash, G.A., Yousef, T.A. and Mefreh, M., 2015. Synthesis, spectral characterization, computational calculations and biological activity of complexes

designed from NNO donor Schiff-base ligand. *Spectrochimica Acta Part A: Molecular and Biomolecular Spectroscopy*, *146*, pp.163-176.

[21]   Bartyzel, A., 2018. Synthesis, thermal behaviour and some properties of CuII complexes with N, O-donor Schiff bases. *Journal of Thermal Analysis and Calorimetry*, *131*(2), pp.1221-1236.

[22]   Guo, Y., Hu, X., Zhang, X., Pu, X. and Wang, Y., 2019. The synthesis of a Cu (ii) Schiff base complex using a bidentate N 2 O 2 donor ligand: crystal structure, photophysical properties, and antibacterial activities. *RSC advances*, *9*(71), pp.41737-41744.

[23]   Elsherif, K.M., Zubi, A., Shawish, H., Almelah, E. and Abajja, S., 2019. UV-VIS Absorption Spectral Studies of N, N′-Bis (salicylidene) ethylenediamine (Salen) in Different Solvents. *Iraqi Journal of Science*, pp.204-210.

[24]   Kavitha, N. and Alivelu, M., 2021. Investigation of Structures, QTAIM, RDG, ADMET, and docking properties of SASC compound using experimental and theoretical approach. *Computational and Theoretical Chemistry*, *1201*, p.113287.

[25]   Tomczyk, D., Nowak, L., Bukowski, W., Bester, K., Urbaniak, P., Andrijewski, G. and Olejniczak, B., 2014. Reductive and oxidative electrochemical study and spectroscopic properties of nickel (II) complexes with N2O2 Schiff bases derived from (±)-trans-N, N′-bis (salicylidene)-1, 2-cyclohexanediamine. *Electrochimica Acta*, *121*, pp.64-77.

[26]   Arjmand, F., Sayeed, F. and Muddassir, M., 2011. Synthesis of new chiral heterocyclic Schiff base modulated Cu (II)/Zn (II) complexes: their comparative binding studies with CT-DNA, mononucleotides and cleavage activity. *Journal of Photochemistry and Photobiology B: Biology*, *103*(2), pp.166-179.

[27]   Haribabu, P., Patil, Y.P., Hussain Reddy, K. and Nethaji, M., 2014. Synthesis, crystal structure, DNA interaction and cleavage activities of mononuclear and trinuclear copper (II) complexes. *Transition Metal Chemistry*, *39*(2), pp.167-175.

[28]   Ara Elachi K., "Synthesis, Spectral and Thermal Characterization of Cu(II) Complexes Containing Schiff Base Ligands and Their Antibacterial Activity Study," *Am. J. Mater. Synth. Process.*, vol. 4, no. 1, p. 43, 2019.

[29]   C. Karakaya, B. Dede, and E. Cicek, "Novel metal(II) complexes with bidentate Schiff base ligand: Synthesis, spectroscopic properties and dye decolorization functions," *Acta Phys. Pol. A*, vol. 129, no. 2, pp. 208–212, 2016.

[30]   Ulusoy, M., Karabıyık, H., Kılınçarslan, R., Aygün, M., Cetinkaya, B. and García-Granda, S., 2008. Co (II) and Cu (II) Schiff base complexes of bis (N-(4-diethylamino-2-methylphenyl)-3, 5-di-tert-butylsalicylaldimine): Electrochemical and X-ray structural study. *Structural Chemistry*, *19*(5), pp.749-755.

[31]   UÇAN, S.Y., SYNTHESIS AND SPECTROSCOPIC CHARACTERIZATION OF BIDENTATE SCHIFF BASE AND ZINC (II) COMPLEX. *Eurasian Journal of Science Engineering and Technology*, *1*(1), pp.35-40.

[32]   Yilmaz, I. and Çukurovali, A., 2003. Salicylaldehyde thiazolyl hydrazones as ligands. *Heteroatom Chemistry: An International Journal of Main Group Elements*, *14*(7), pp.617-621.

[33]   Matsuo, H., Miyazaki, Y., Takemura, H., Matsuoka, S., Sakashita, H. and Yoshimura, K., 2004. 11B NMR study on the interaction of boric acid with Azomethine H. *Polyhedron*, *23*(6), pp.955-961.

[34]   Berman, A.M. and Johnson, J.S., 2004. Copper-catalyzed electrophilic amination of diorganozinc reagents. *Journal of the American Chemical Society*, *126*(18), pp.5680-5681.

[35]   Salih, K.S., Shraim, A.M., Al-Mhini, S.R., Al-Soufi, R.E. and Warad, I., 2021. New tetradentate Schiff base Cu (II) complexes: synthesis, physicochemical, chromotropism, fluorescence, thermal, and selective catalytic oxidation. *Emergent Materials*, *4*(2), pp.423-434.

[36]   Gokulnath, G., Manikandan, R., Anitha, P. and Umarani, C., 2021. SYNTHESIS, CHARACTERIZATION AND ANTIBACTERIAL STUDIES OF Co (II), Ni (II) AND Cu (II) COMPLEXES CONTAINING TRIPHENYLPHOSPHINE AND SCHIFF BASE LIGAND BASED ON SALICYLALDEHYDE. *spectrum*, *14*(4), pp.2692-2697.

[37]   Elantabli, F.M., Radebe, M.P., Motswainyana, W.M., Owaga, B.O., El-Medani, S.M., Ekengard, E., Haukka, M., Nordlander, E. and Onani, M.O., 2017. Thiophene based imino-pyridyl palladium (II) complexes: Synthesis, molecular structures and Heck coupling reactions. *Journal of Organometallic Chemistry*, *843*, pp.40-47.

[38]   Pettersen, E.F., Goddard, T.D., Huang, C.C., Couch, G.S., Greenblatt, D.M., Meng, E.C. and Ferrin, T.E., 2004. UCSF Chimera—a visualization system for exploratory research and analysis. *Journal of computational chemistry*, *25*(13), pp.1605-1612.

[39]   Sumrra, S.H., Ibrahim, M., Ambreen, S., Imran, M., Danish, M. and Rehmani, F.S., 2014. Synthesis, spectral characterization, and biological evaluation of transition metal complexes of bidentate N, O donor Schiff bases. *Bioinorganic chemistry and applications*, *2014*.

[40]   Srinivas, M., Vijayakumar, G.R., Mahadevan, K.M., Nagabhushana, H. and Naik, H.B., 2017. Synthesis, photoluminescence and forensic applications of blue light emitting azomethine-zinc (II) complexes of bis (salicylidene) cyclohexyl-1, 2-diamino based organic ligands. *Journal of Science: Advanced Materials and Devices*, *2*(2), pp.156-164.

[41]   Kafi-Ahmadi, L. and Marjani, A.P., 2019. Mononuclear Schiff base complexes derived from 5-azophenylsalicylaldehyde with Co (ii), Ni (ii) ions: Synthesis, characterization, electrochemical study and antibacterial properties. *South African Journal of Chemistry*, *72*, pp.101-107.

[42]   Khanmohammadi, H. and Darvishpour, M., 2009. New azo ligands containing azomethine groups in the pyridazine-based chain: Synthesis and characterization. *Dyes and Pigments*, *81*(3), pp.167-173.

[43]   Holeček, J., Lyčka, A., Micák, D., Nagy, L., Vankó, G., Brus, J., Raj, S. and Fun, H.K., 1999. Infrared, 119 Sn, 13 C and 1 H NMR, 119 Sn and 13 C CP/MAS NMR and Mössbauer Spectral Study of Some Tributylstannyl Citrates and Propane-1, 2, 3-tricarboxylates. *Collection of Czechoslovak Chemical Communications*, *64*(6), pp.1028-1048.

[44]   Dehghani-Firouzabadi, A.A. and Firouzmandi, S., 2017. Synthesis and characterization of a new unsymmetrical potentially pentadentate Schiff base ligand and related complexes with manganese (II), nickel (II), copper (II), zinc (II) and cadmium (II). *Journal of the Brazilian Chemical Society*, *28*, pp.768-774.

[45]   Ommenya, F.K., Nyawade, E.A., Andala, D.M. and Kinyua, J., 2020. Synthesis, characterization and antibacterial activity of Schiff base, 4-Chloro-2-{(E)-[(4-fluorophenyl) imino] methyl} phenol metal (II) complexes. *Journal of Chemistry*, *2020*.

[46]   Davidson, J.T., Lum, B.J., Nano, G. and Jackson, G.P., 2018. Comparison of measured and recommended acceptance criteria for the analysis of seized drugs using gas chromatography–mass spectrometry (GC–MS). *Forensic Chemistry*, *10*, pp.15-26.

[47]   Elgrishi, N., Rountree, K.J., McCarthy, B.D., Rountree, E.S., Eisenhart, T.T. and Dempsey, J.L., 2018. A practical beginner's guide to cyclic voltammetry. *Journal of chemical education*, *95*(2), pp.197-206.

[48]   Koudehi, M.F. and Pourmortazavi, S.M., 2017. Synthesis and application of carbowax/polypyrrole nanocomposite for fabrication of electrochemical sensor to detect 2, 4-DNT vapor. *Materials Research Express*, *4*(8), p.086303.

[49]   Nazim, M., Ameen, S., Akhtar, M.S. and Shin, H.S., 2019. Electrochemical Detection of Chloride Ions by Copper (II) Complex with Mixed Ligand of Oxindole Derivative and Dithiocarbamates Moiety. *Applied Sciences*, *9*(7), p.1358.

[50]   S. Hamnca, "Electrochemical Screening of Antibiotic Residues in Water By," no. November, 2015.

[51]   Laviron, E.J.J., 1979. General expression of the linear potential sweep voltammogram in the case of diffusionless electrochemical systems. *Journal of Electroanalytical Chemistry and Interfacial Electrochemistry*, *101*(1), pp.19-28.

[52]   Janeva, M., Kokoskarova, P., Maksimova, V. and Gulaboski, R., 2019. Square-wave Voltammetry of Two-step Surface Electrode Mechanisms Coupled with Chemical Reactions–A Theoretical Overview. *Electroanalysis*, *31*(12), pp.2488-2506.

[53]   Fernández-G, J.M., Hernández-Ortega, S., Cetina-Rosado, R., Macías-Ruvalcaba, N. and Aguilar-Martínez, M., 1998. The crystal structures and electrochemical studies of three 2, 3-naphthalenic Schiff base copper (II) complexes. *Polyhedron*, *17*(15), pp.2425-2432.

[54]   Tojo, G. and Fernández, M.I., 2006. *Oxidation of alcohols to aldehydes and ketones: a guide to current common practice*. Springer Science & Business Media.

[55]   Arends, I.W. and Sheldon, R.A., 2004. Modern oxidation of alcohols using environmentally benign oxidants. *Modern oxidation methods*, pp.83-118.

[56]   Figiel, P.J., Kirillov, A.M., Karabach, Y.Y., Kopylovich, M.N. and Pombeiro, A.J., 2009. Mild aerobic oxidation of benzyl alcohols to benzaldehydes in water catalyzed by aqua-soluble multicopper (II) triethanolaminate compounds. *Journal of Molecular Catalysis A: Chemical*, *305*(1-2), pp.178-182.

[57]   Ng, K.Y., Tu, L.C., Wang, Y.S., Chan, S.I. and Yu, S.S.F., 2008. Probing the hydrophobic pocket of the active site in the particulate methane monooxygenase (pMMO) from Methylococcus capsulatus (Bath) by variable stereoselective alkane hydroxylation and olefin epoxidation. *ChemBioChem*, *9*(7), pp.1116-1123.

[58]   Wertz, S. and Studer, A., 2013. Nitroxide-catalyzed transition-metal-free aerobic oxidation processes. *Green chemistry*, *15*(11), pp.3116-3134.

[59]   Nutting, J.E., Rafiee, M. and Stahl, S.S., 2018. Tetramethylpiperidine N-oxyl (TEMPO), phthalimide N-oxyl (PINO), and related N-oxyl species: electrochemical properties and their use in electrocatalytic reactions. *Chemical reviews*, *118*(9), pp.4834-4885.

[60]   Gamez, P., Arends, I.W., Reedijk, J. and Sheldon, R.A., 2003. Copper (II)-catalysed aerobic oxidation of primary alcohols to aldehydes. *Chemical communications*, (19), pp.2414-2415.

[61]   Kumpulainen, E.T. and Koskinen, A.M., 2009. Catalytic activity dependency on catalyst components in aerobic copper–TEMPO oxidation. *Chemistry–A European Journal*, *15*(41), pp.10901-10911.

[62]   Brioche, J., Masson, G. and Zhu, J., 2010. Passerini three-component reaction of alcohols under catalytic aerobic oxidative conditions. *Organic Letters*, *12*(7), pp.1432-1435.

[63]   Figiel, P.J., Leskelä, M. and Repo, T., 2007. TEMPO-Copper (II) Diimine-Catalysed Oxidation of Benzylic Alcohols in Aqueous Media. *Advanced Synthesis & Catalysis*, *349*(7), pp.1173-1179.

[64]   Hoover, J.M. and Stahl, S.S., 2011. Highly practical copper (I)/TEMPO catalyst system for chemoselective aerobic oxidation of primary alcohols. *Journal of the American Chemical Society*, *133*(42), pp.16901-16910.

[65]   Mannam, S. and Sekar, G., 2009. An enantiopure galactose oxidase model: synthesis of chiral amino alcohols through oxidative kinetic resolution catalyzed by a chiral copper complex. *Tetrahedron: Asymmetry*, *20*(4), pp.497-502.

[66]   Lin, L., Liuyan, J. and Yunyang, W., 2008. Base promoted aerobic oxidation of alcohols to corresponding aldehydes or ketones catalyzed by CuCl/TEMPO. *Catalysis Communications*, *9*(6), pp.1379-1382.

[67]   Ragagnin, G., Betzemeier, B., Quici, S. and Knochel, P., 2002. Copper-catalysed aerobic oxidation of alcohols using fluorous biphasic catalysis. *Tetrahedron*, *58*(20), pp.3985-3991.

Chapter 4

4.1 Conclusion and Future work

4.1.1 Conclusion

In this work, we have successfully synthesized 10 new compounds (5 ligands and their copper (II) complexes). The work initially synthesized the salicylaldimine ligand using the literature methods with great yields [1]. The salicylaldiminato-copper (II) complexes were synthesized using the Schiff base ligands. Subsequent to the investigations conducted in this study, the salicylaldimine Schiff base ligands HL^1-HL^5 and their salicylaldiminato-copper (II) complexes were fully characterized. Consequently, our objective one of the syntheses of both ligands and the complexes were successful.

The compounds were characterized using analytical techniques (FTIR, NMR. UV-Vis, Elemental Analysis, Mass spec, and CV). The FTRI spectra had the azomethine moiety stretching frequency at a range of 1612-1662 cm^{-1} as expected which proved the presence of the Schiff base condensation products. The ligands' ^1H- NMR spectroscopy as well as their $^{13}C\{^1H\}$-NMR spectra were well discussed and confirmed that the compounds were duly prepared. Copper (II) complexes are not characterized by NMR because Cu isotopes are quadrupolar and normally yield broad signals, which in medium and large molecules may be too broad to be observed with a high-resolution NMR spectrometer. Again our second objective was achieved from the full characterization of the prepared compounds by suing the standard analytical techniques including CV studies.

Furthermore all the compounds absorbed in the UV-Vis region. All ligands showed two peaks and the bands assigned to π - π * transition of the aromatic ring and n - π * of the phenyl ring, and a peak attributed to the C=N group. On the other hand with the complexes we observed 3 peaks attributed to π - π *, n - π * and LMCT.

Furthermore, the mass spectroscopy showed interesting results, where the calculated molecular weight of the compounds was very close to that of the observed compound and these results are in agreement with the results received from elemental analysis which were indicative of the compounds purity,

The complexes were further characterized by cyclic voltammetry. According to the data we obtained, the unmodified GCE showed no peaks before the addition of the copper (II) complexes into the solution. However, after the addition of the complexes, an intense redox

peaks were observed with the Epa which may be attributed to the free copper ions in the solution. Cathodic and anodic currents increased with scan rate at 50 mV/s and 100 mV/s, respectively. Furthermore, a literature confirmation was achieved in which as the scan rates increase, the cathodic potential (Epc) shifts to more negative potentials while the anodic potential (Epa) shifts to more positive potentials in order to detect copper ions. Therefore the CV confirmed the successful formation of Copper (II) complexes.

Our last objective was not fully achieved however, complex 1 was tested for catalytic activity unfortunately the obtained results did not show any conclusive results which was attributed to the following factors

- The samples aliquoted stayed for long time in the refrigerator due to the covid-19 pandemic lockdown.

- The further delay in testing the samples was due to the delay in delivering of the gas for the GC.

4.1.2 Future Work

The synthesized and characterized complexes were employed as catalyst precursors in the mild oxidation of alcohol oxidation, however, the oxidation results were not fully obtained. Therefore, for future work, there is a need to investigate the catalytic activity of the synthesized ligands and the copper (II) complexes and study the catalytic cycle of these new complexes as compared to reported studies [1].

We also wish to expand the scope of this study by investigating the use of salicylaldimine ligands that are endowed with a pyrrole/thiophene moiety, followed by the synthesis of salicylaldiminato-copper (II) complexes anchored by the resulting ligands and to fully characterize complexes and test their catalytic performance in the mild oxidation of alcohols.

Ligands 1 and 2 formed crystals however we were unable to obtain the crystal structure results as they were not yet available, against due to covid-19 pandemic, the results can be further used to identify the actual structure of the ligands.

Furthermore, the preliminary catalytic studies was conducted only for one of the complexes. The rest of the complexes should also have their catalytic abilities tested because this is very important for our objective of finding highly selective mild oxidants of the alcohols to produce value added organic substrates.

4.2 References

[1]   A. V. Busa, R. Lalancette, E. Nordlander, and M. Onani, "New copper(II) salicylaldimine derivatives for mild oxidation of cyclohexane," *J. Chem. Sci.*, vol. 130, no. 6, 2018.

Appendix 1
Spectra of synthesized compounds
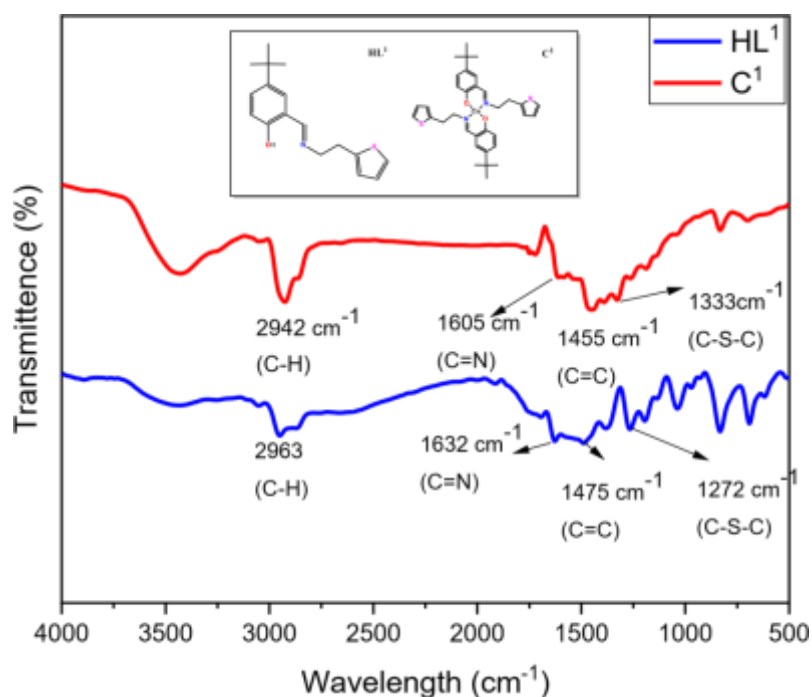
Figure 3.3. FTIR spectra of **HL^1** and **C^1.**
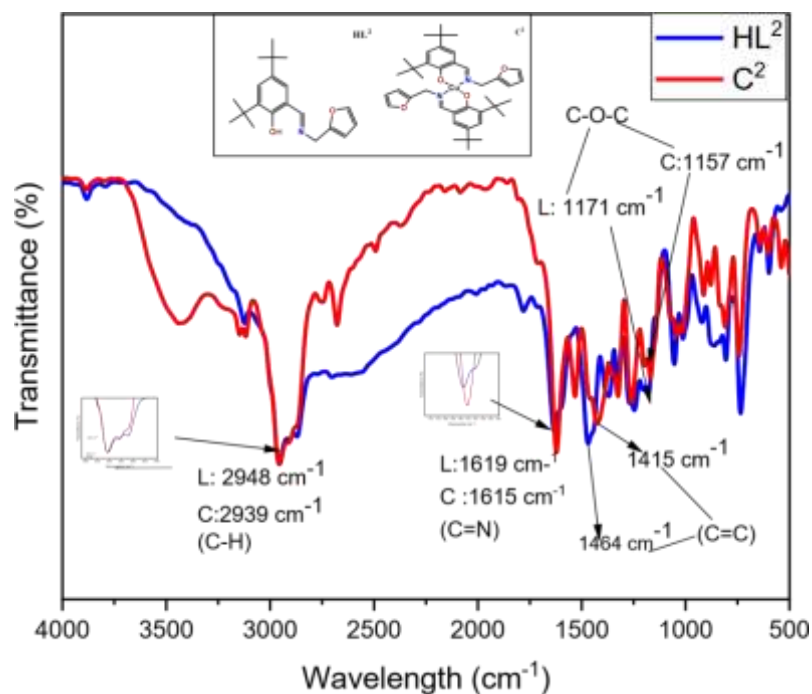
Figure 3.4. FTIR spectra of **HL^2** and **C^2**.
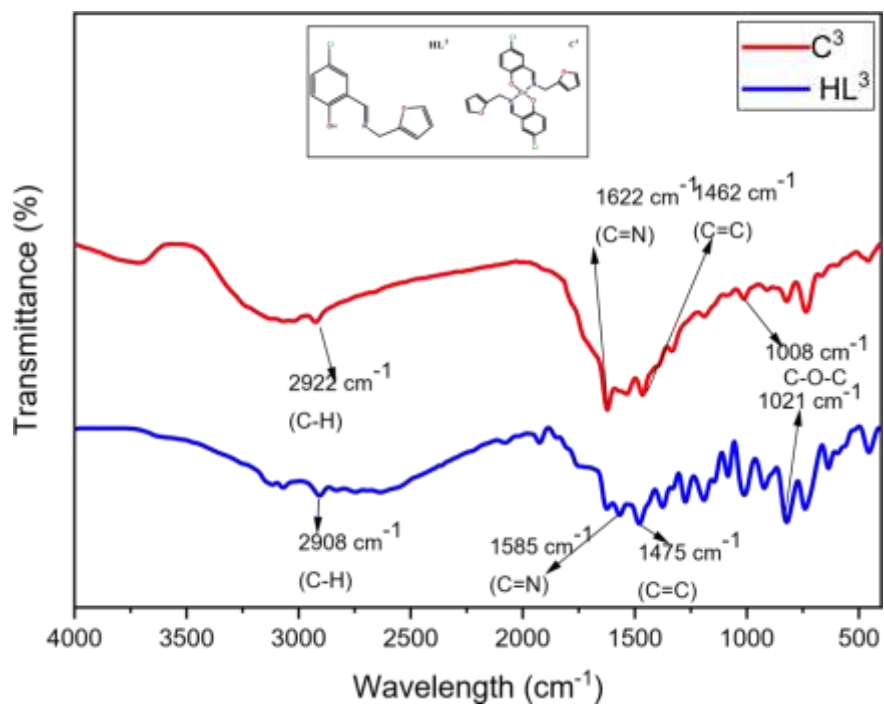
Figure 3.5. FTIR spectra of **HL³** and **C³**.

Figure 3.6. FTIR spectra of **HL⁴** and **C⁴**.

99
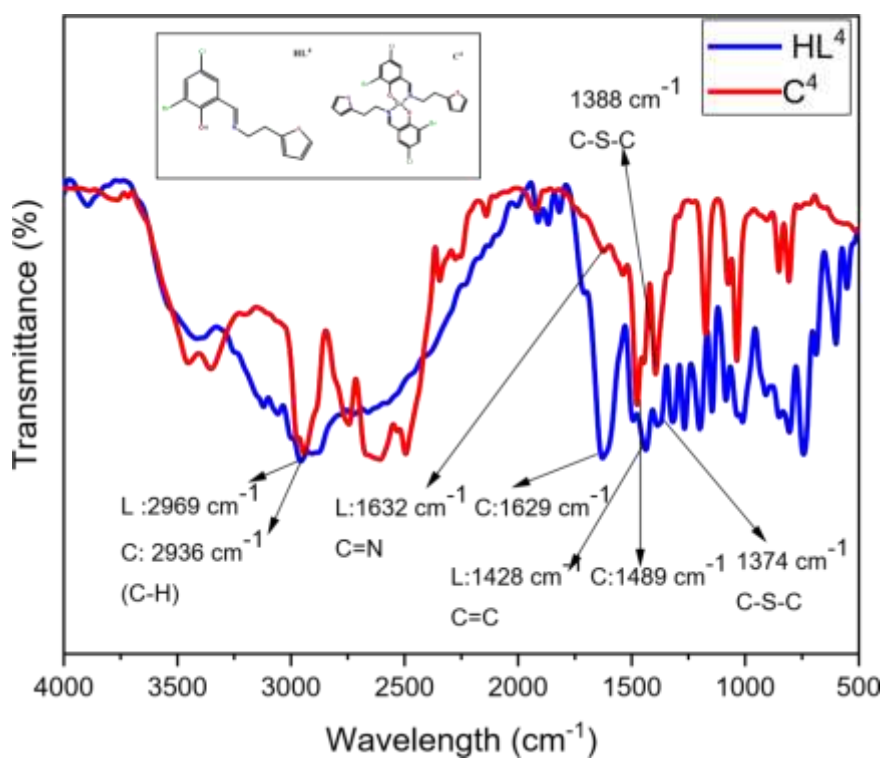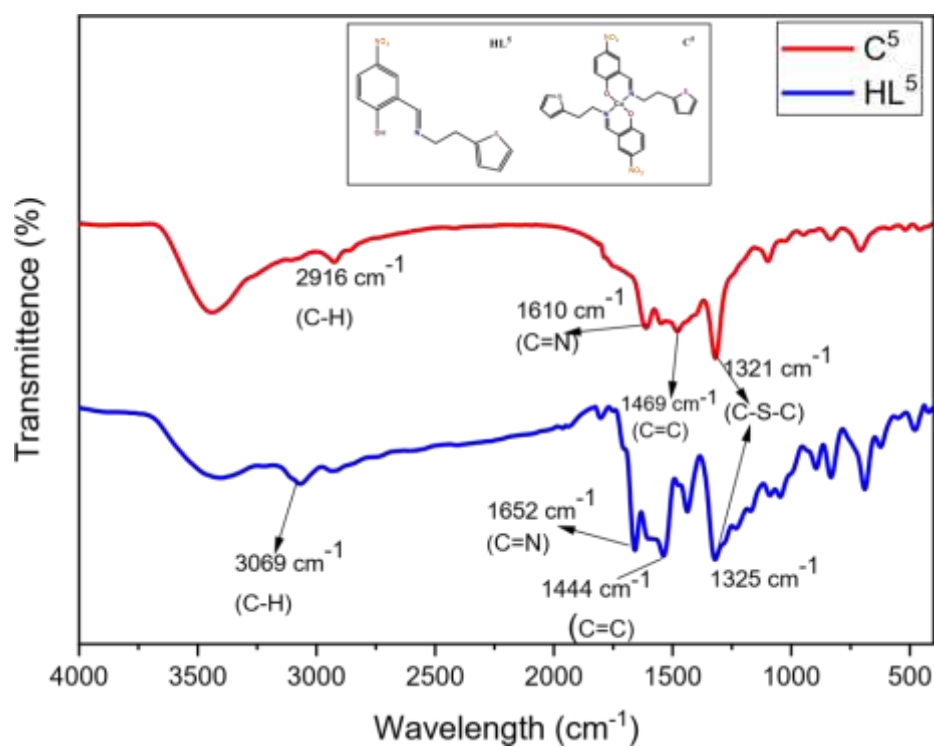
Figure 3.7. FTIR spectra of **HL⁵** and **C⁵**.

Figure 3.8. UV-vis spectra of **HL¹** and **C¹**in **DMSO.**

100
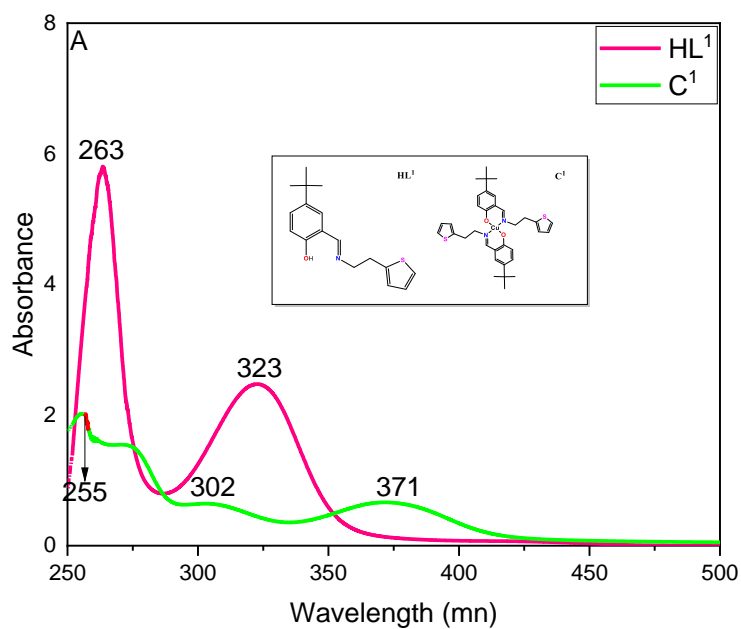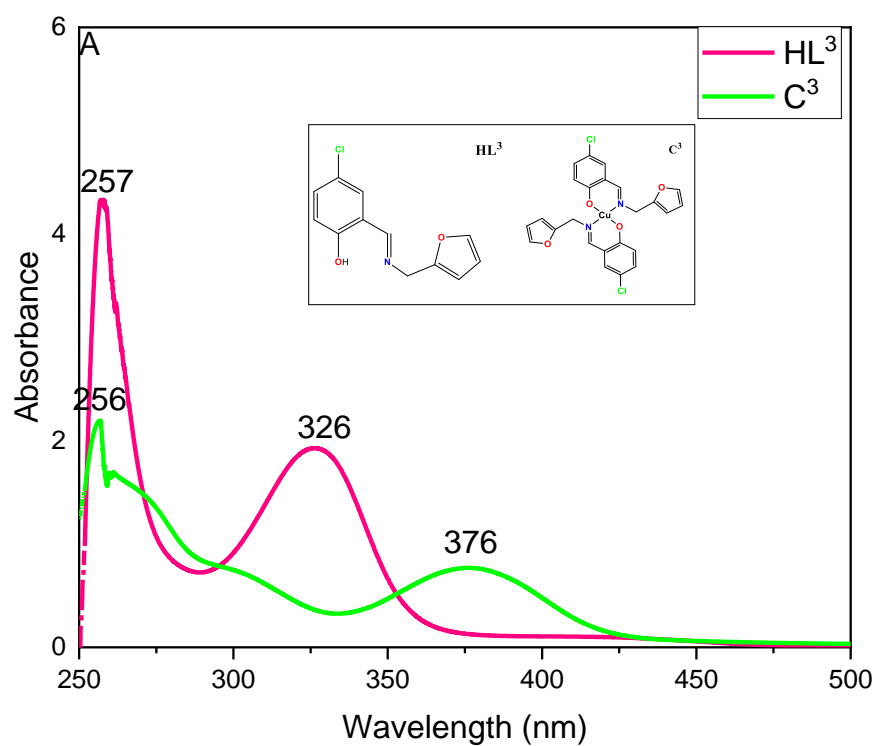
Figure 3.9. UV-Vis spectra of **HL²** and **C²** in **DMSO.**

Figure 3.10. UV-vis spectra of **HL³** and **C³** in **DMSO.**

101
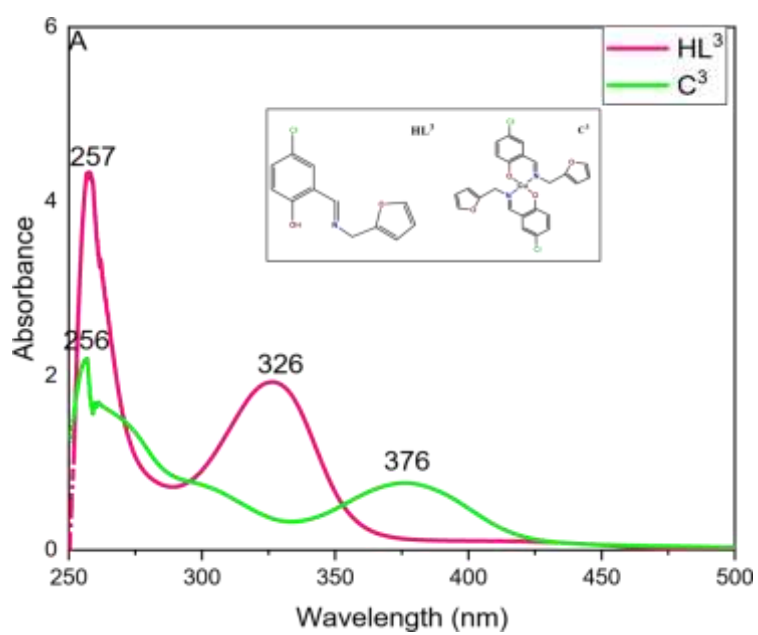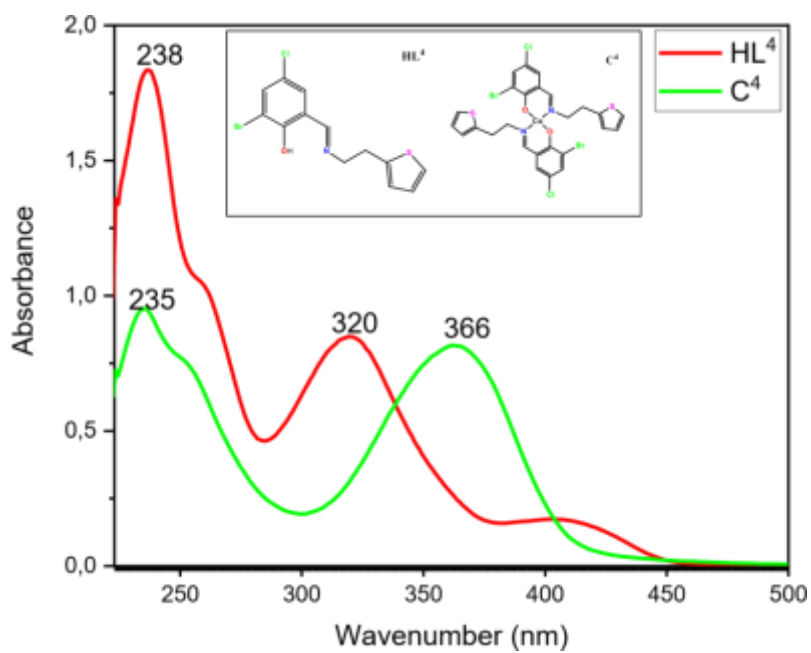
Figure 3.11. UV-vis spectra of **HL^4** and **C^4** in **DMSO.**
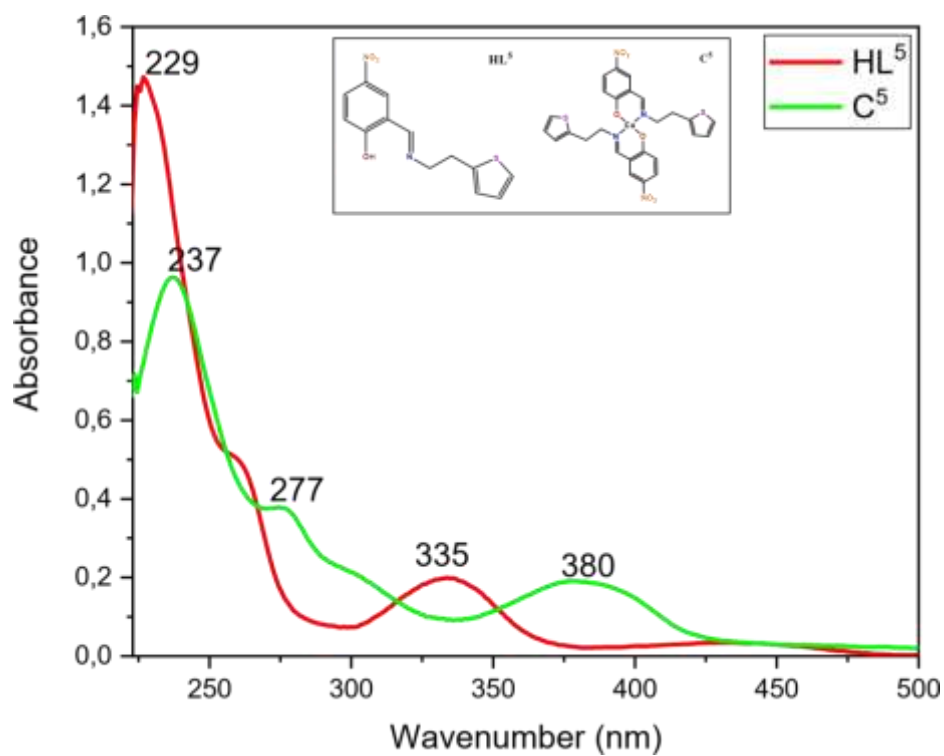
Figure 3.12. UV-vis spectra of **HL^5** and **C^5** in **DMSO.**
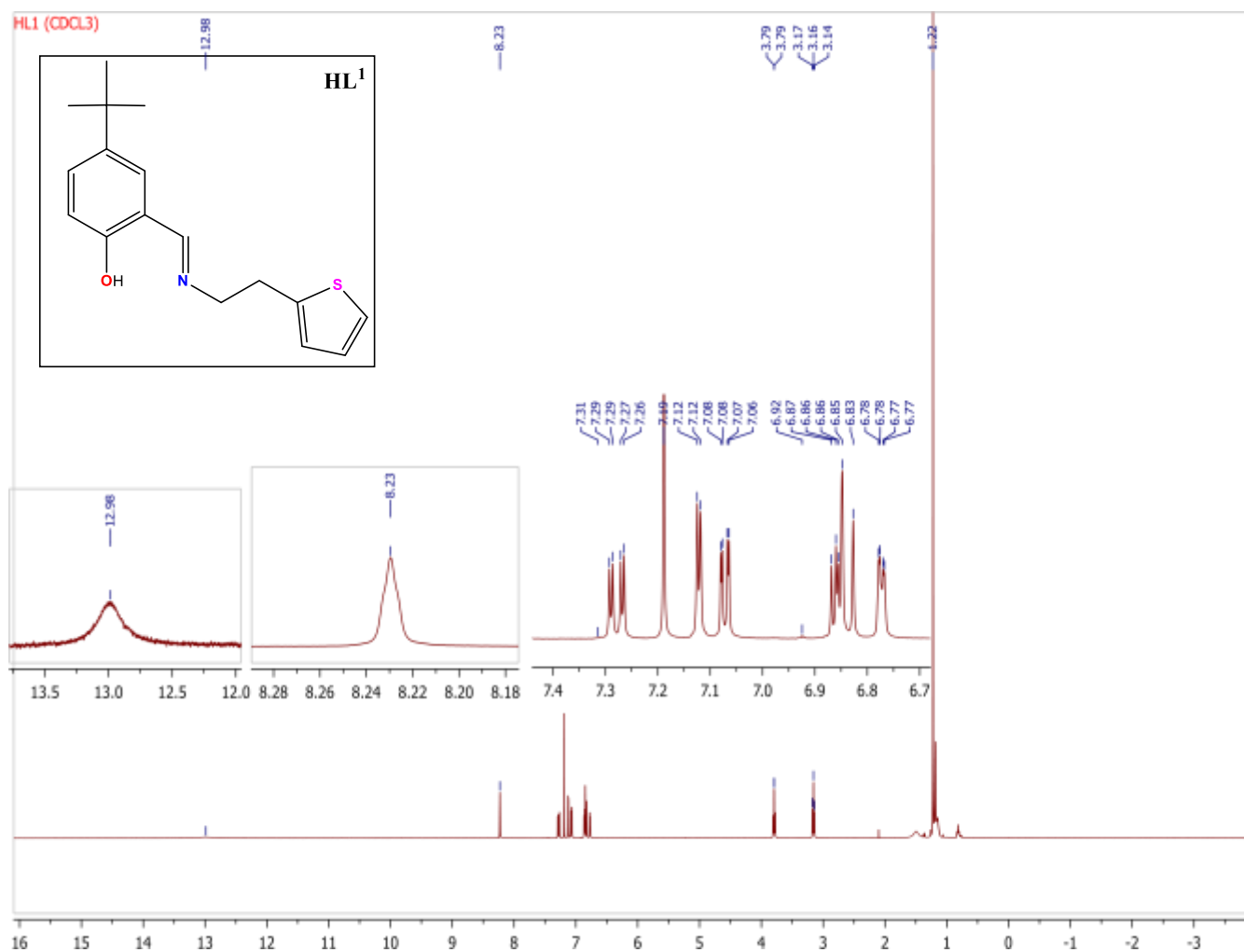
Figure 3.13. ^{1}H NMR spectrum of ligand **HL^1** in CDCl$_3$
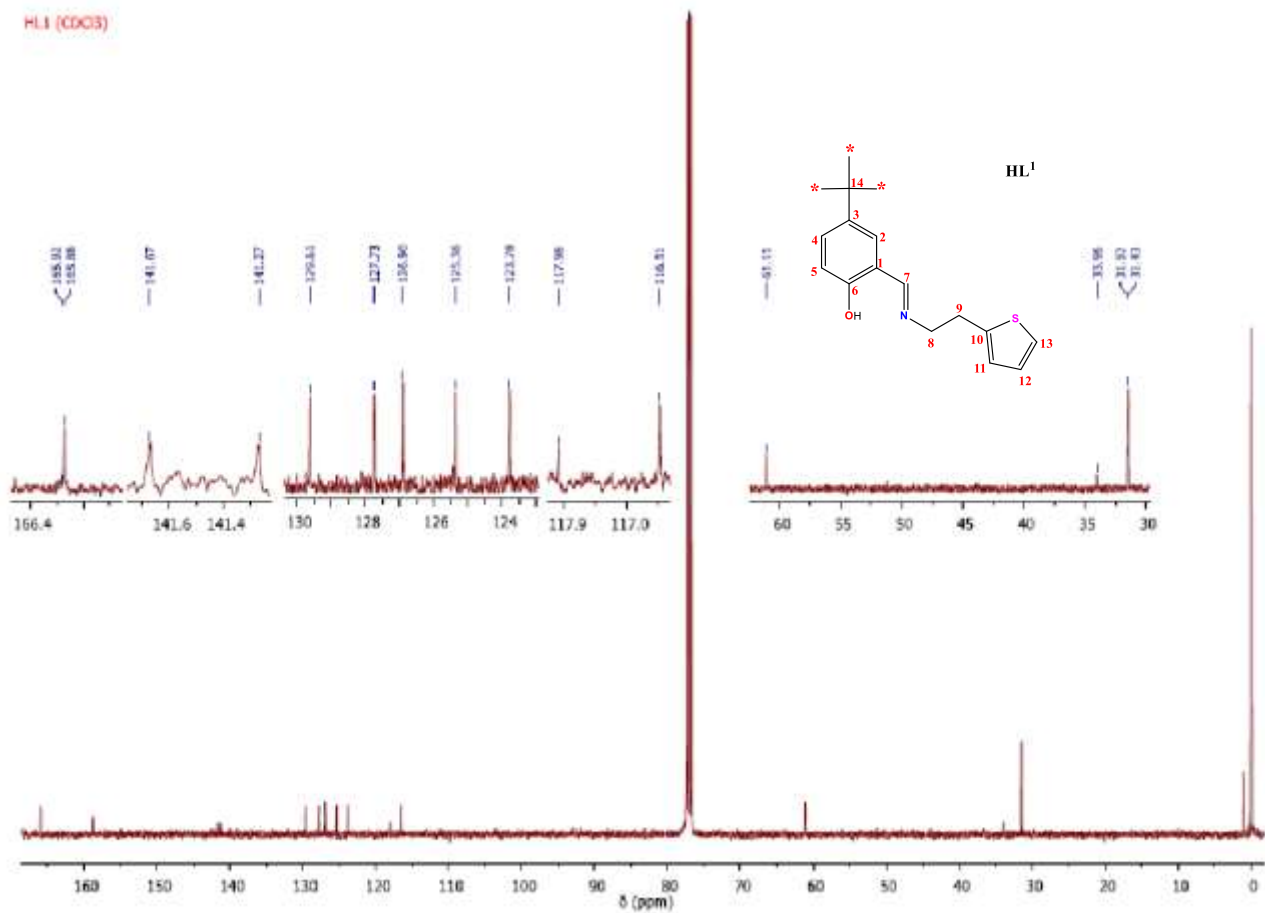
Figure 3.14. ^{13}C NMR spectrum of ligand **HL^1** in CDCl$_3$

104

Figure 3.15. ¹H NMR spectrum of ligand **HL²** in CDCl₃

105

Figure 3.16. ^{13}C NMR spectrum of ligand **HL²** in CDCl₃

106

Figure 3.17. ^{1}H NMR spectrum of ligand **HL^3** in CDCl$_3$

107
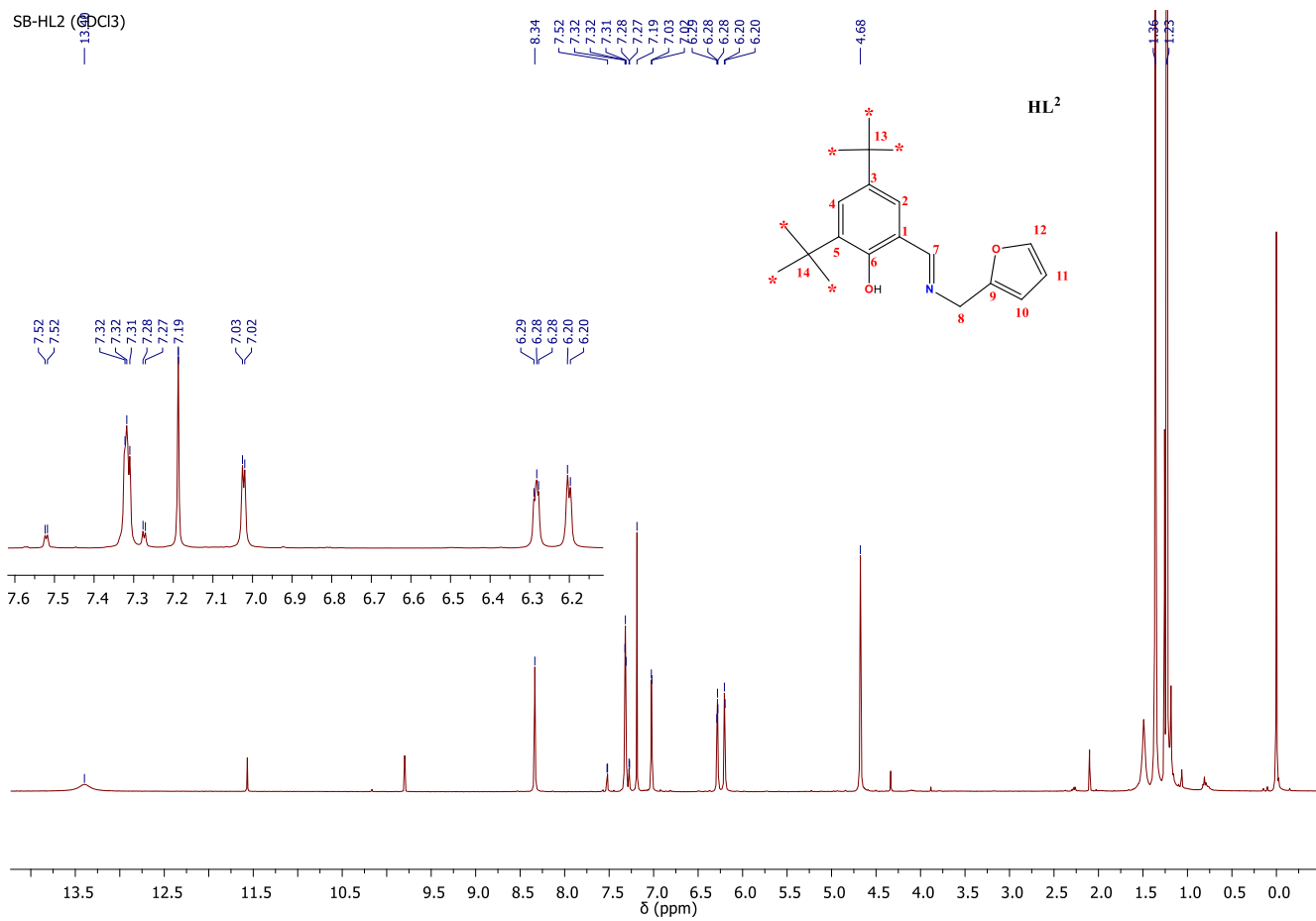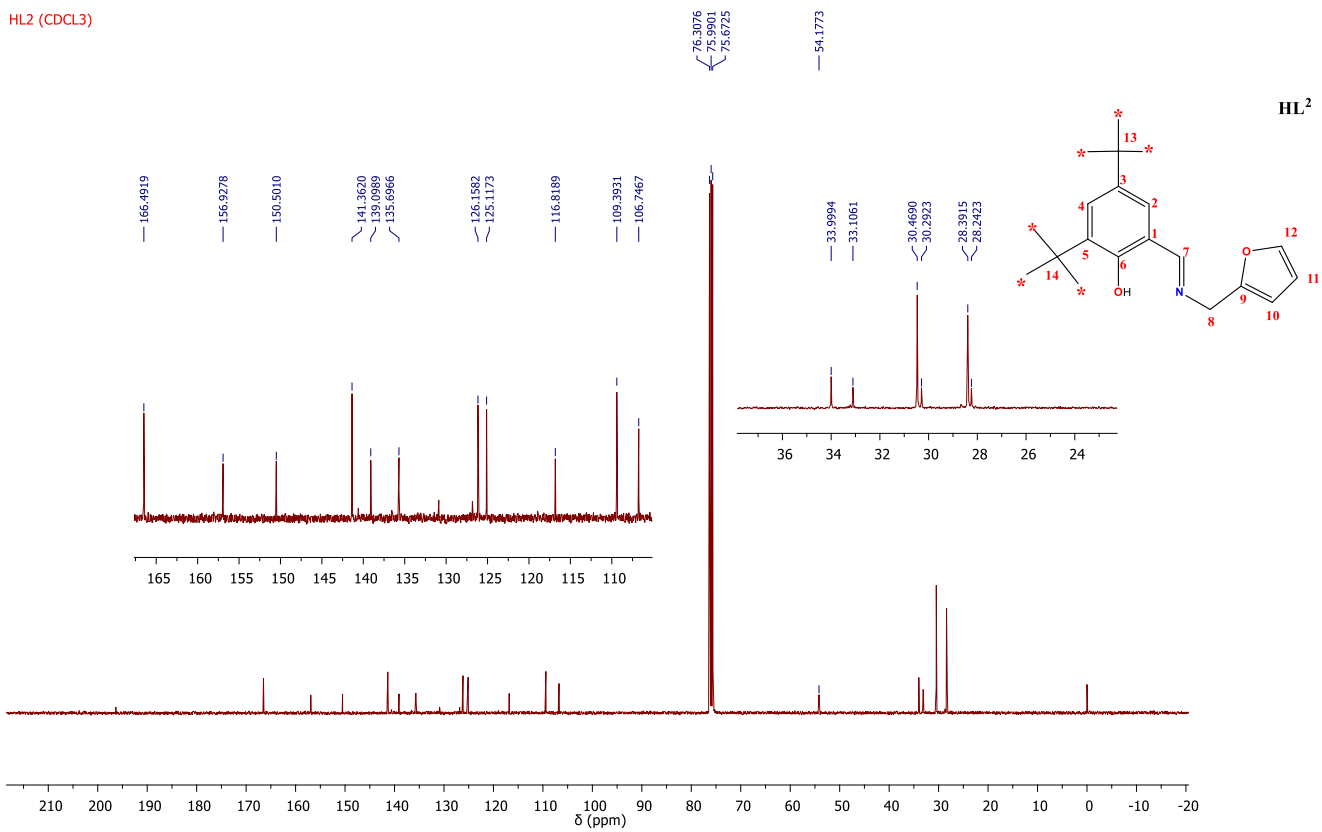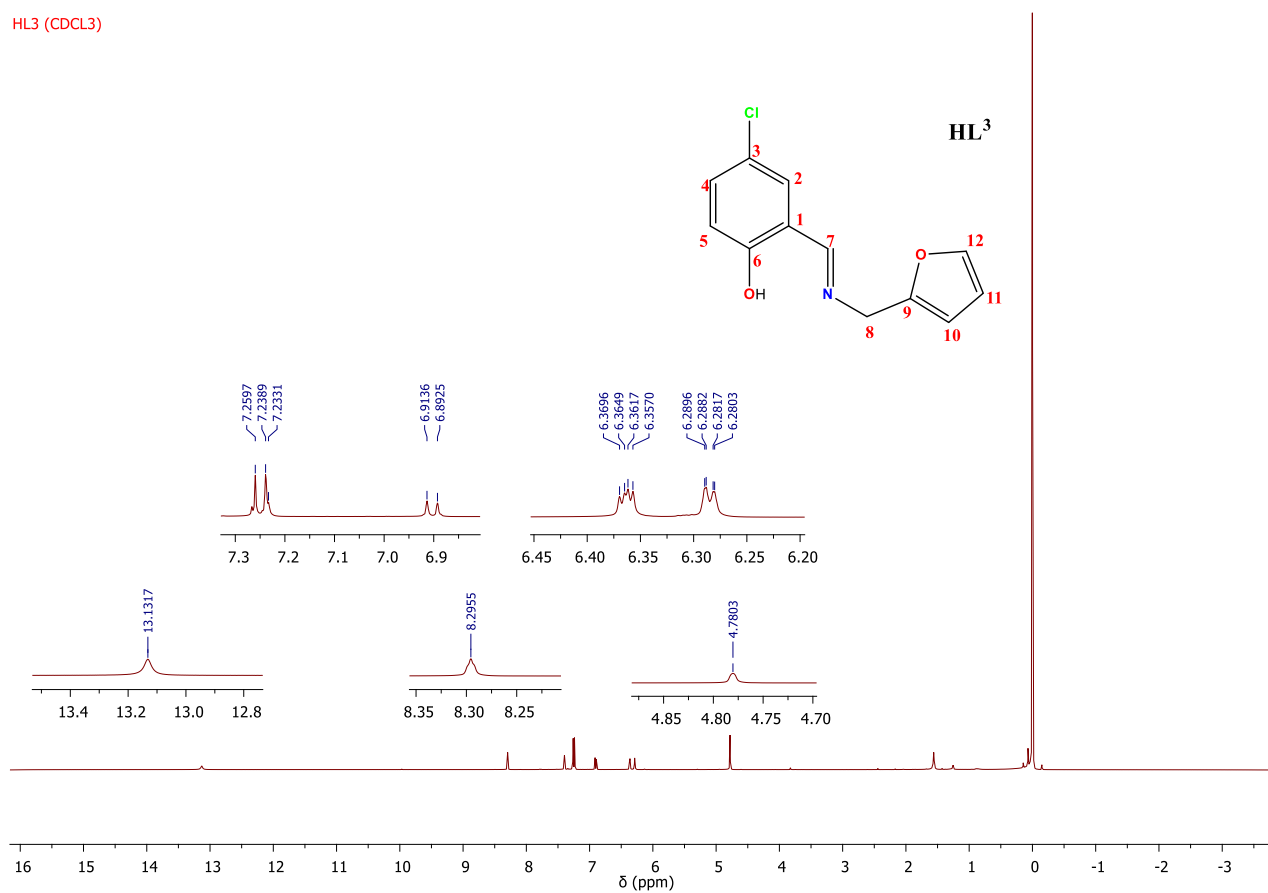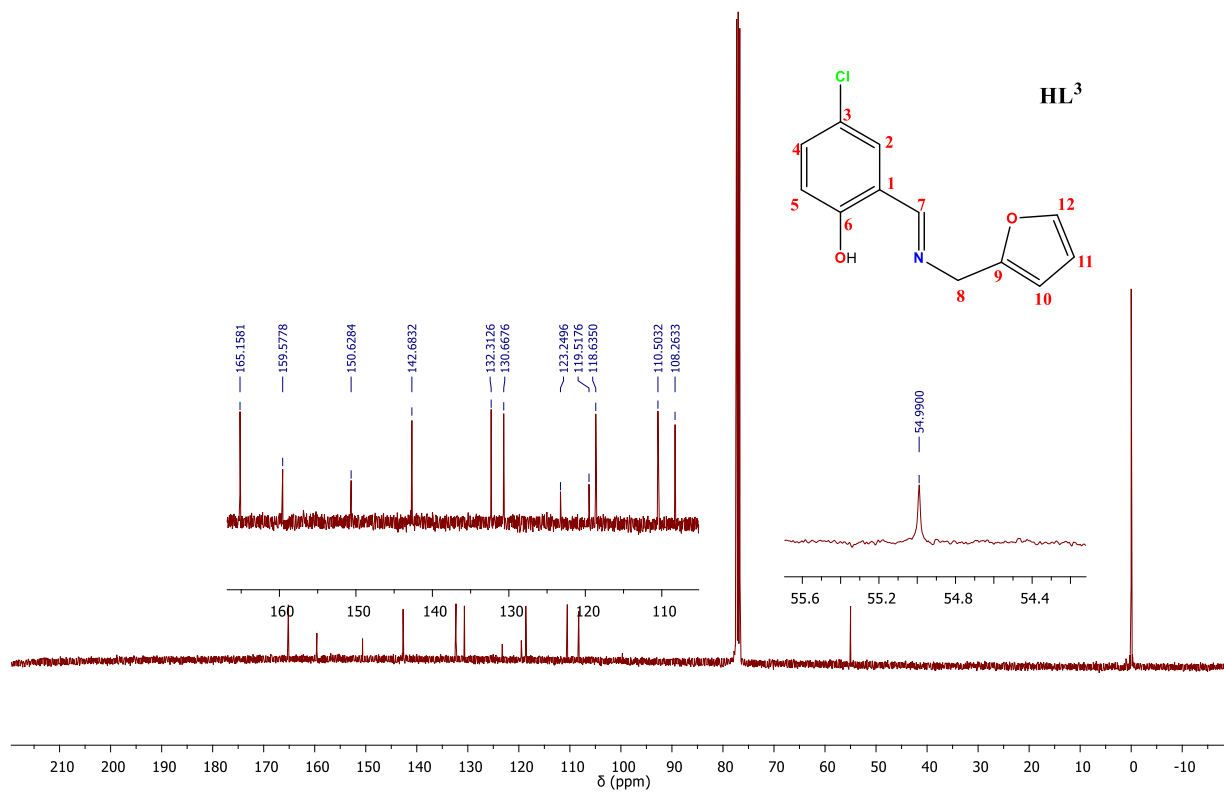
Figure 3.18. ^{13}C NMR spectum of ligand **HL^3** in CDCl$_3$

Figure 3.19. ¹H NMR spectrum of ligand **HL⁴** in CDCl₃

109
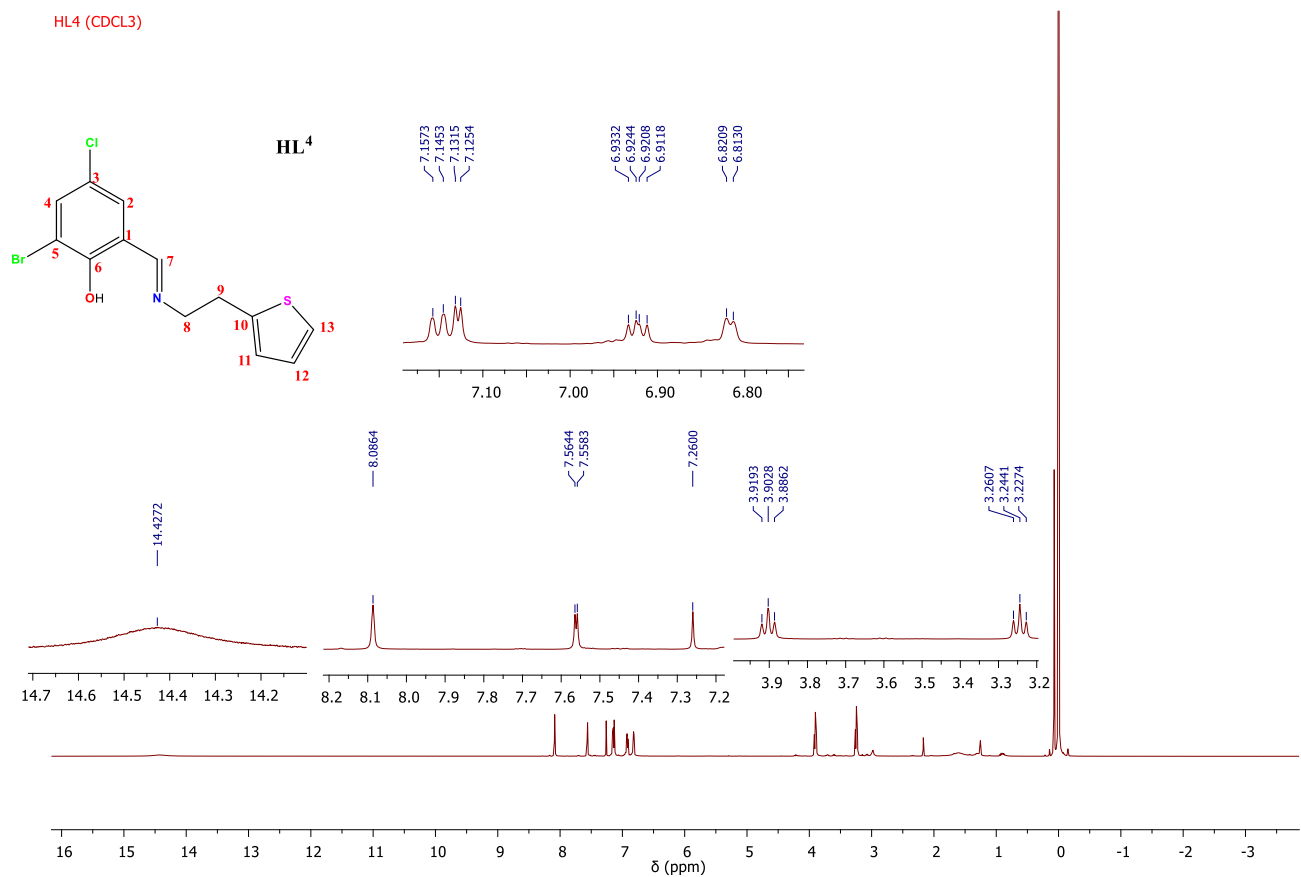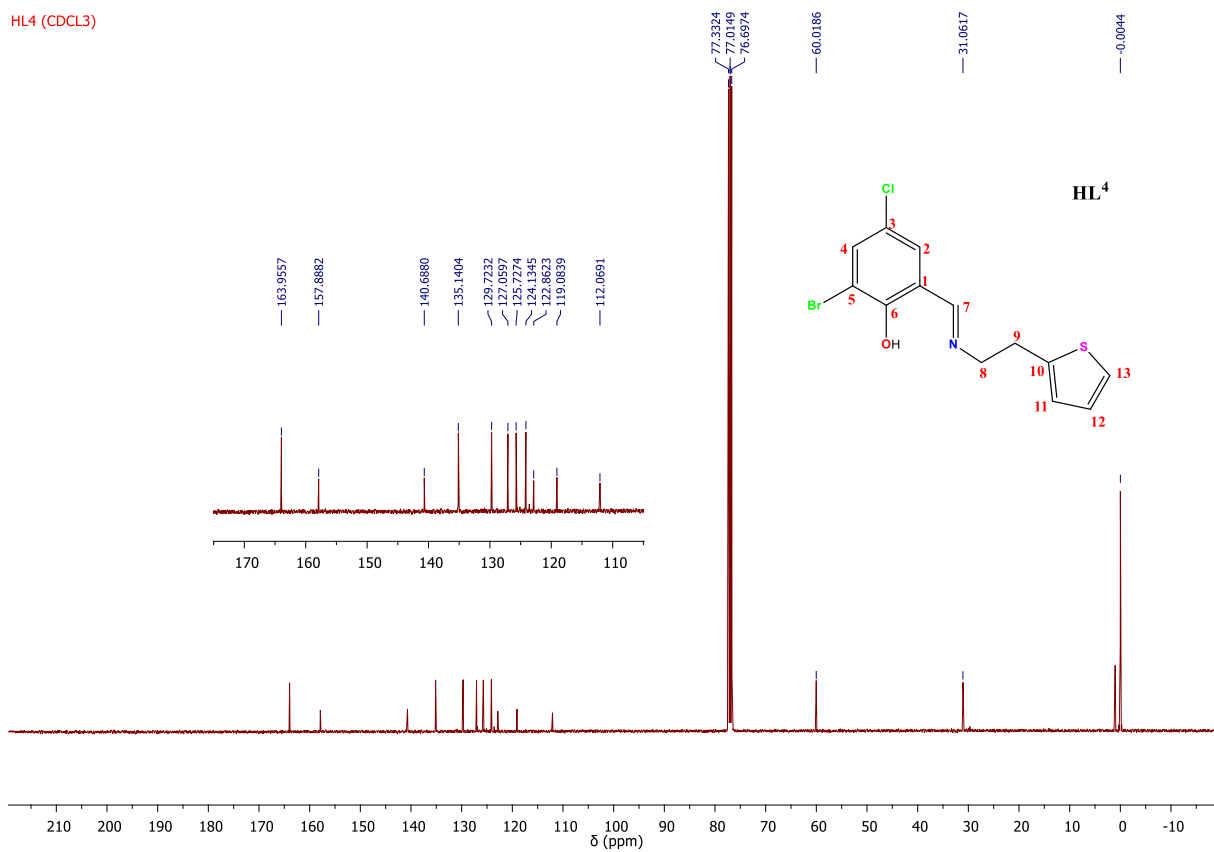
Figure 3.20. ^{13}C NMR spectrum of ligand **HL^4** in CDCl$_3$

Figure 3.21. ^{1}H NMR spectrum of ligand **HL^5** in CDCl$_3$
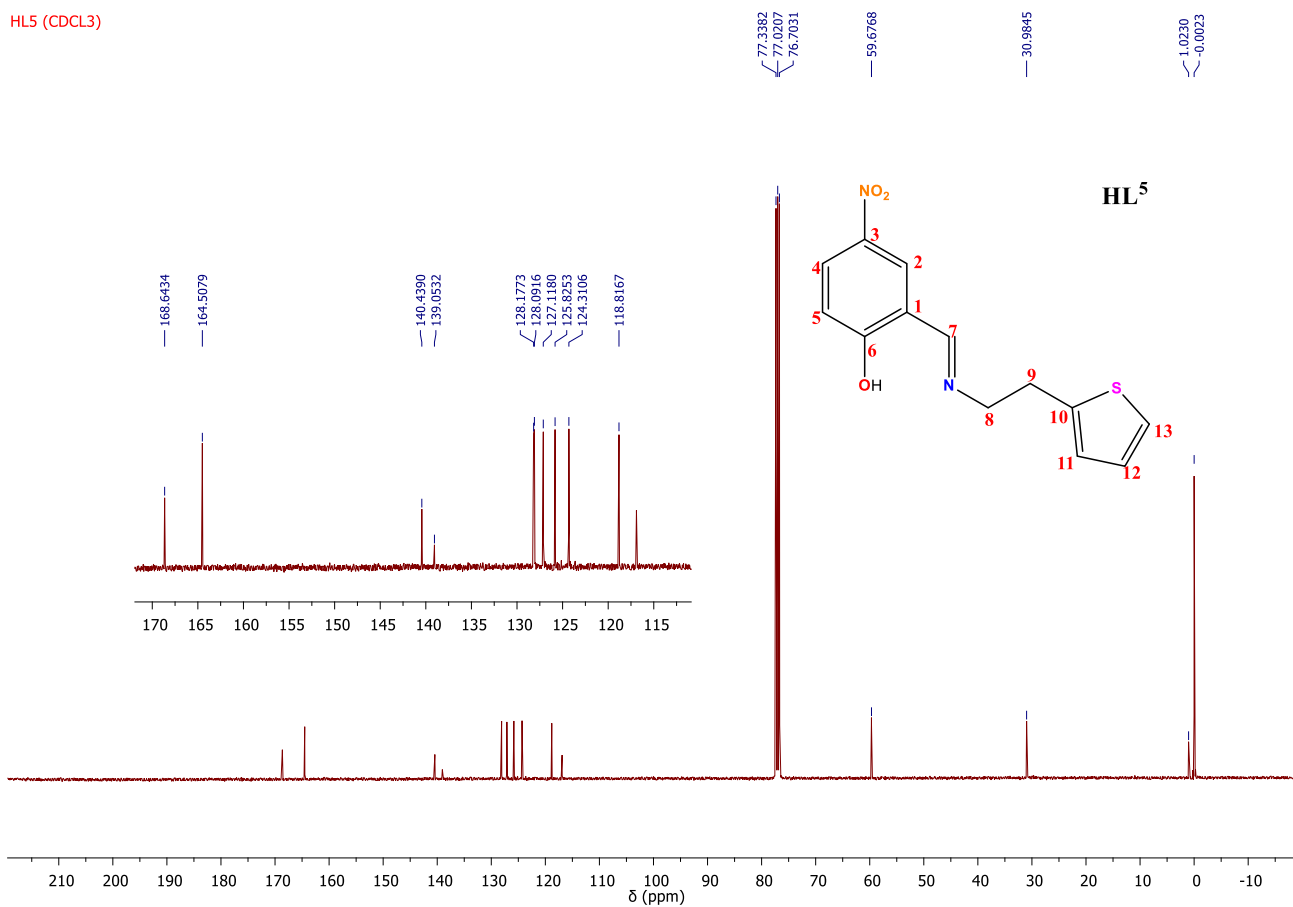
Figure 3.22. ^{13}C NMR spectrum of ligand **HL^5** in CDCl$_3$

112
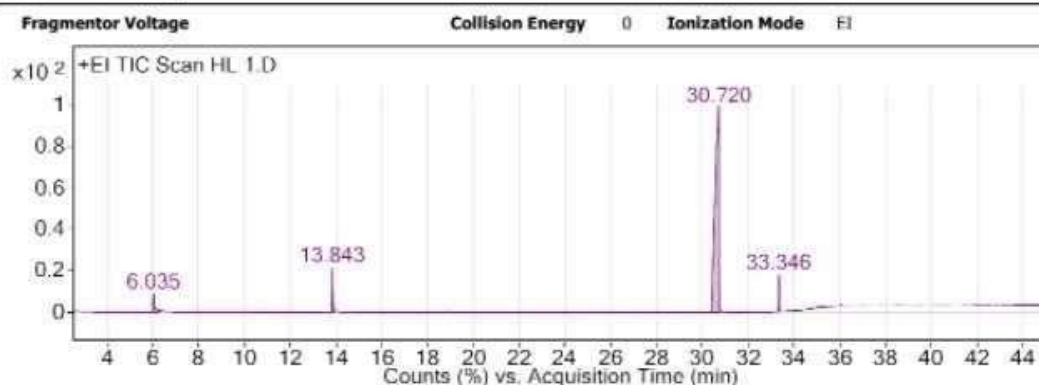
GC-MS retention time of **HL¹**
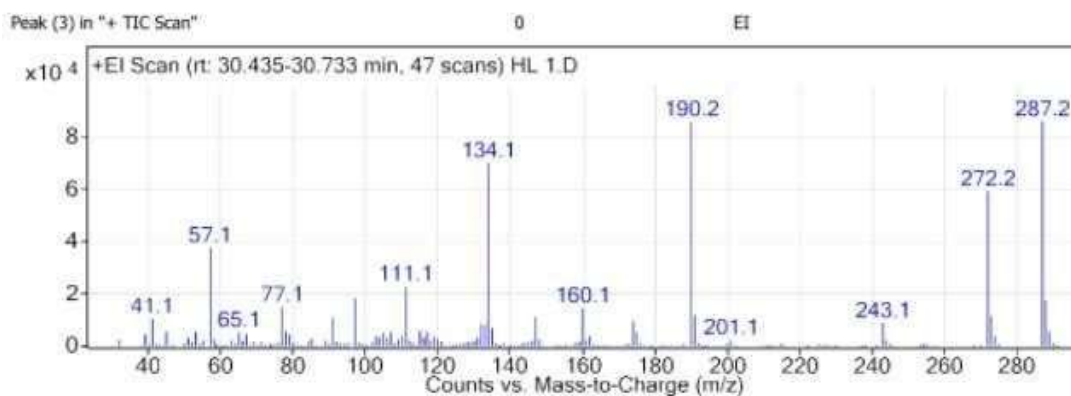
Figure 3.23. GC-MS of **HL¹**
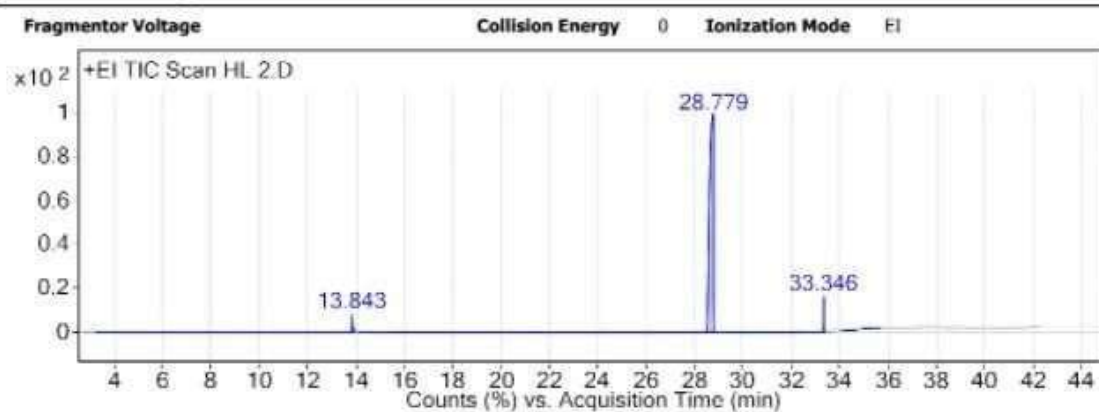
GC-MS Retention time of **HL²**

113
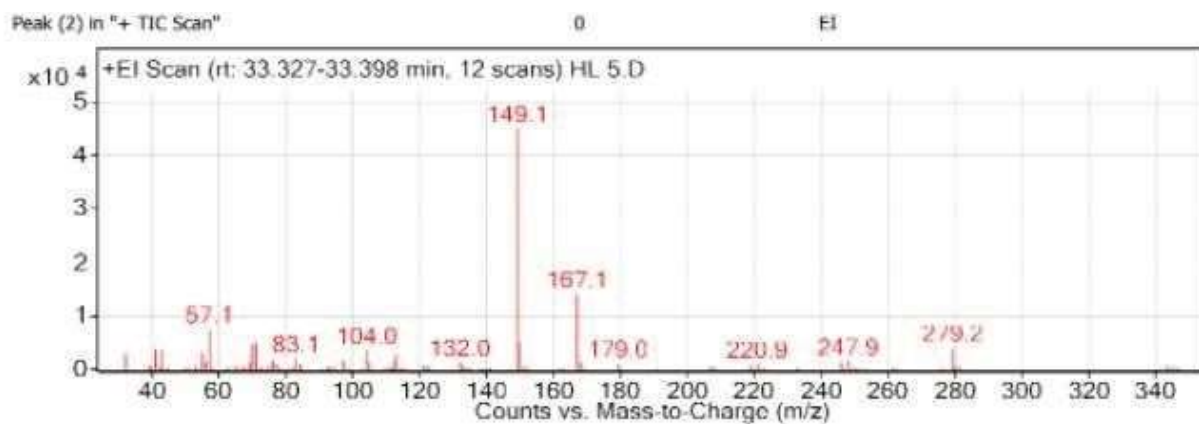
Figure 3.24. GC-MS of **HL²**
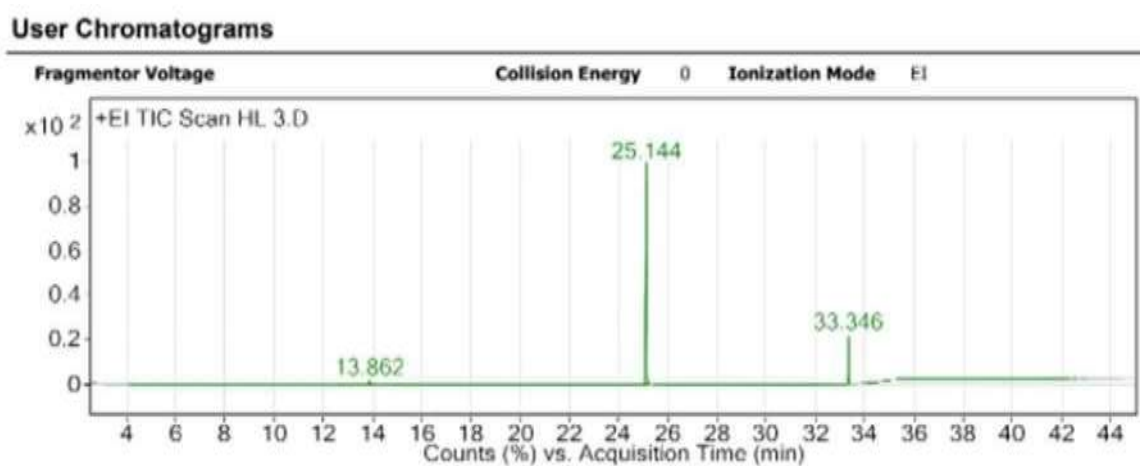
GC-MS Retention time of **HL³**
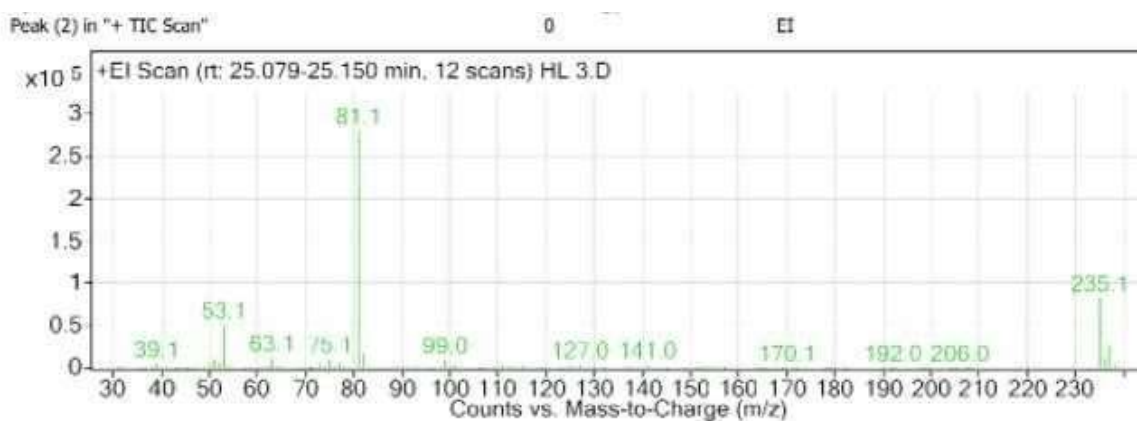
Figure 3.25. GC-MS of **HL³**

User Chromatograms
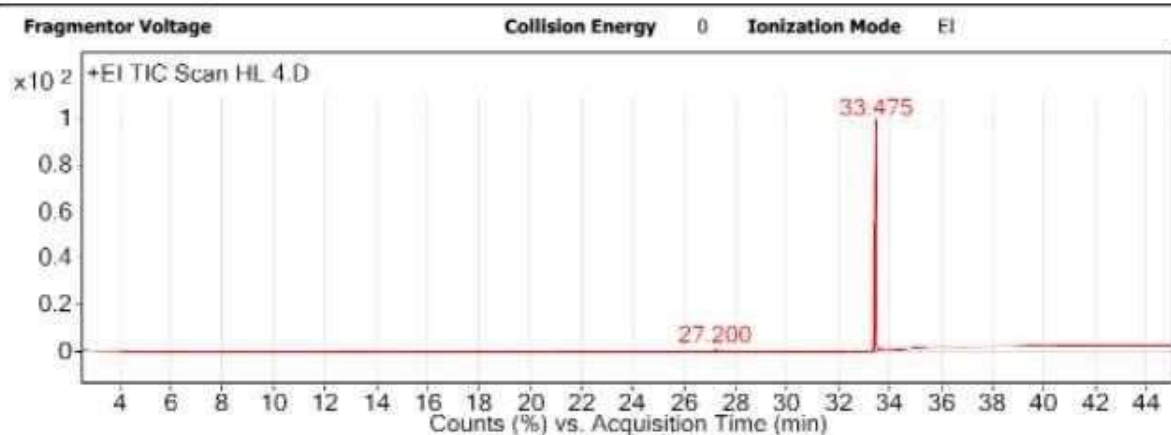
GC-MS Retention time of **HL**[4]
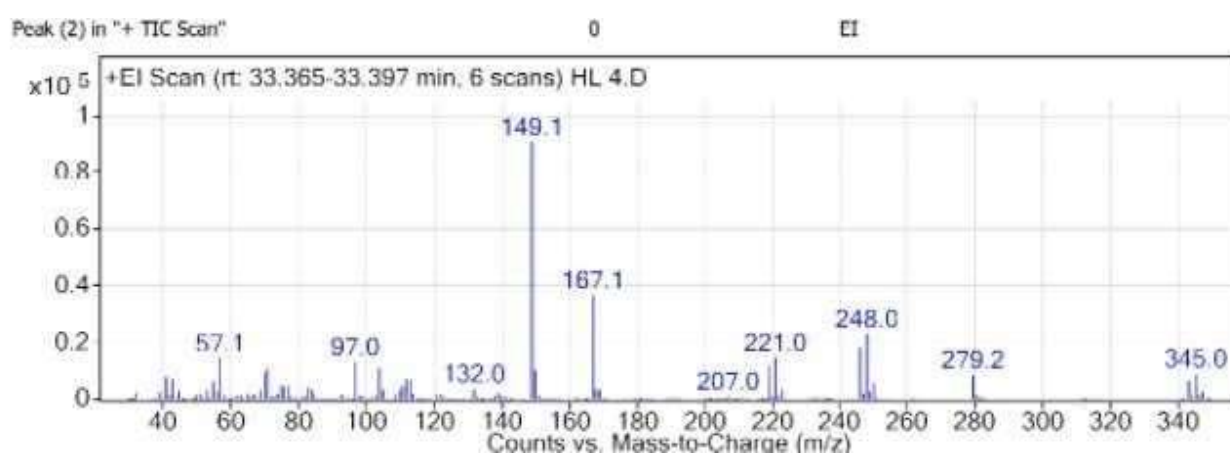
Figure 3.26. GC-MS of **HL**[4]

User Chromatograms
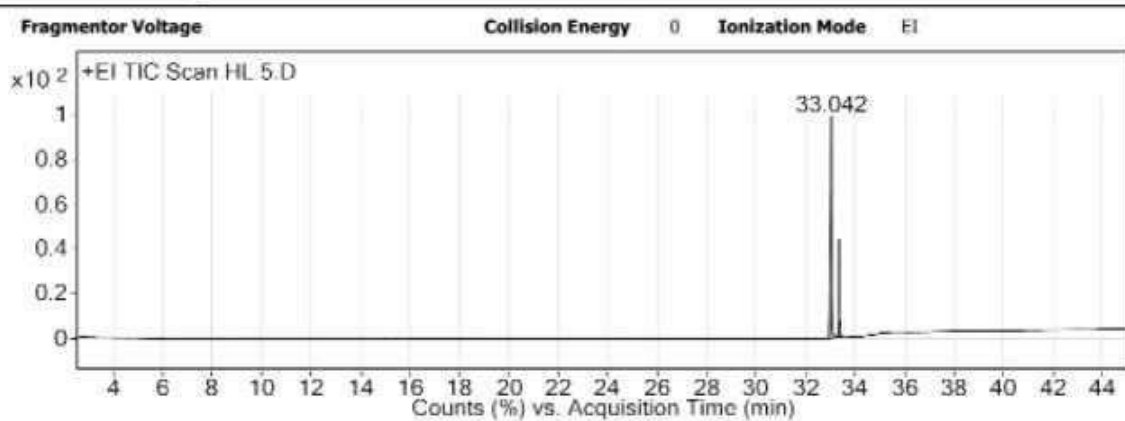
GC-MS Retention time of **HL**[5]
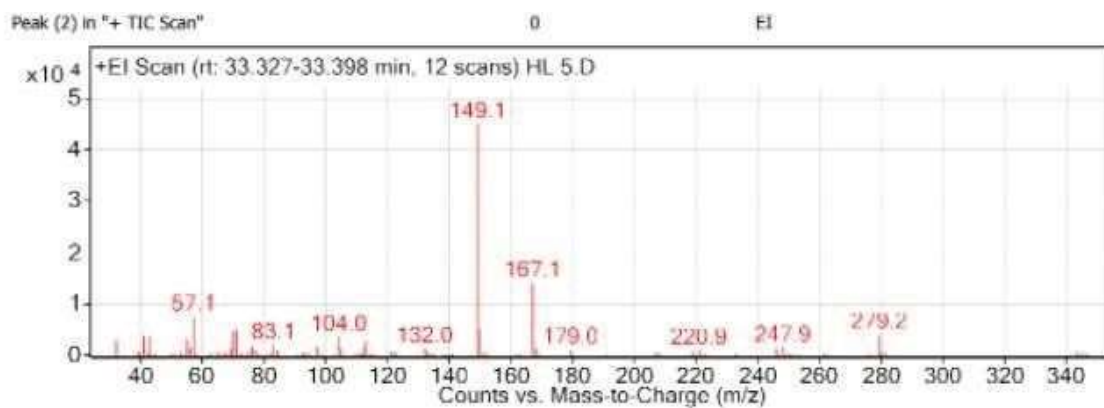
Figure 3.27. GC-MS of **HL**[5]
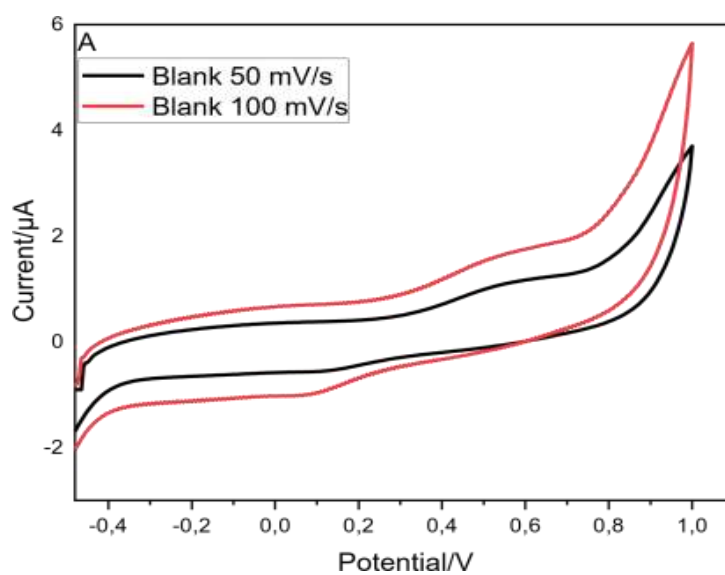
Figure: 3.28. Cyclic voltammogram of unmodified **GCE** in at scan rate of 50 and 100 mV/s.
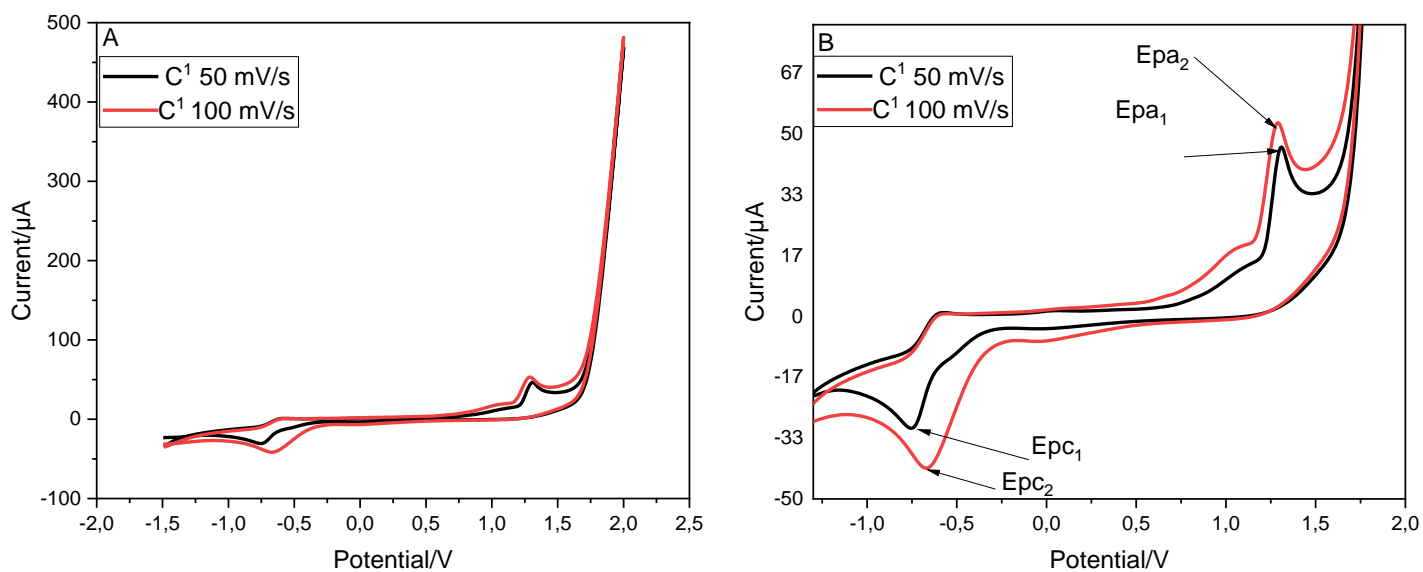
Figure 3.29. (a) Cyclic voltammogram of **Complex 1(C^1)** in 0.3 M of TBAP solution at scan rate of 50 and 100 mV/s. **(b)** zoomed in cyclic voltammogram of **(C^1)**.

Figure 3.30. (a) Cyclic voltammogram of **complex 2 (C^2)** in 0.3 M of TBAP solution at scan rate of 50 and 100 mV/s. **(b)** zoomed in cyclic voltammogram of **(C^2)**

117

Figure 3.31. (a) Cyclic voltammogram of **complex 3 (C^3)** in 0.3 M of TBAP solution at scan rate of 50 and 100 mV/s. **(b)** zoomed in cyclic voltammogram of (**C^3**)

118
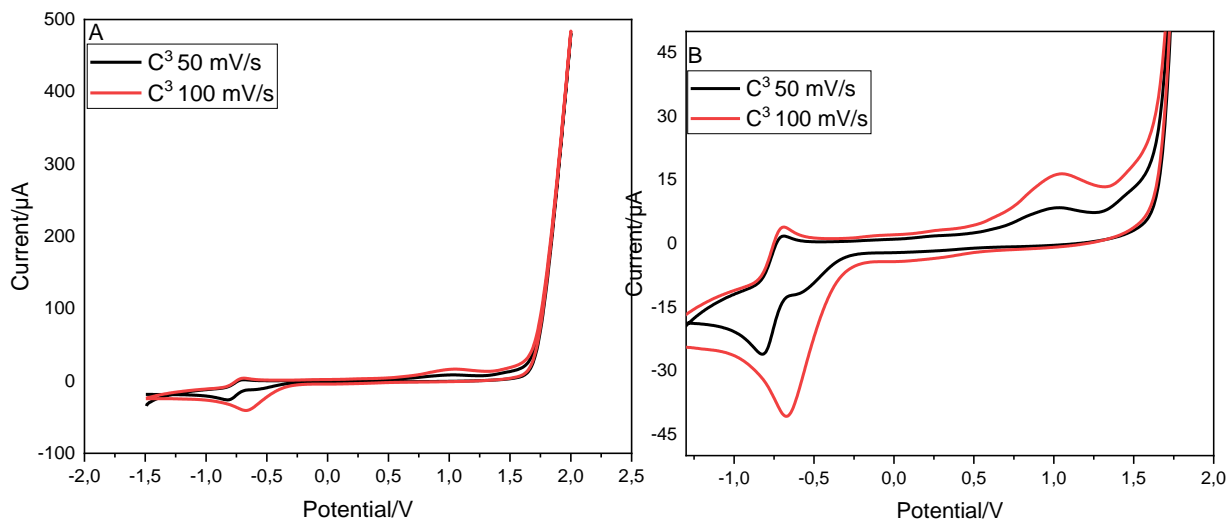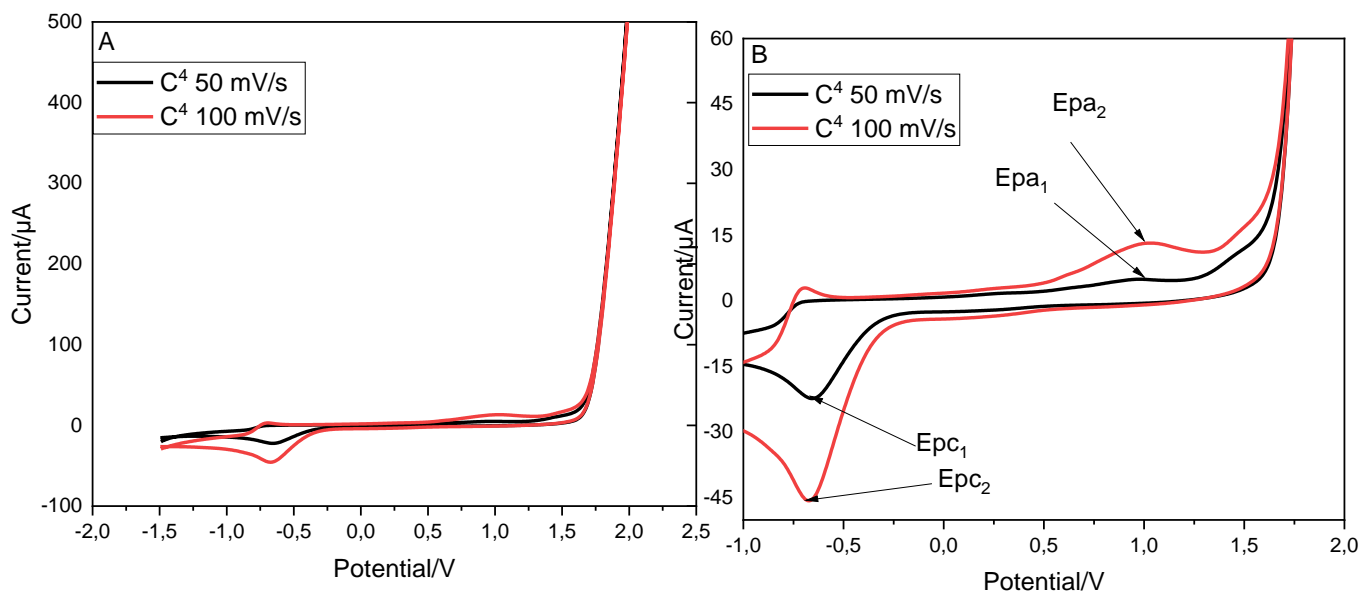
Figure 3.32. (a)Cyclic voltammogram of **complex 4 (C^4)** in 0.3 M of TBAP solution at scan rate of 50 and 100 mV/s. **(b)** Zoomed in cyclic voltammogram of **(C^4)**

Figure 3.33. (a) Cyclic voltammogram of **complex 5 (C^5)** in 0.3 M of TBAP solution at scan rate of 50 and 100 mV/s. **(b)** zoomed in cyclic voltammogram of **(C^5)**

Appendix 2 Preliminary results for complex 1 catalysis
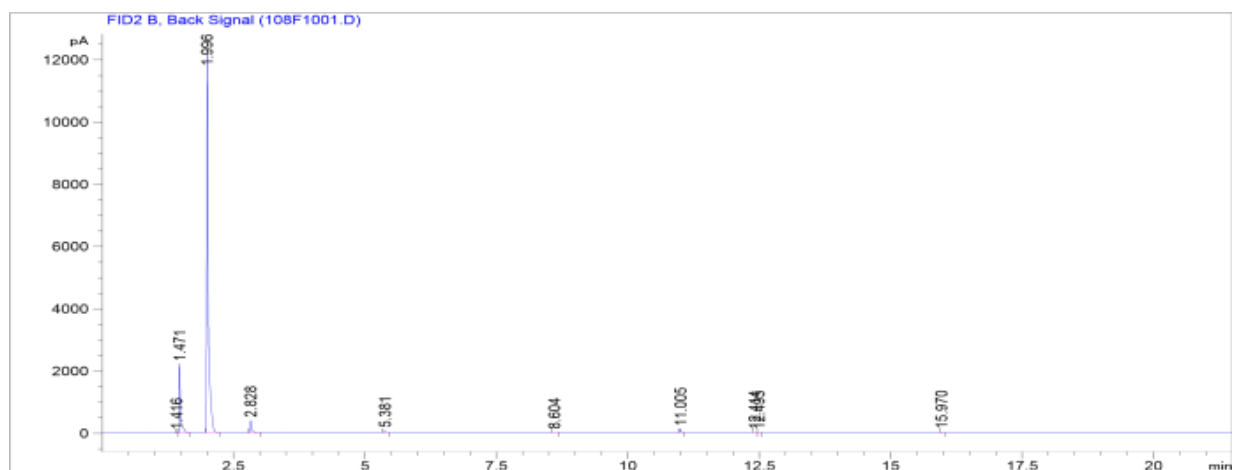
Figure 3.34. Sample of the chromatogram after 12 hours of catalysis reaction.

119
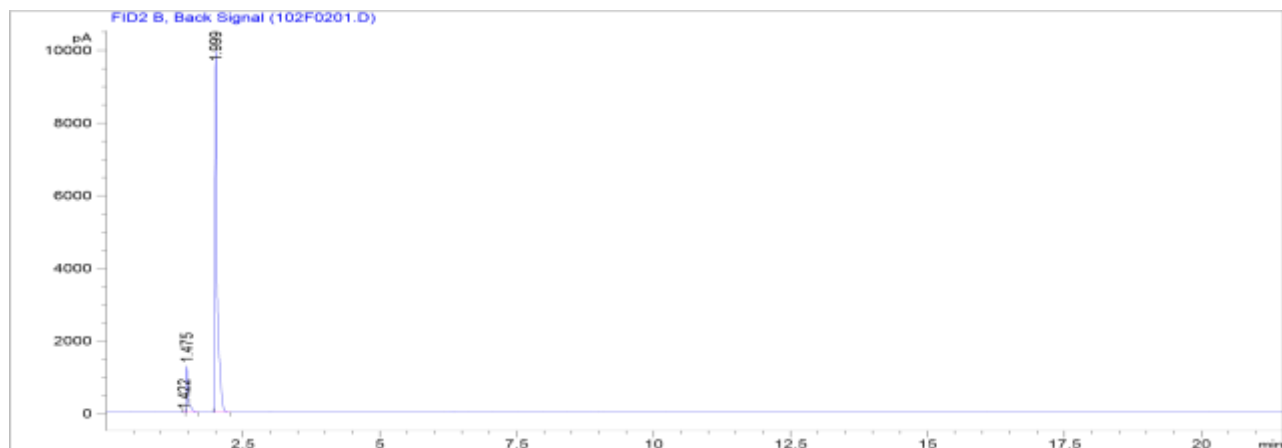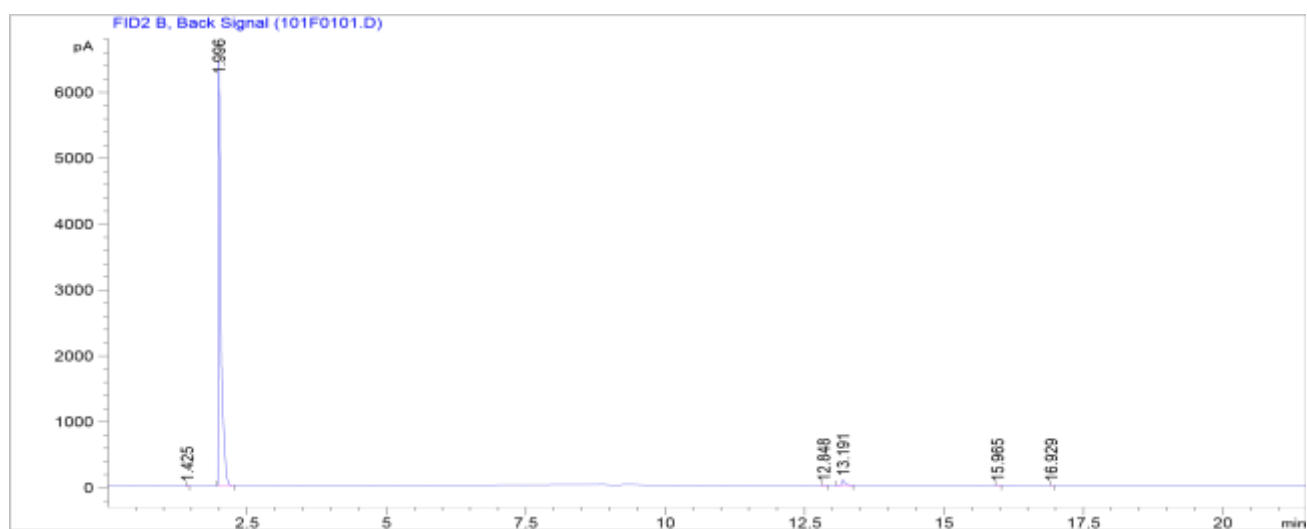
DCM and Ether

DCM
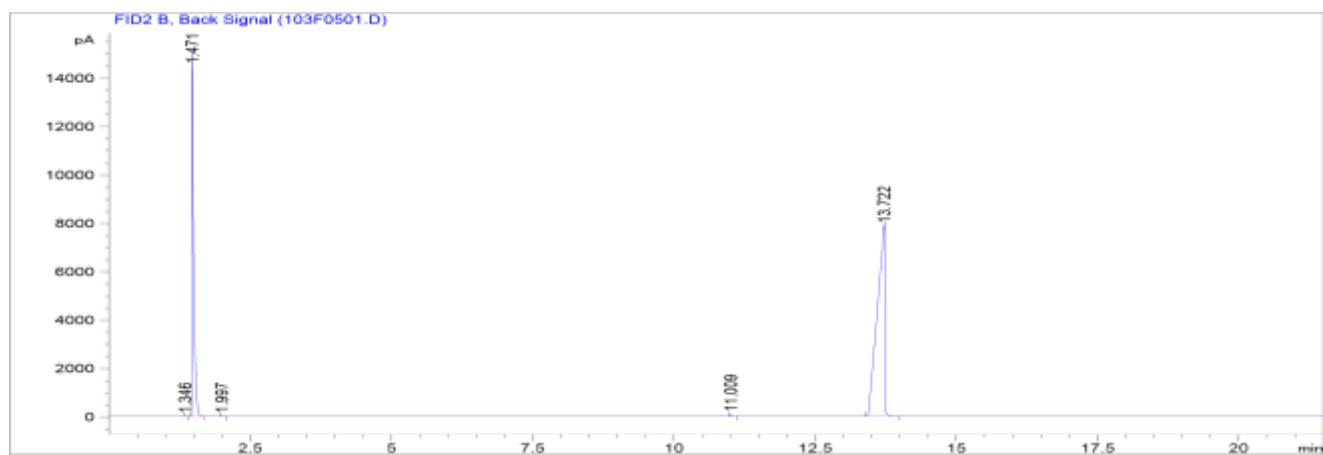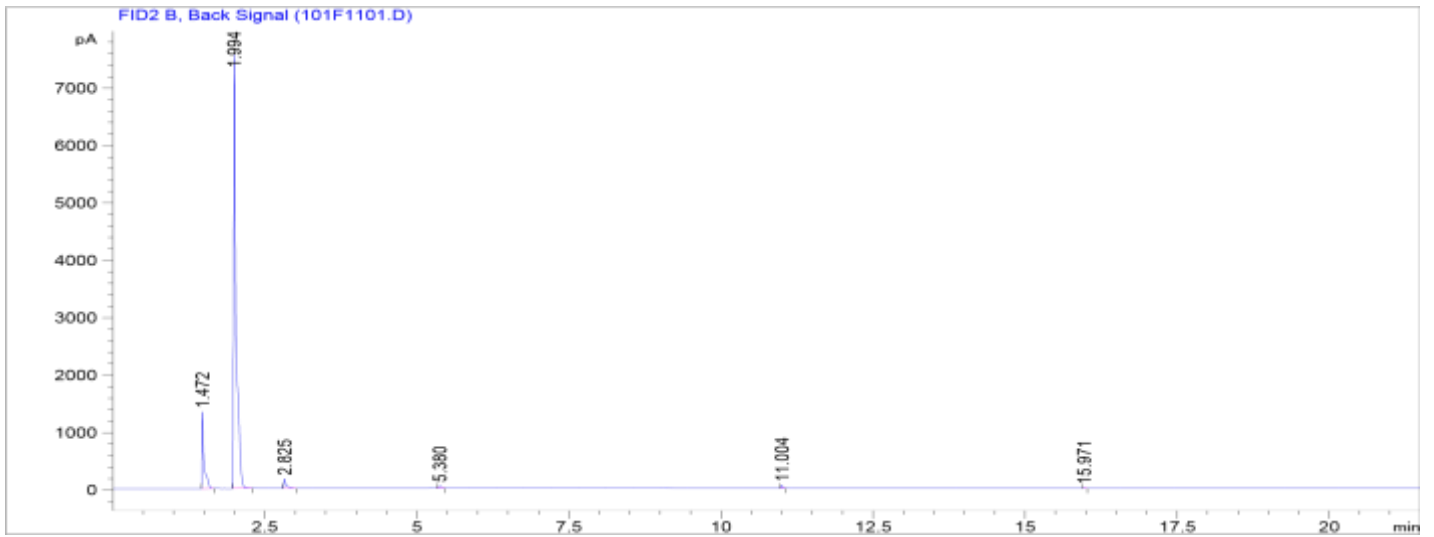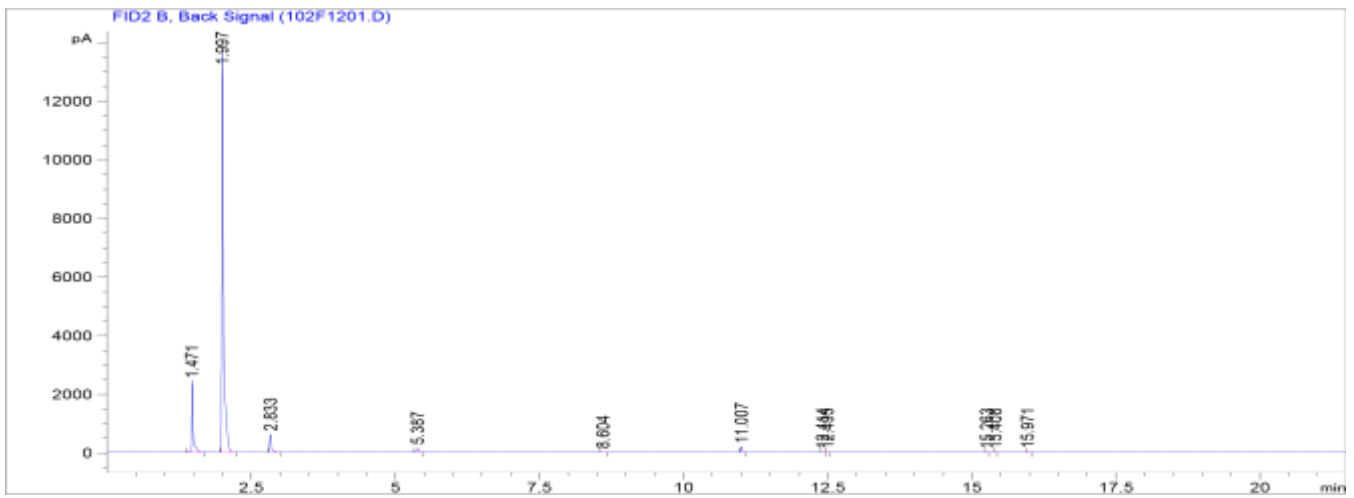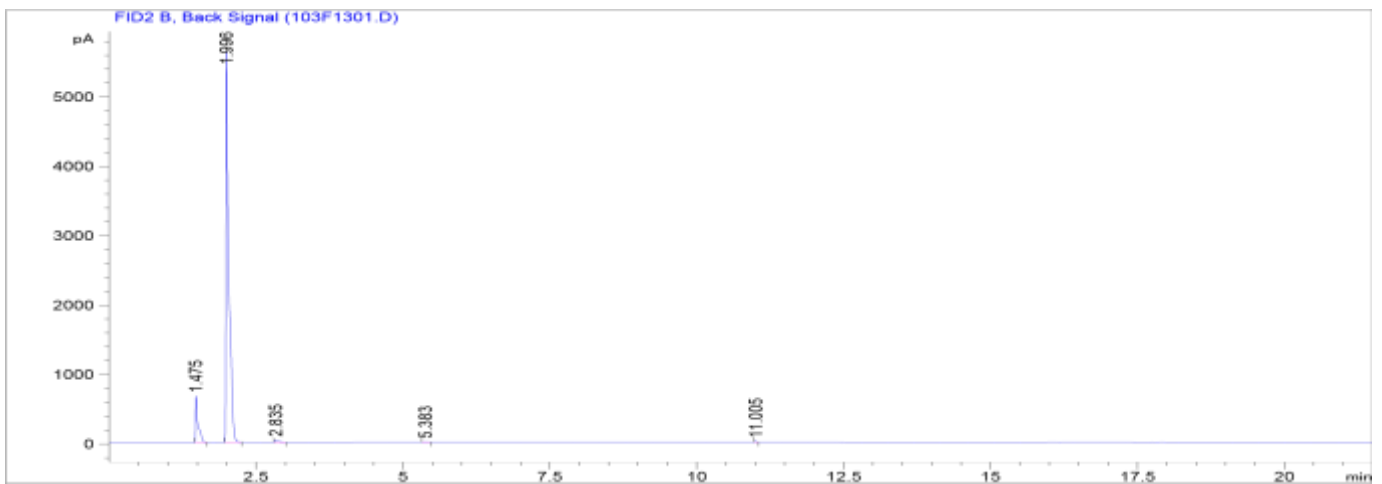

Starting material: Decant, DCM and Ether

120

Time zero

1 Hour

121

3 Hours

6 Hours

122
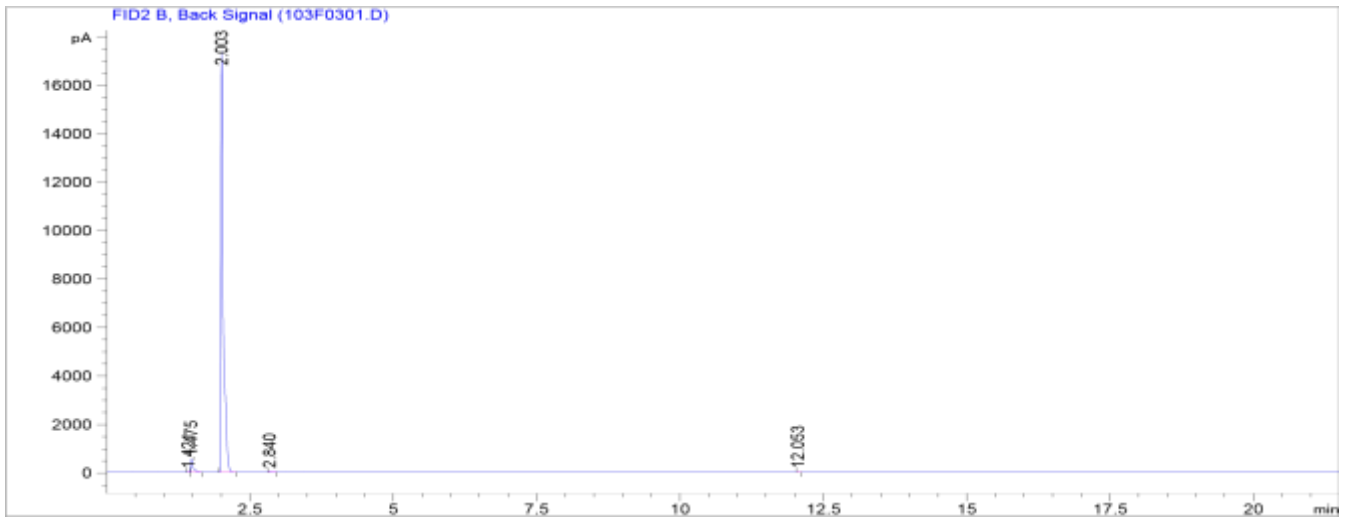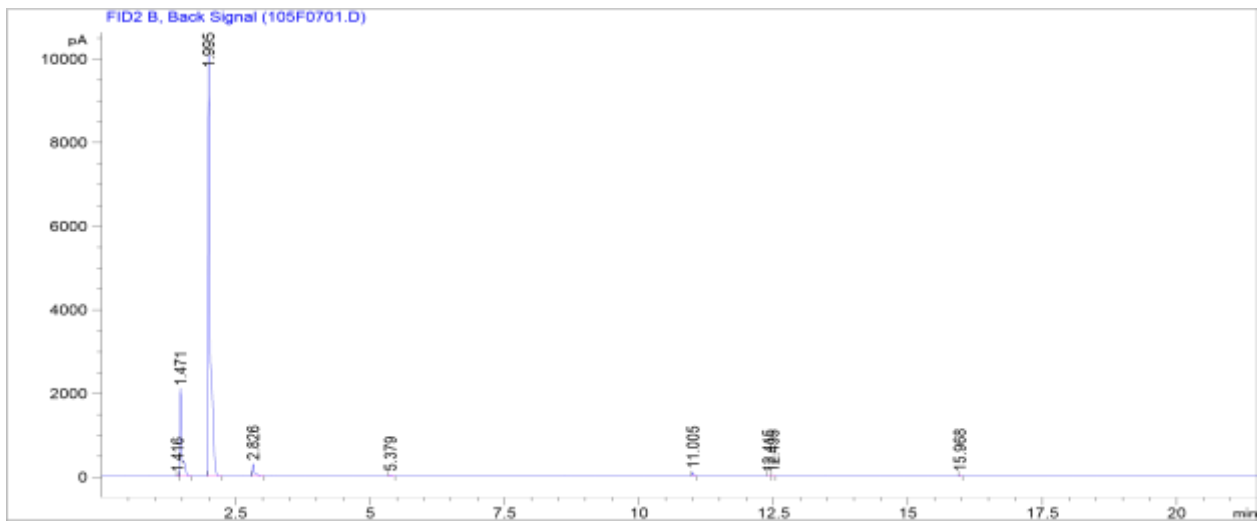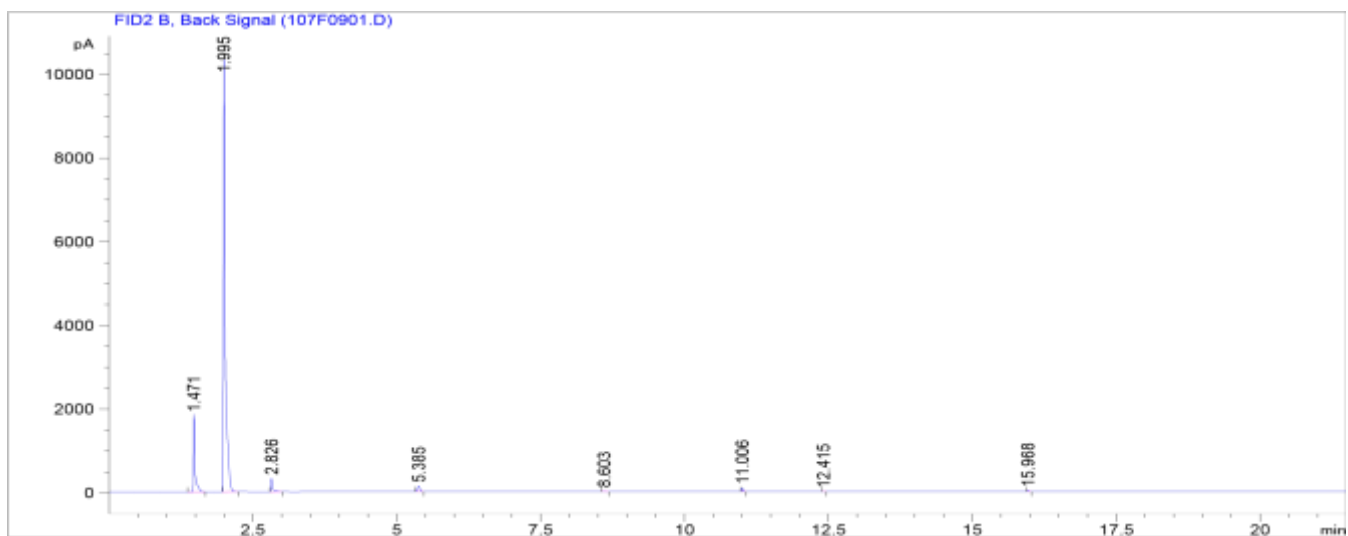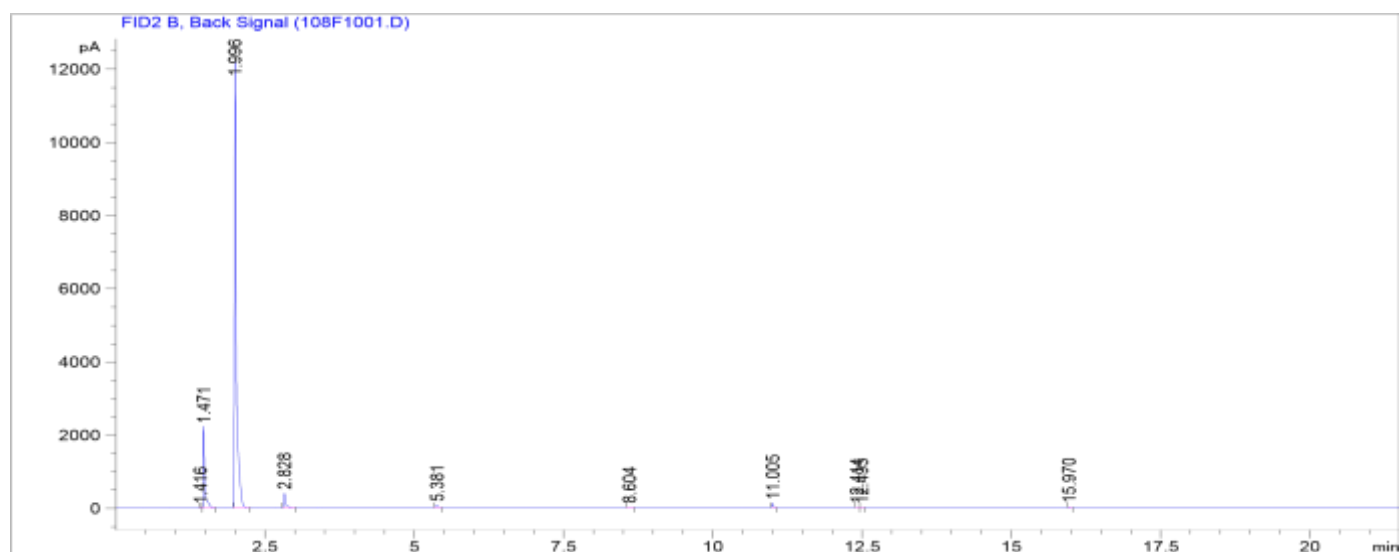
12 Hours

24 Hours

36 Hours

123